

# Event generators for the Higgs boson searches at the LHC

B. Di Micco

CERN, Università degli Studi di Roma Tre

LNF Spring Institute  
16<sup>th</sup> May 2012, Frascati

# Outline

- Higgs production cross section
- Higgs  $p_T$  and jet binning
- Background treatment in the  $H \rightarrow \gamma\gamma$  channel
- jet bin uncertainties
- Underlying Event tuning
- Parton shower effect on the differential Higgs distributions
- The  $H \rightarrow WW \rightarrow l\nu l\nu$  channel
- The  $H \rightarrow WW \rightarrow 4l$
- Heavy Higgs and signal-background interference,

## Event generators

LO+corrections

Pythia, Pythia8, Herwig, Herwig++

Multi-leg generators

Alpgen, Sherpa, Madgraph with matching to Pythia6

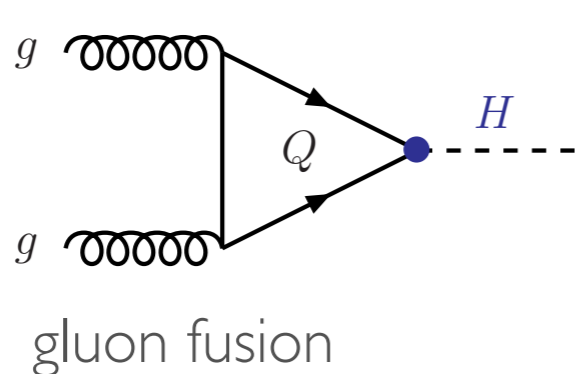
NLO generators

MC@NLO + Herwig, Powheg+Herwig, Pythia6, Pythia8

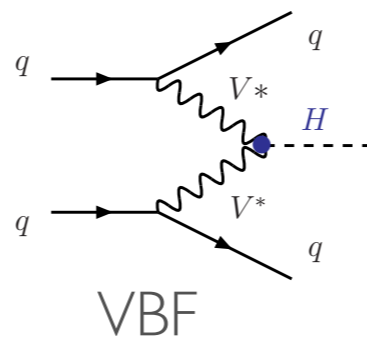
General approach:

Use NLO generators as much as possible, use multi-leg generators to describe jet sensitive process (correct them with data when needed), use LO+corrections only when there aren't alternative (correct them at truth level to NLO predictions when possible).

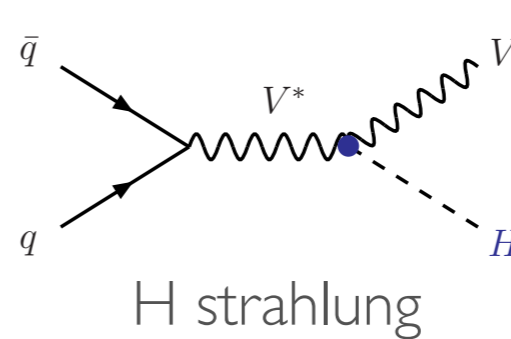
# Higgs production



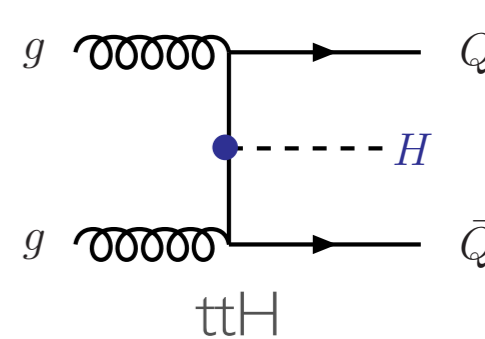
10 pb



0.96 pb

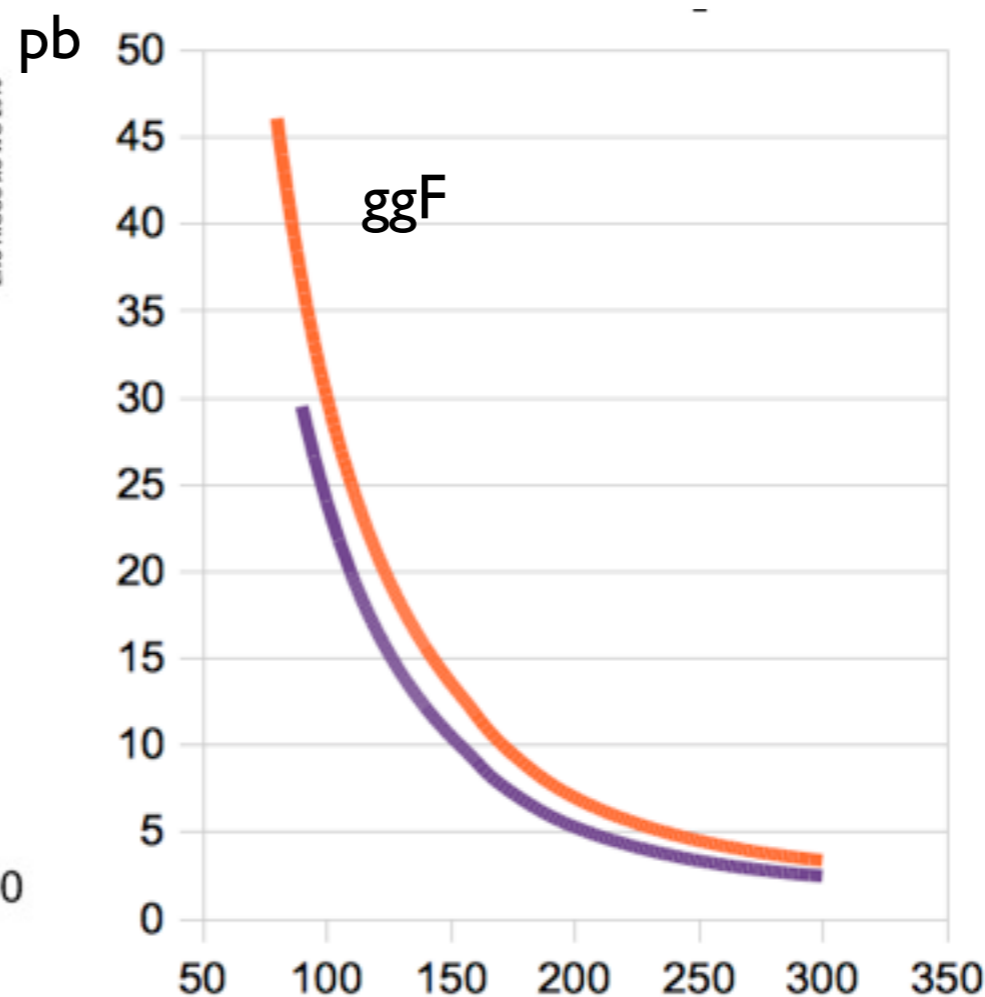
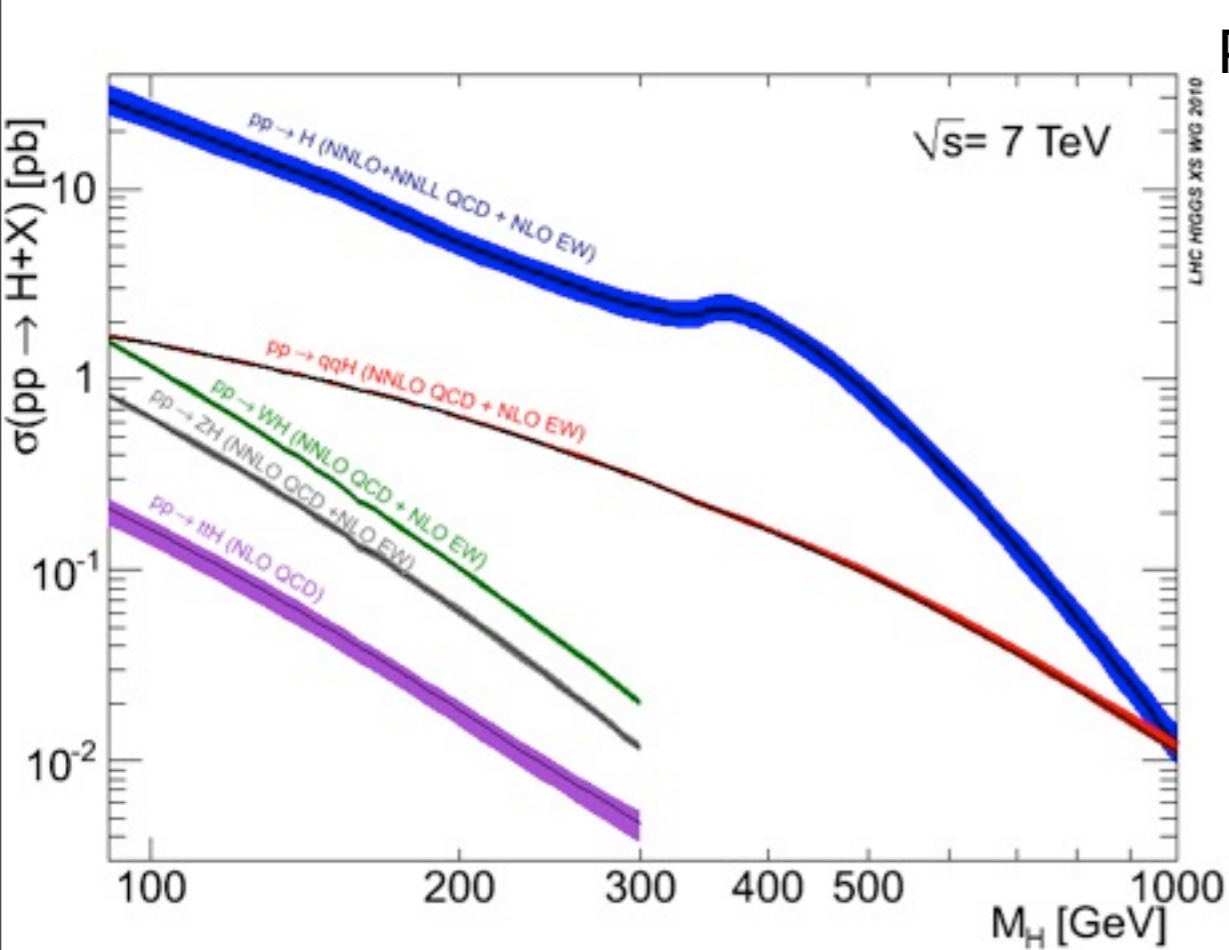


0.47 pb



0.05 pb

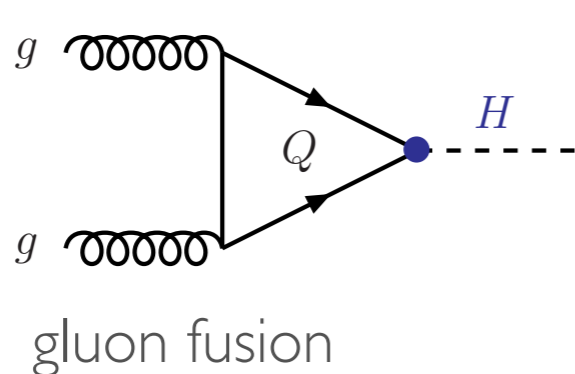
$\sigma$   
( $m_H = 150$  GeV)



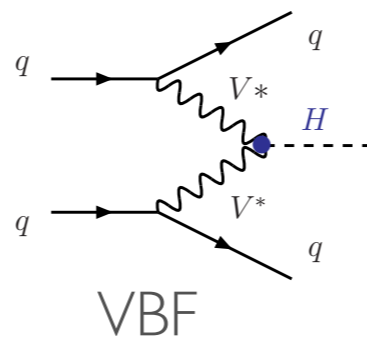
NNLO+NNLL  
+EW corrections  
dFG (De Florian,  
Grazzini)



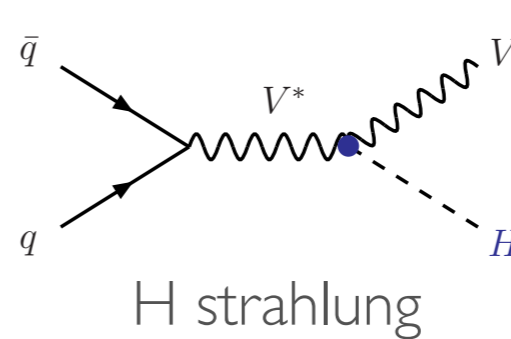
# Higgs production



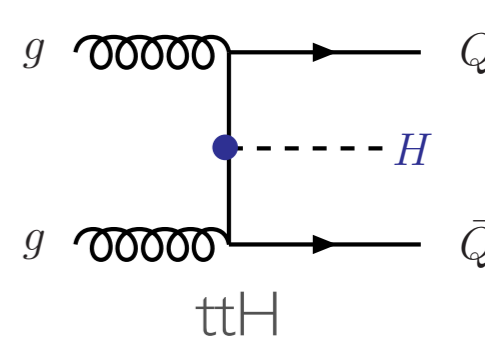
10 pb



0.96 pb

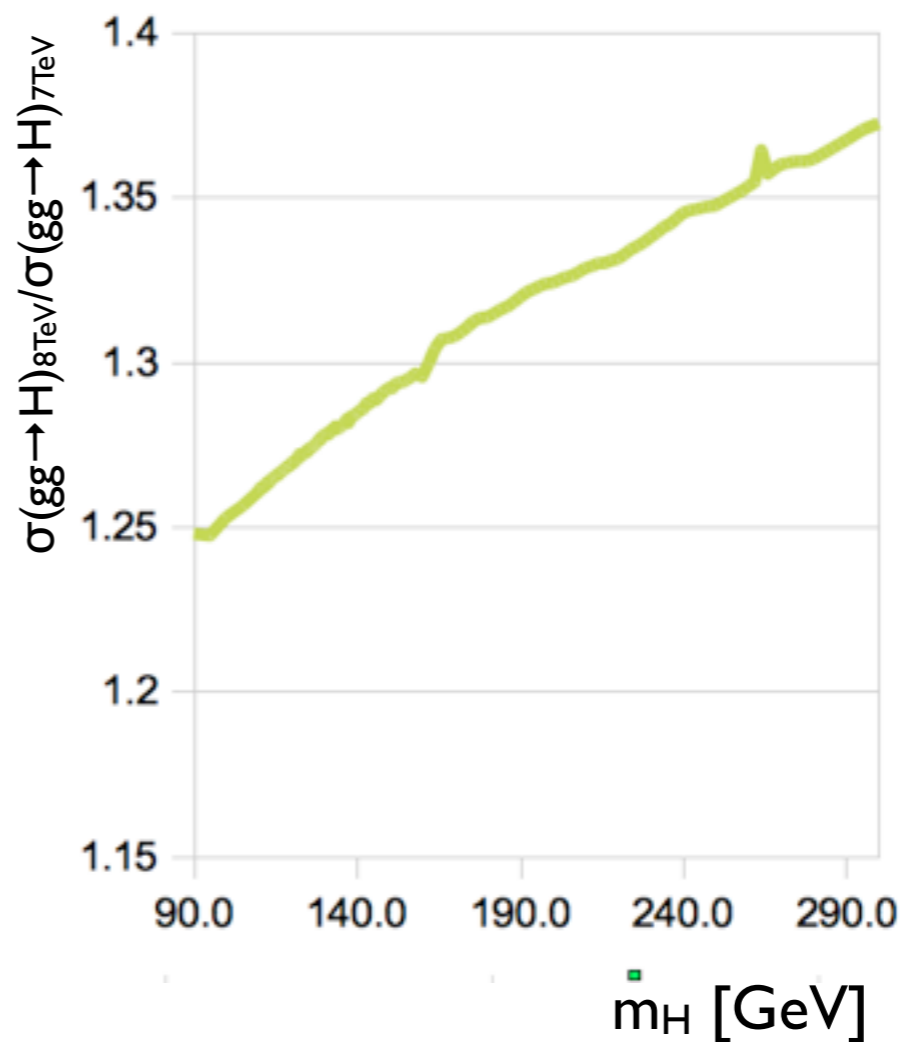
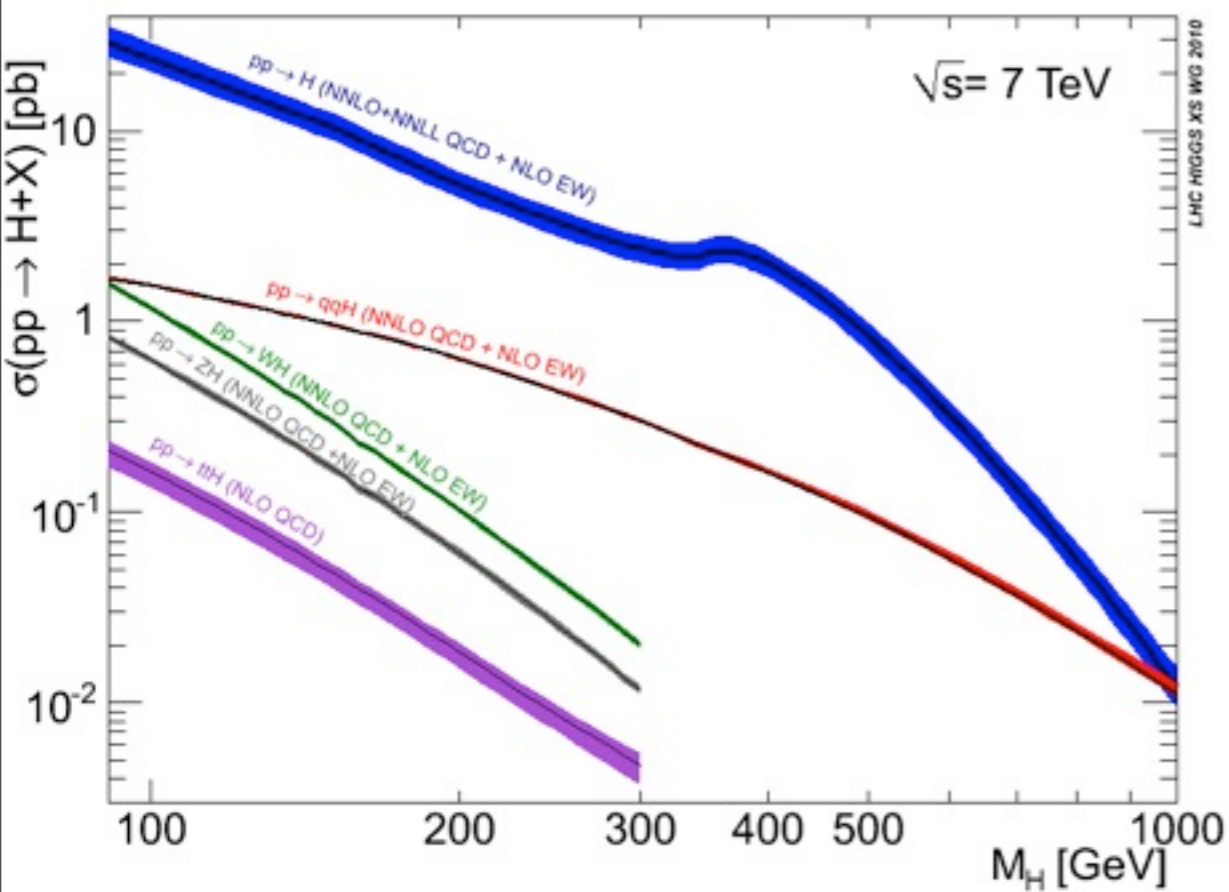


0.47 pb



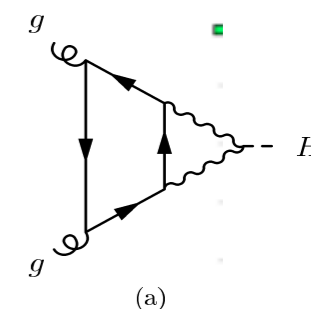
0.05 pb

$\sigma$   
( $m_H = 150$  GeV)



NNLO+NNLL  
+NLO EW  
corrections

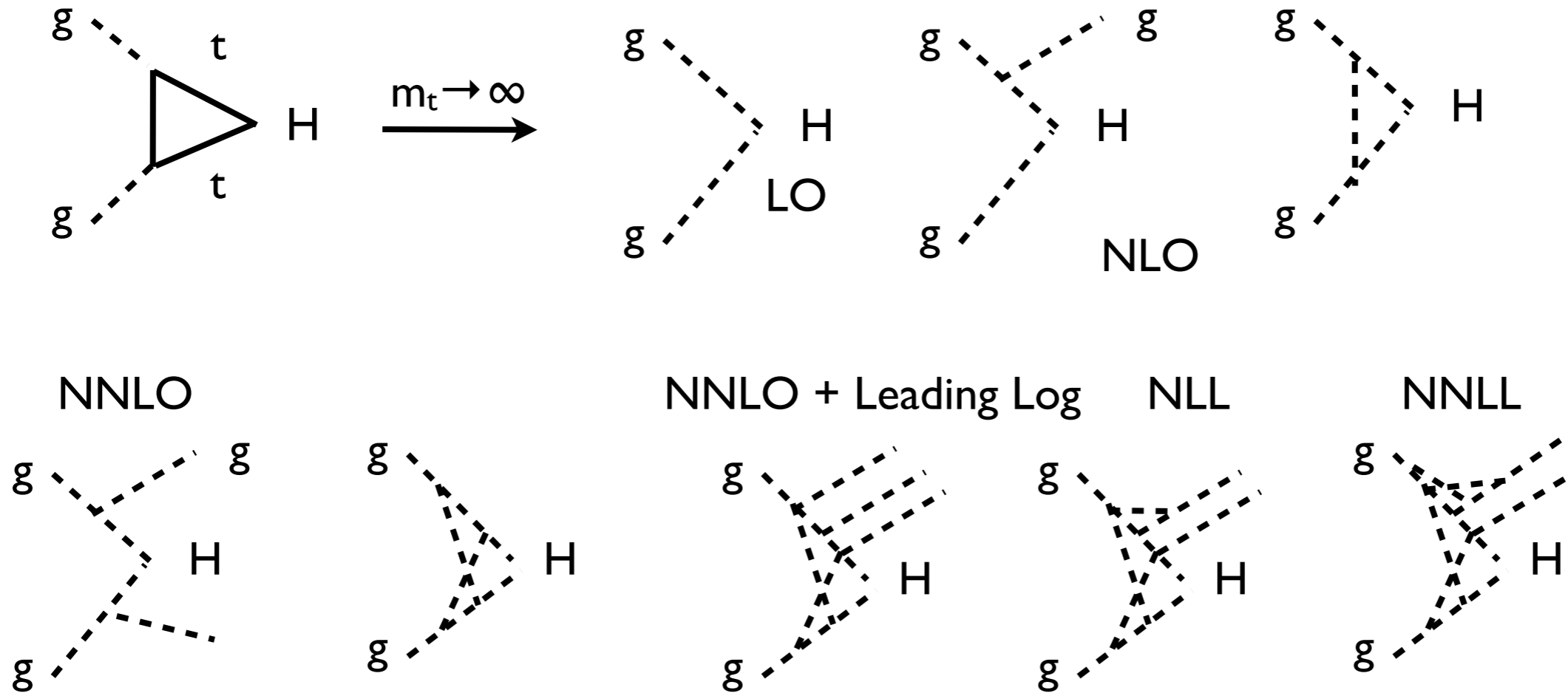
light quark contribution at  
2 loops.



U. Aglietti,  
R. Bonciani,  
G. De Grassi,  
A. Vicini

# Finite quark effects and $N^k$ Leading log resummation

H couplings to fermions is proportional to  $m_f$ , top contributions dominates.  
In the limit  $m_t \rightarrow \infty$



Resummation in practice means to sum up all particle irreducible diagrams at LO, NLO or NNLO (LL, NLL, NNLL) in soft and collinear approximation. The LL case is performed by the parton showers. Observables like inclusive cross sections and differential distributions can be evaluated applying resummation techniques.

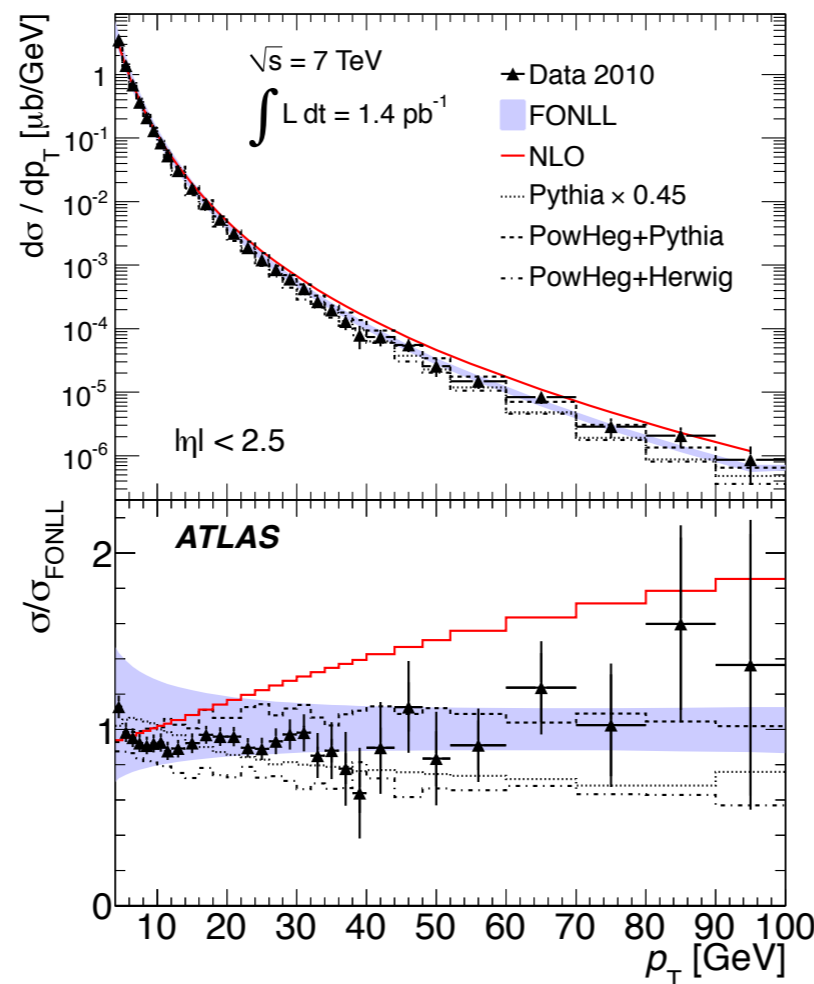
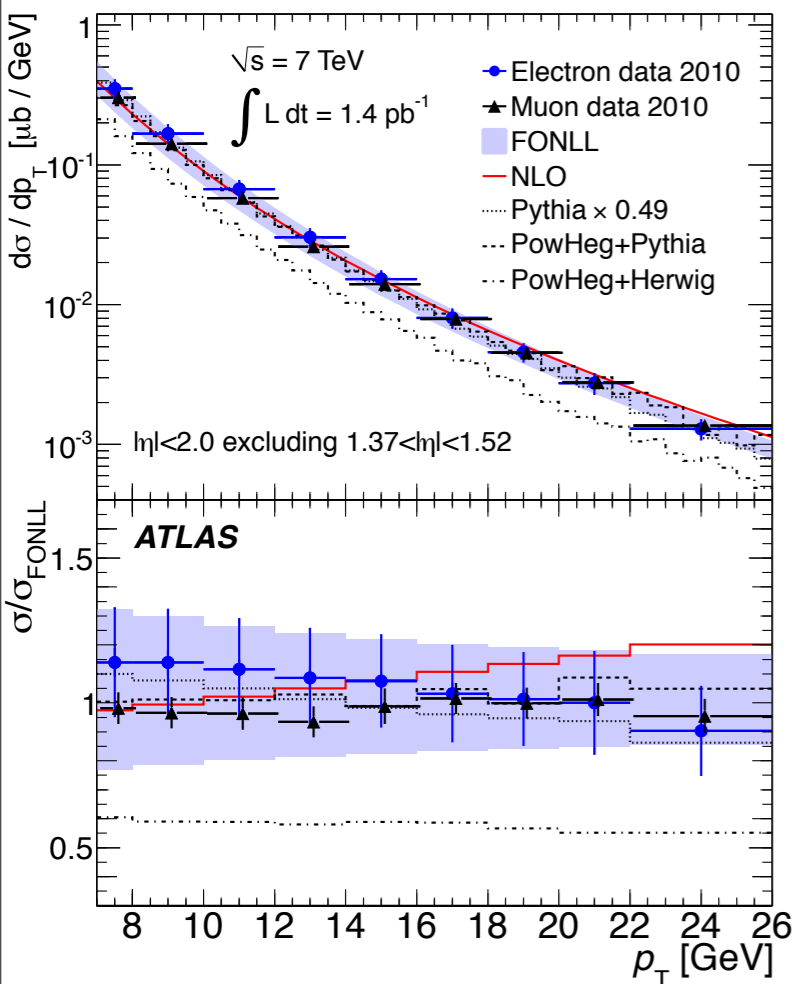
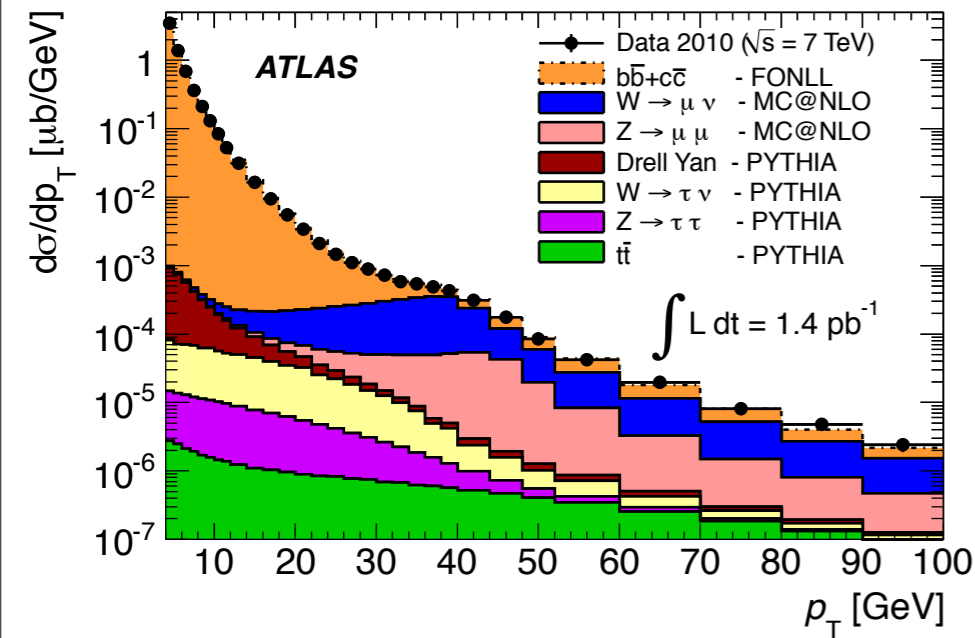
# Resummation at work.

- Inclusive cross section compared with MC@NLO and FONLL predictions;

- W/Z contribution subtracted at cross section level with MC@NLO;

- $$\sigma_{\text{HF}}^{\mu} = 0.818 \pm 0.003_{\text{stat.}} \pm 0.045_{\text{syst.}} \mu\text{b}$$

$$\sigma_{\text{FONLL}} = 0.840^{+0.158}_{-0.103} \mu\text{b}$$



- Agreement of the FONLL prediction over six order of magnitudes;

- Large deviation between the NLO computation and NLO+NLL at high pT;

- First direct observation of the NLL contribution to the heavy quark production cross section.

8 10 15 14 16 18 20 22 24 26  
[GeV] p<sub>T</sub>

7 10 50 30 40 20 60 80 90 100  
[GeV] p<sub>T</sub>

# The factorisation theorem.

Cross section in hh collision are evaluated according to the formula:

$$\frac{d\sigma}{dy dp_T^2}(y, p_T, m_H, s) = \sum_{a_1, a_2} \int_0^1 dx_1 \int_0^1 dx_2 f_{a_1/h_1}(x_1, \mu_F^2) f_{a_2/h_2}(x_2, \mu_F^2) \times \frac{d\hat{\sigma}_{a_1 a_2}}{d\hat{y} dp_T^2}(\hat{y}, p_T, m_H, \hat{s}; \alpha_S(\mu_R^2), \mu_R^2, \mu_F^2),$$

factorisation scale

pdf momentum fraction of the partons inside the proton

renormalisation scale

$$\hat{y} = y - \frac{1}{2} \ln \frac{x_1}{x_2}, \quad \hat{s} = x_1 x_2 s.$$

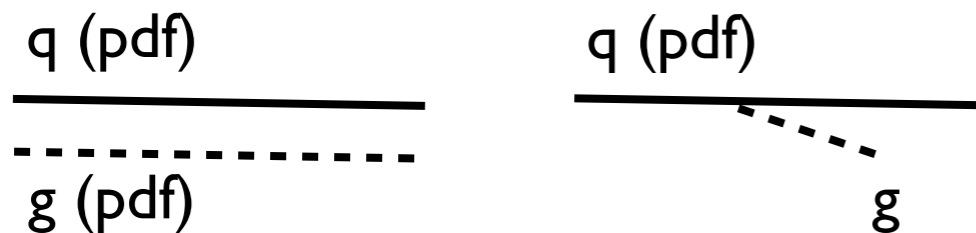
Renormalisation scale is needed to compute  $\alpha_s$  that shows an arbitrary scale dependence when computed at fixed order.

Factorisation scale: we have to decide what to put in the pdf, and what in the ME

roughly  $p_T^g < \mu_F$  pdf, otherwise take q pdf and ME

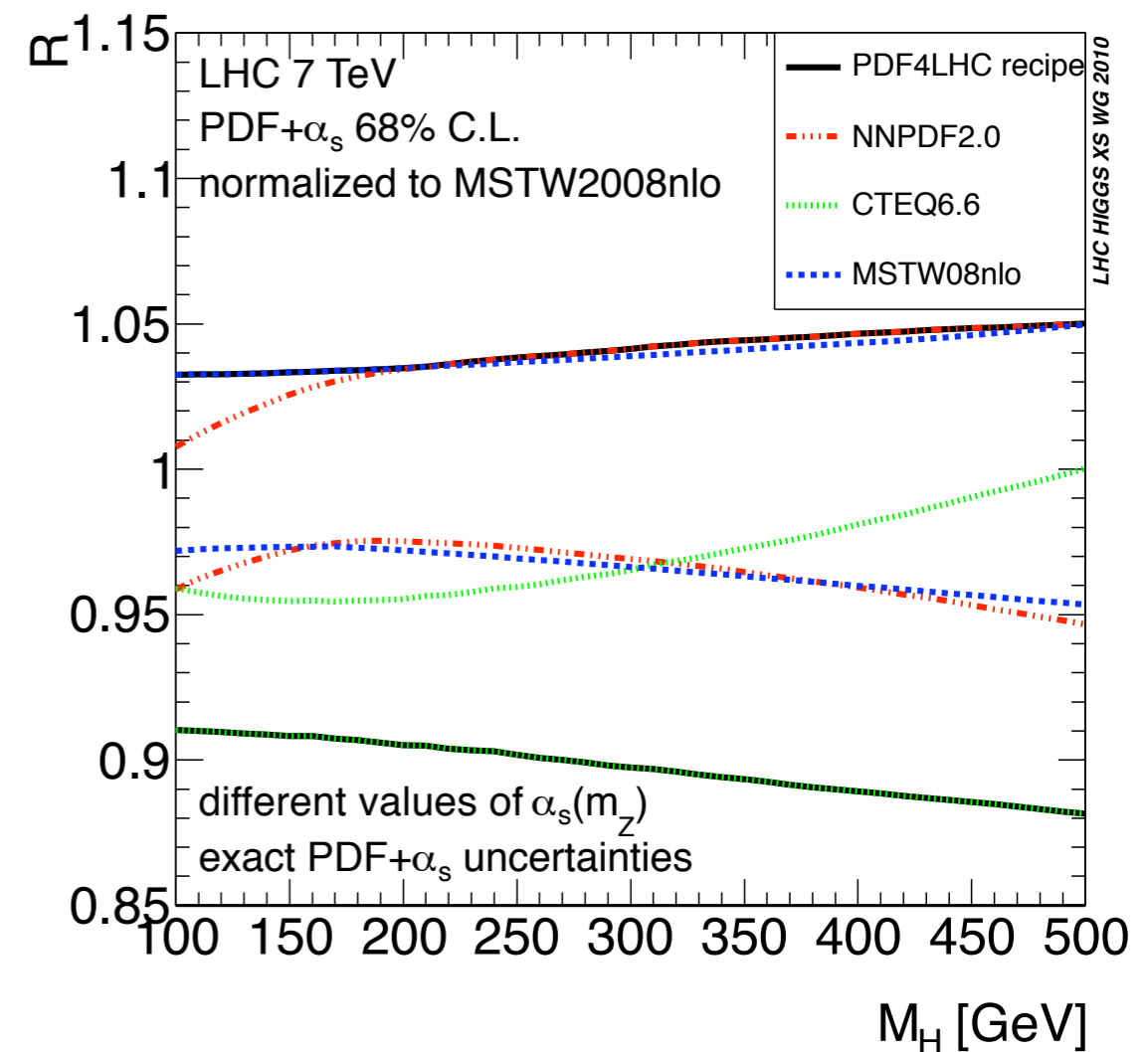
If we could sum up all order we could in principle cancel out the  $\mu_F, \mu_R$  dependence.

Scale dependence of the results gives an estimate of the missing higher order contribution.



# Pdf uncertainty computation

- Pdf are determined by fitting pdf sensitive data in mainly from ep collision (HERA) and also in ppbar and pp collision;
- several pdf sets are available, corresponding to the physics observable used in the determination, the parametrisation used in the pdf description, the theoretical constrains imposed.
- Each set of pdf is provided at LO, NLO and NNLO (according to the order at which the observables are computed) with an error set (a full pdf varied collection, and a recipe to compute its error)
- Uncertainties are computed using the PDF4LHC recommendation, that consists in computing the envelop of the error band from CTEQ6.6, MSTW2008 and NNPDF2.1
- What pdf to chose: NLO for NLO generators, LO for LO and multi-leg generators, LO for parton shower.
- What experimentalist do.  
Generate using one pdf set, reweight to other pdf sets after production (reweighting effect respect full generation is “sometimes” checked. Quantities used for normalisation are instead taken with the full envelope error band.

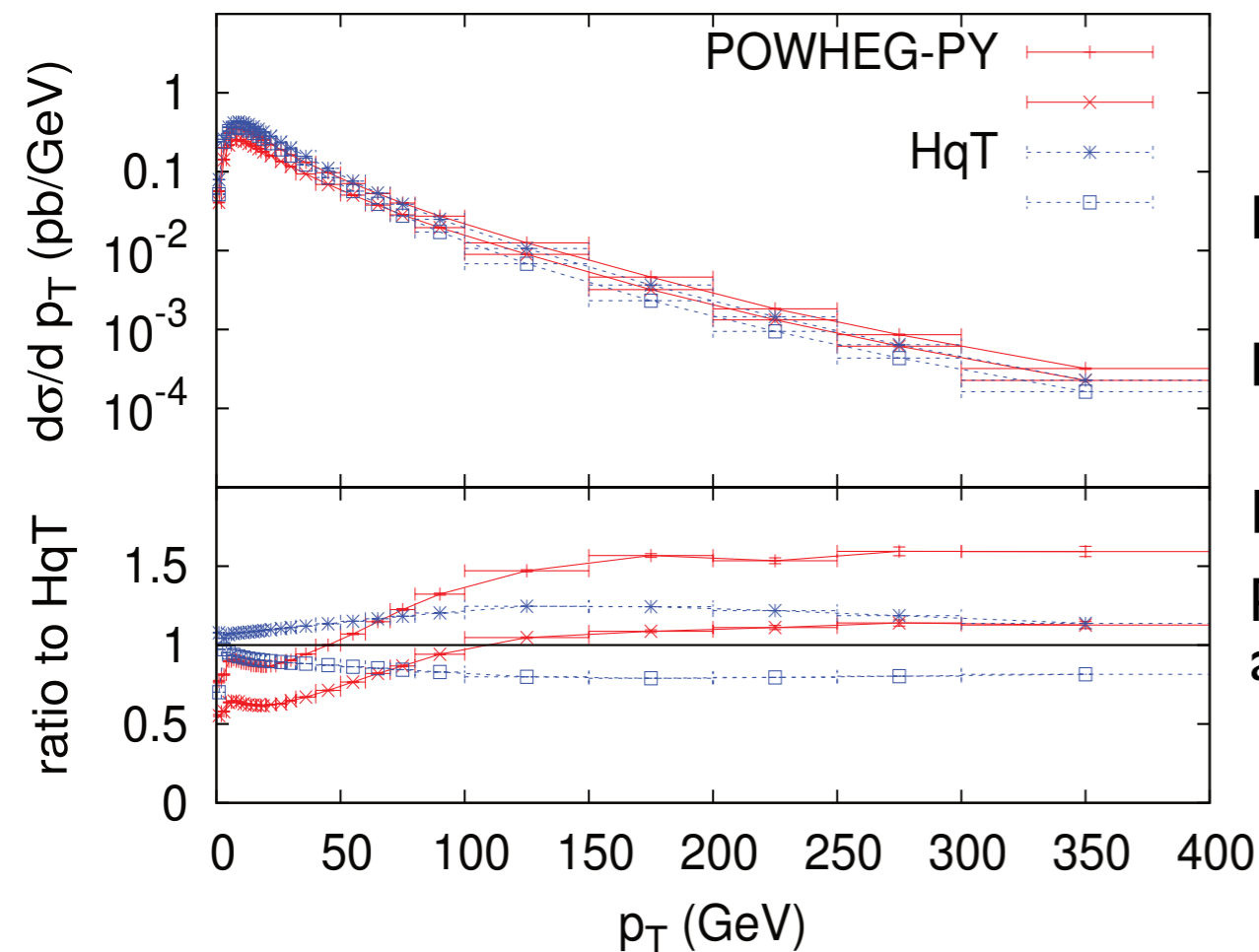
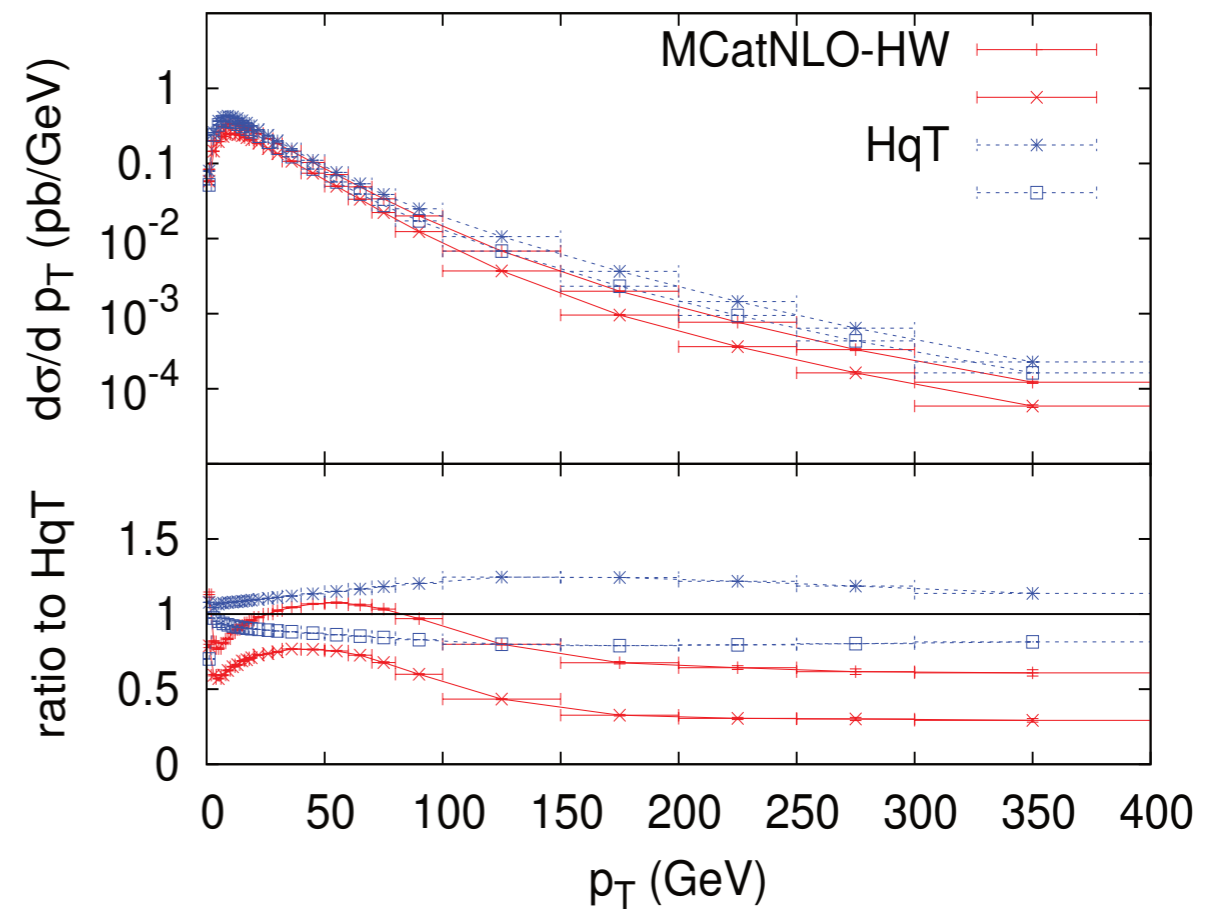


# Higgs $p_T$

Higgs  $p_T$  is  $\sim 0$  at LO (you need a gluon emission to balance the Higgs  $p_T$ ). In NLO MC like Powheg and MC@NLO it is different than zero. Parton shower even computes it at LL.

HqT2.0 evaluates it at NLO+NNLL, in the hard region a switch to the pure NNLO result is performed.

In the soft region Underlying Event effects become important. Comparison performed switching off the underlying events and the hadronisation.



MC@NLO spectrum is softer than HqT at high  $p_T$

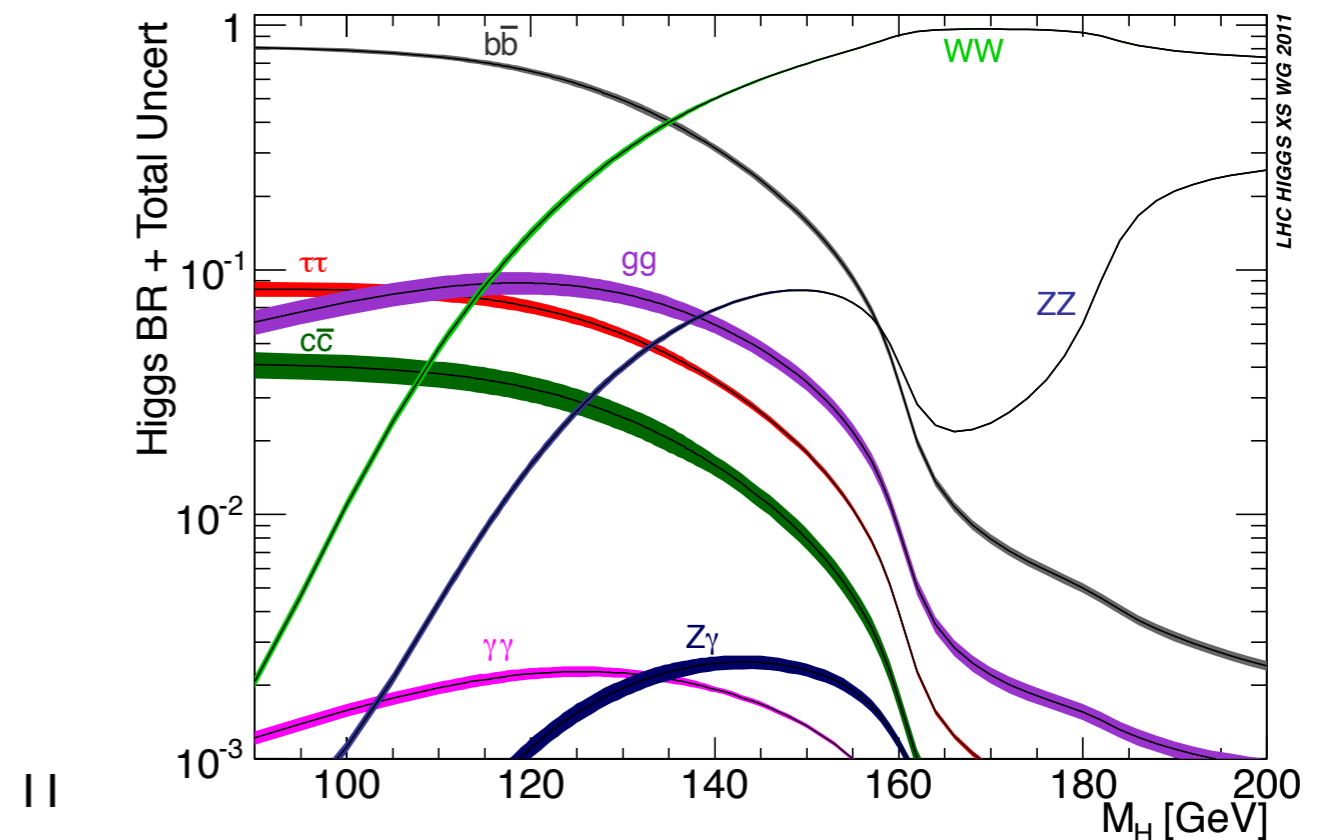
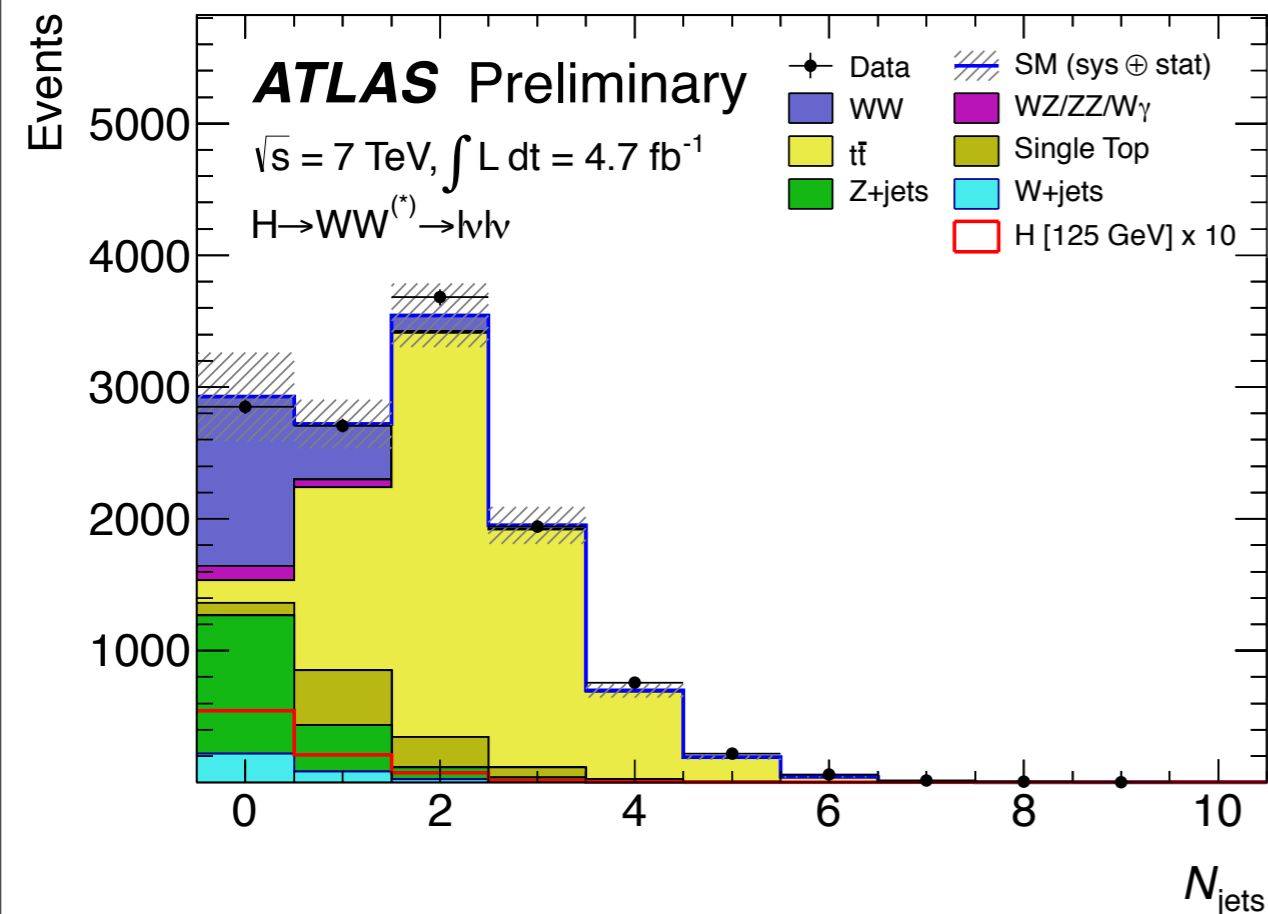
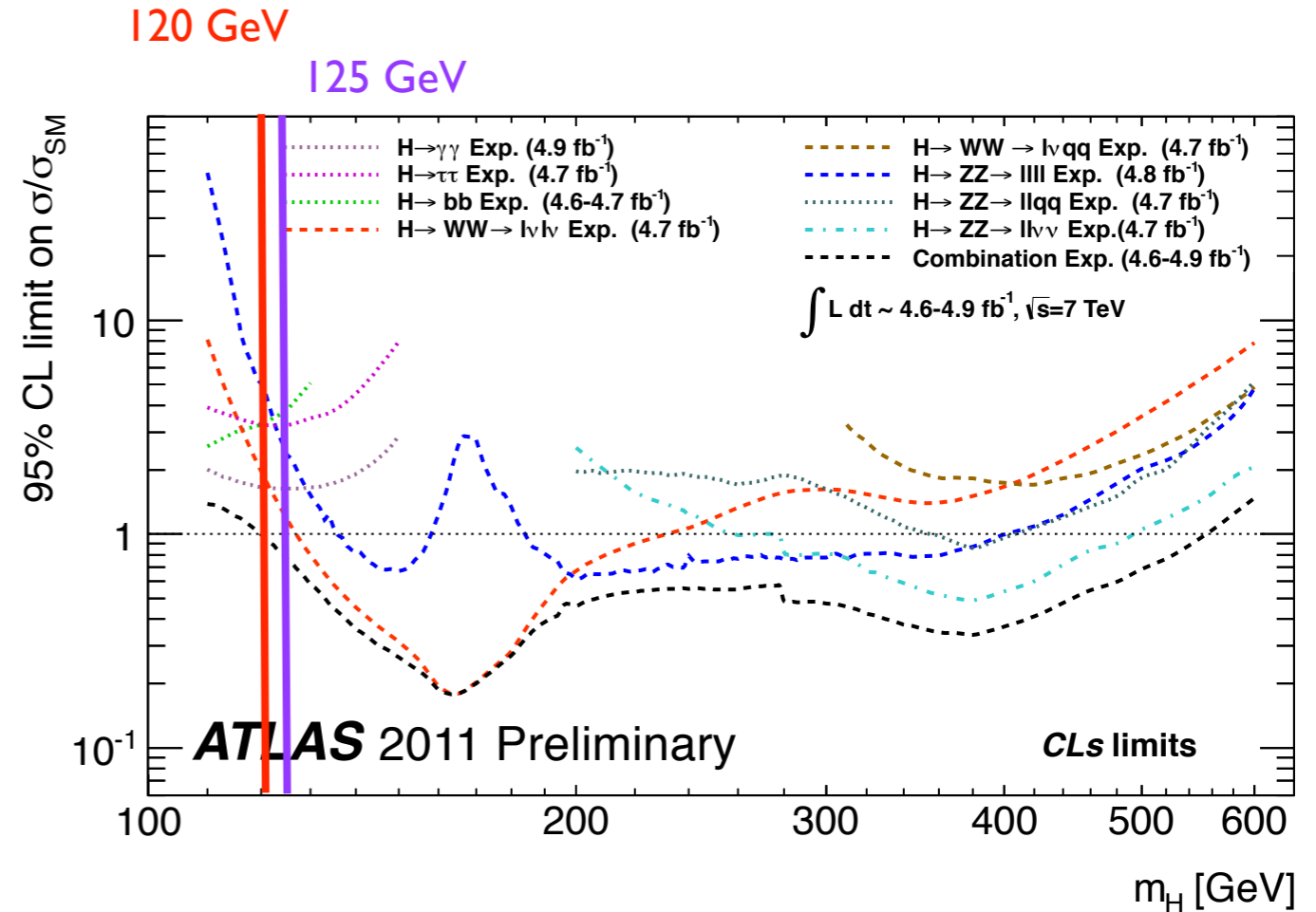
POWHEG + Pythia is harder than MC@NLO.

Reweighting (after!!) UE and hadronisation was performed up to now. This is in principle incorrect at very low  $p_T$ .

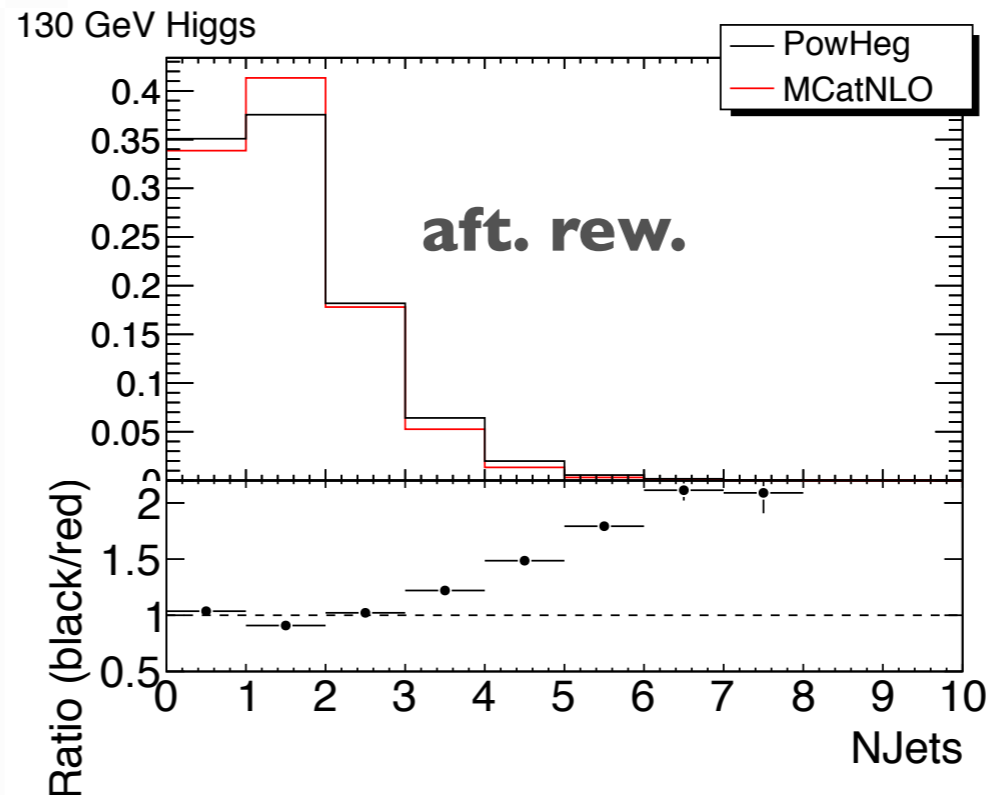
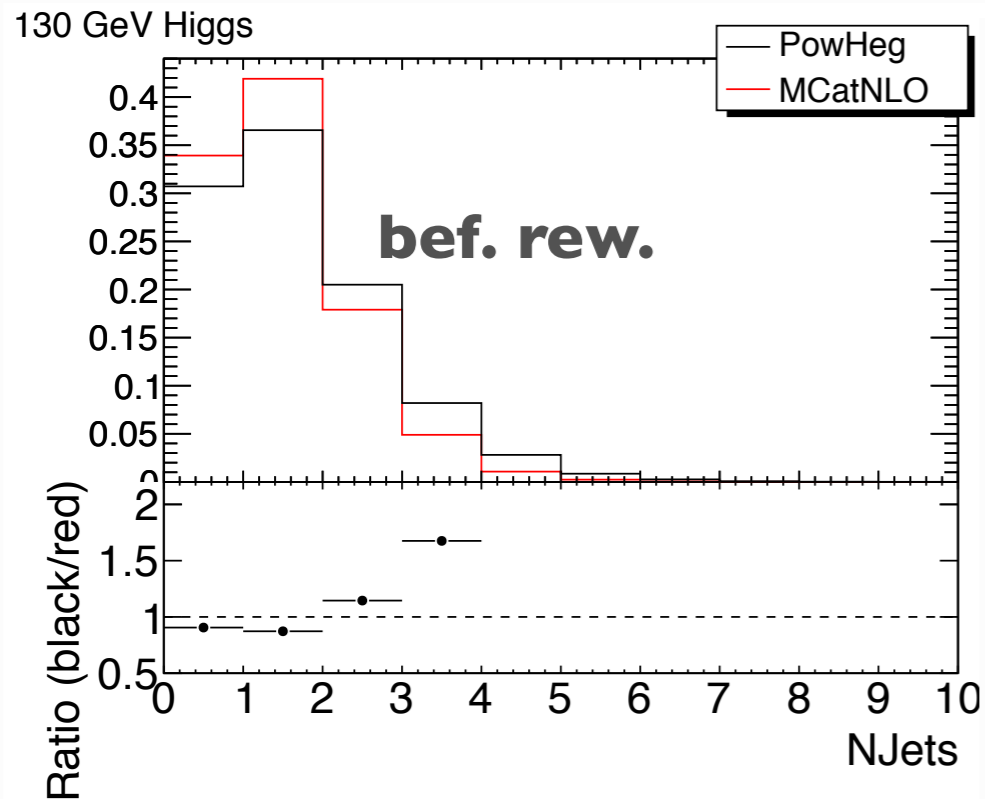


# Jets and the $H \rightarrow WW \rightarrow l\nu l\nu$ channel

- the  $l\nu l\nu$  final state is the most sensitive channel in the range
- needs to be performed in jet bins, to reject  $tt \rightarrow l\nu + N_{\text{jets}}, l\nu l\nu + 2_{\text{jets}} (+n_{\text{jets}})$
- most sensitive channel 0 jet and 1 jet bins
- QCD uncertainties on the background reduced by defined lepton based control regions in the same jet bin.



# Number of jets and Higgs $p_T$



reweighting to HqT2.0 improves the agreement between MC@NLO and Powheg (partially also due to the UE reweighting)

retuning of the showering and the hard component.

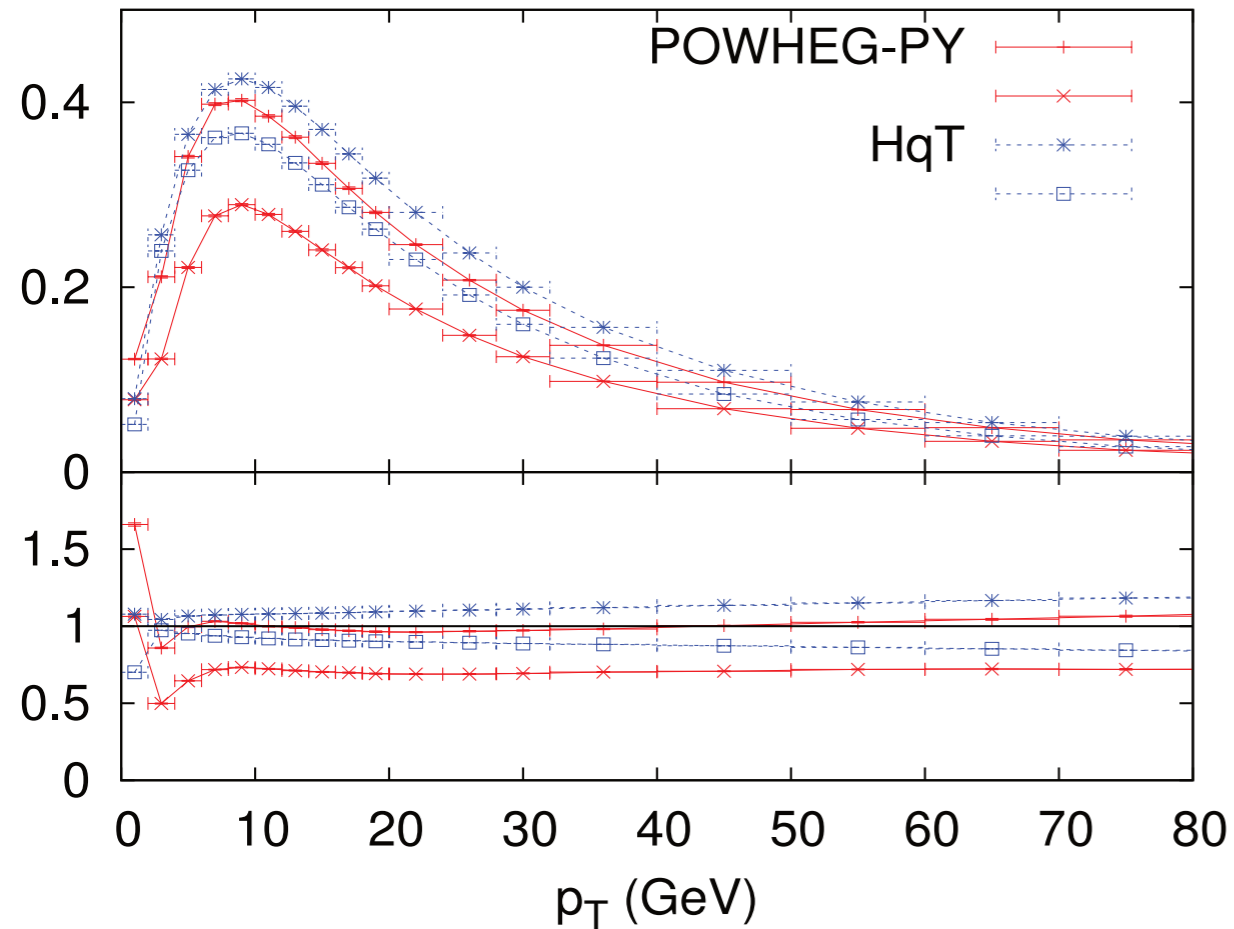
Sudakov contribution from Parton Shower

$$d\sigma^{\text{NLO+PS}} = d\Phi_B \bar{B}^s(\Phi_B) \left[ \Delta^s(p_\perp^{\min}) + d\Phi_{R|B} \frac{R^s(\Phi_R)}{B(\Phi_B)} \Delta^s(p_T(\Phi)) \right] + d\Phi_R R^f(\Phi_R),$$

$$\bar{B}^s = B(\Phi_B) + \left[ V(\Phi_B) + \int d\Phi_{R|B} R^s(\Phi_{R|B}) \right] \cdot \text{NLO hard scattering term.}$$

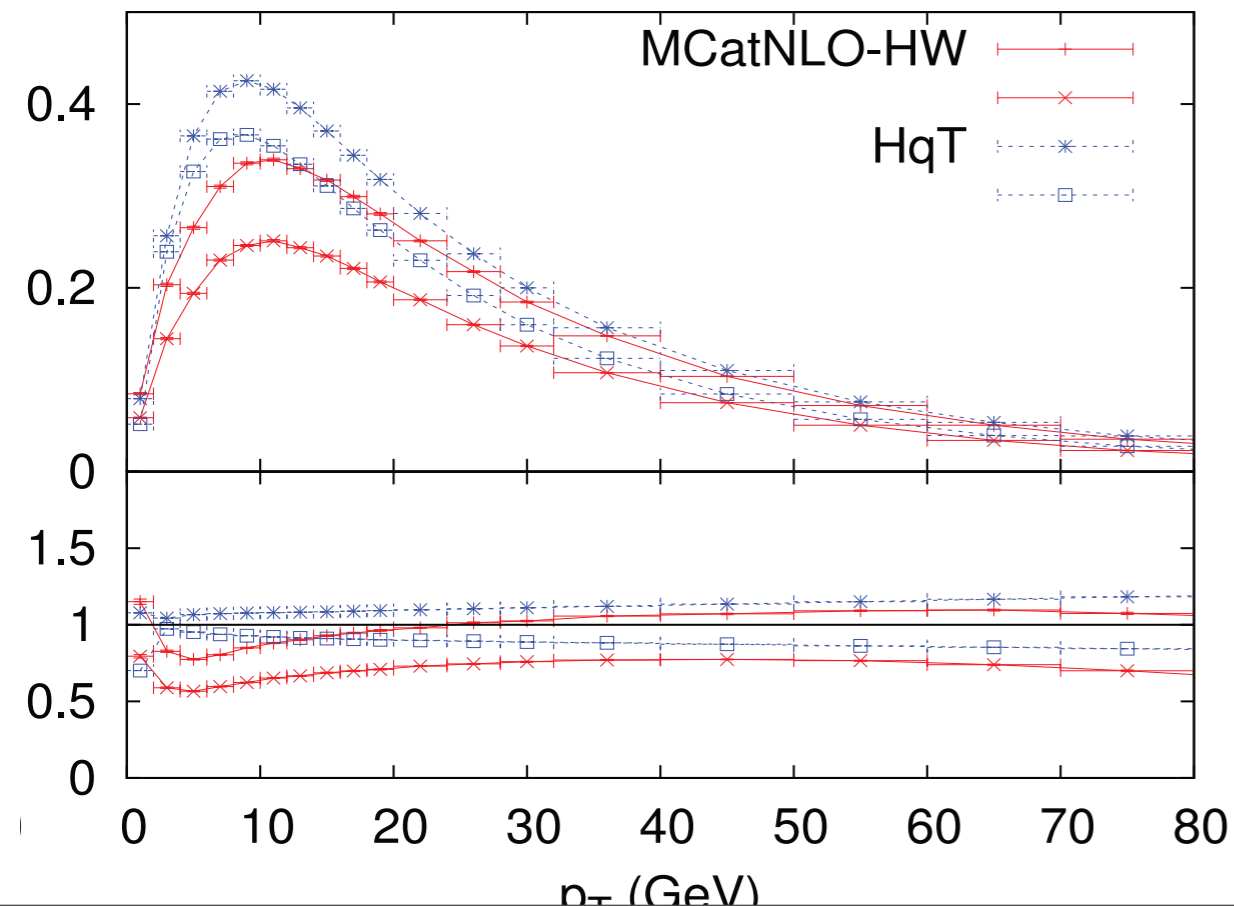


# Corrected $p_T$ distribution.



$h_{\text{fact}}=1.2$  reweighting still needed, but only at very low  $p_T$ .

Reweighting function needs to be evaluated switching off parton shower and hadronisation.



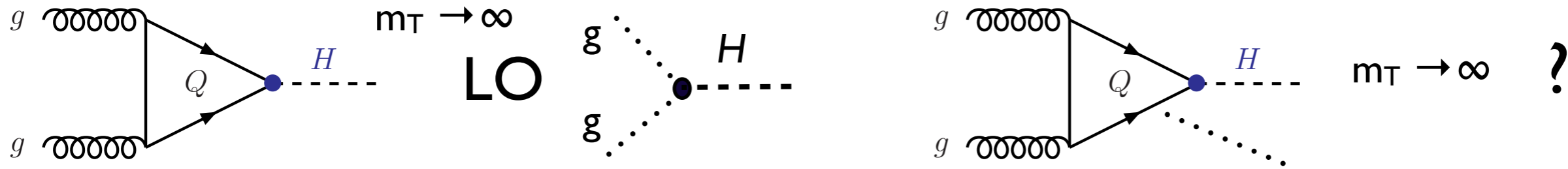
In MC@NLO + Herwig the difference can be recovered by setting the renormalisation and factorisation scale to:

$$\mu_R = \mu_F = m_H$$

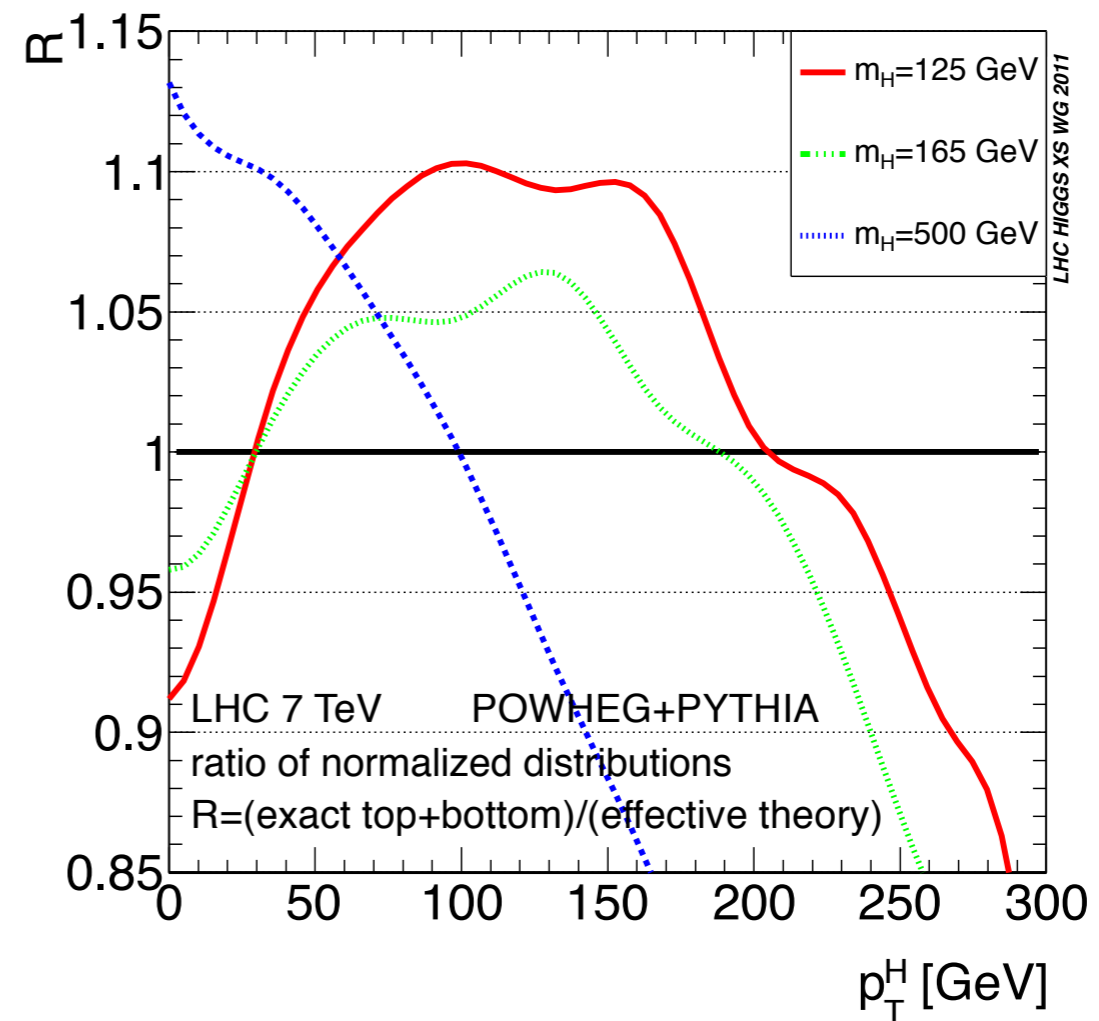
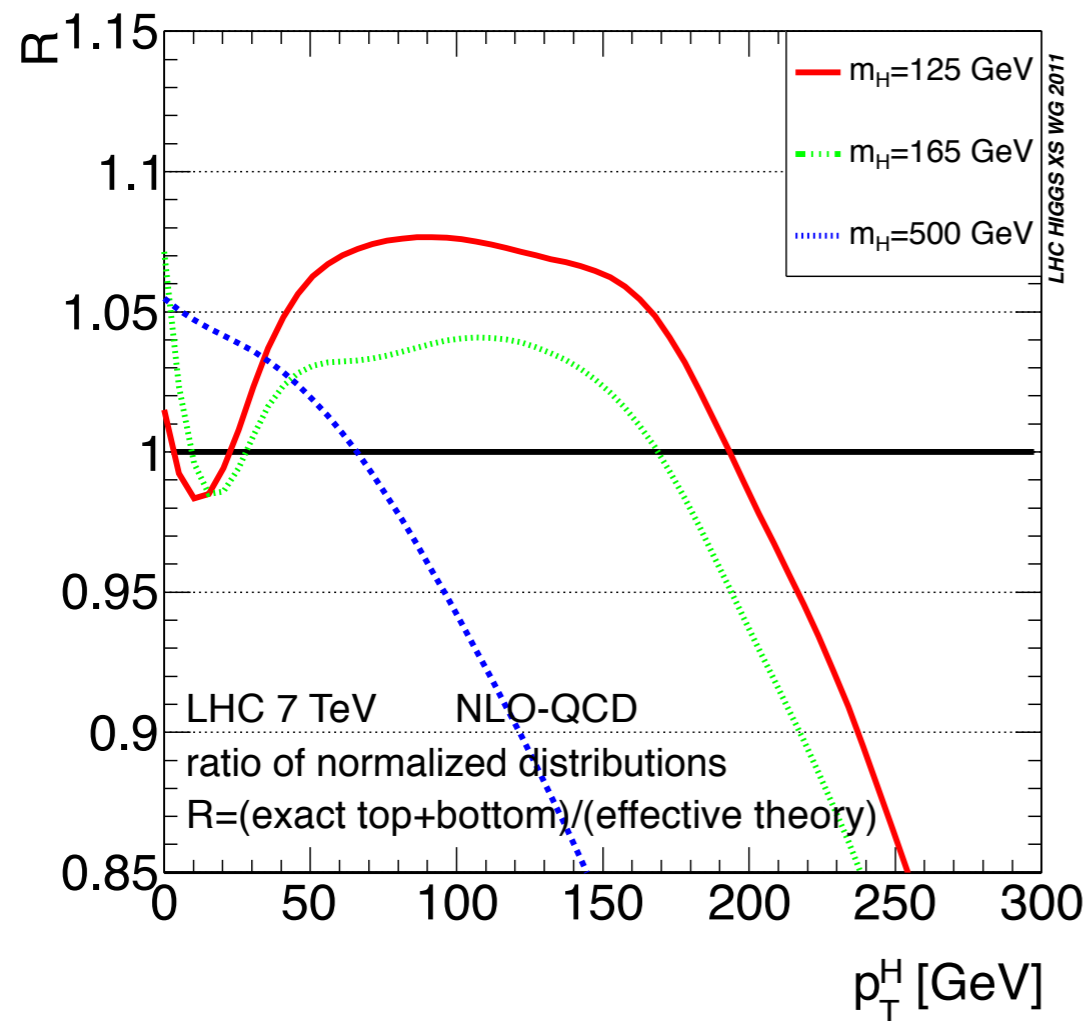
Instead of the dynamic scale:

$$\mu_R = \mu_F = \sqrt{p_T^2 + m_H^2}$$

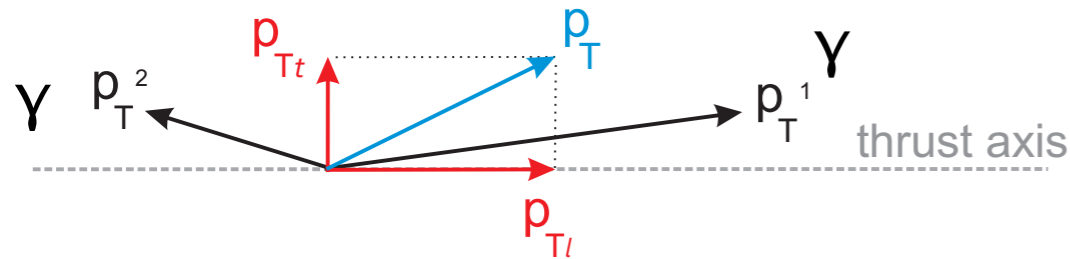
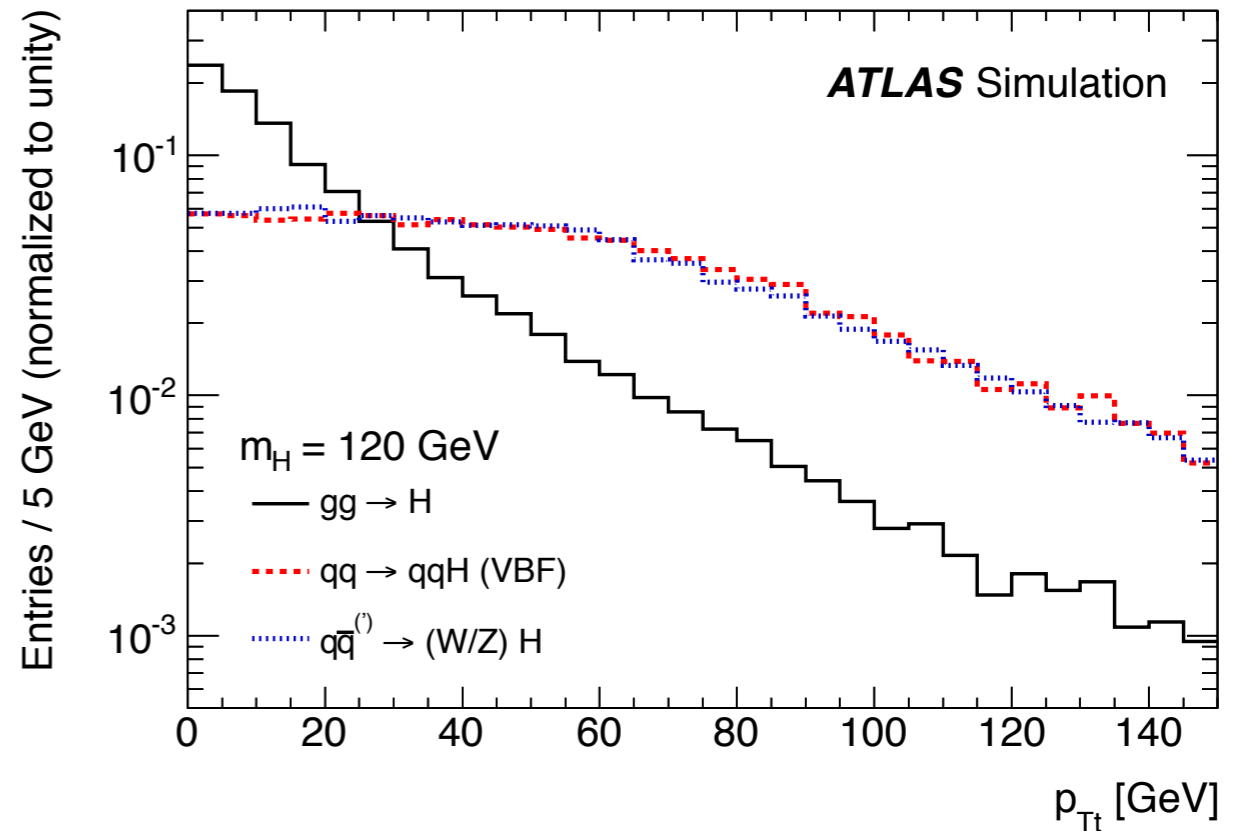
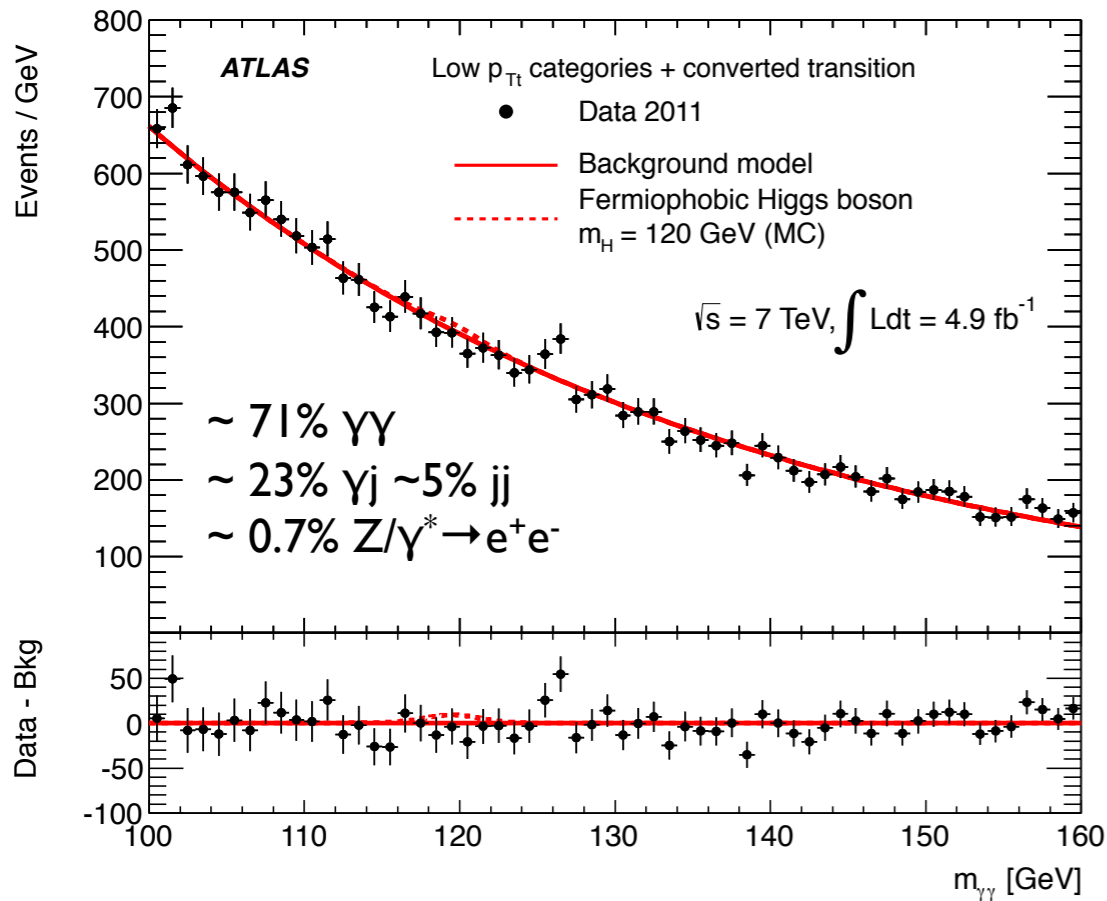
# Finite quark mass effects.



- Finite mass effect for the t and b quark have been implemented in POWHEG @NLO
- important contributions to the Higgs  $p_T$  distribution
- ATLAS MC production includes the HQ mass effect by Bagnasco, De Grassi, Vicini et al. (implemented up to 1 TeV)



# Relevance of Higgs $p_{Tt}$ and $H \rightarrow \gamma\gamma$

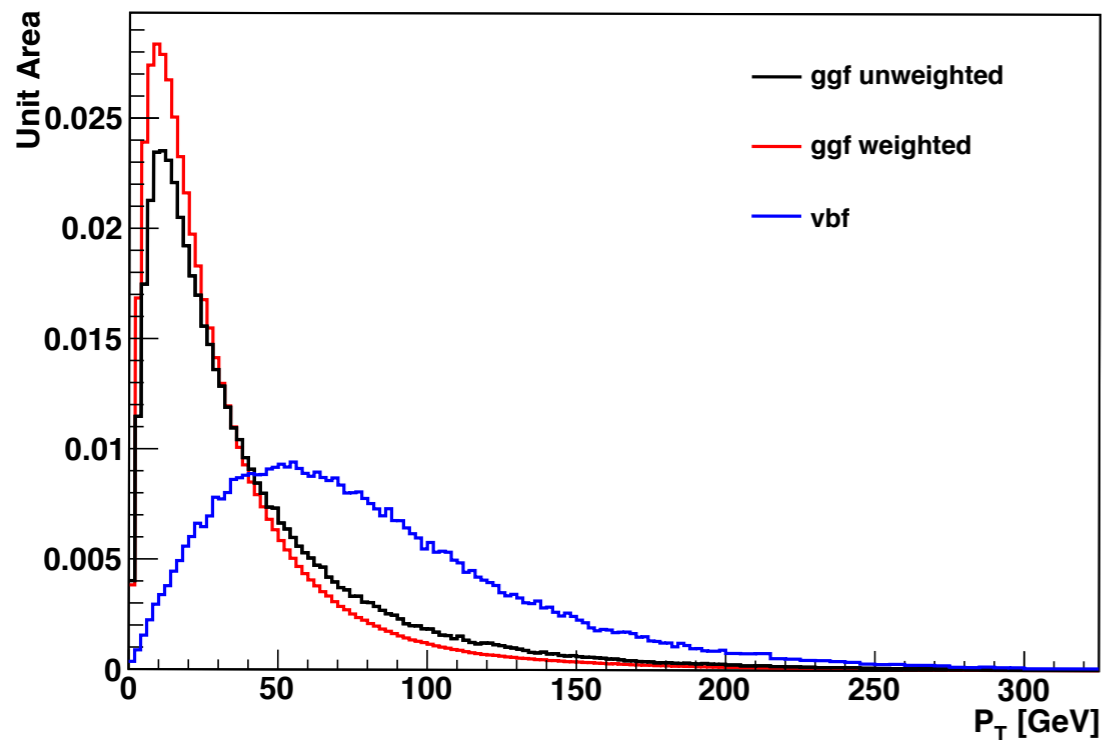


- Thrust axis is such that the 2 photons have equal transverse projections to itself.
- $P_{Tt}$  is the transverse projection of the total photon  $p_{Tt}$  on the thrust axis.
- Main advantages: it is more linked to the photon angle than to the photon energy ( $p_{Tt}$  is zero if the two photons are aligned) resulting in an improved resolution

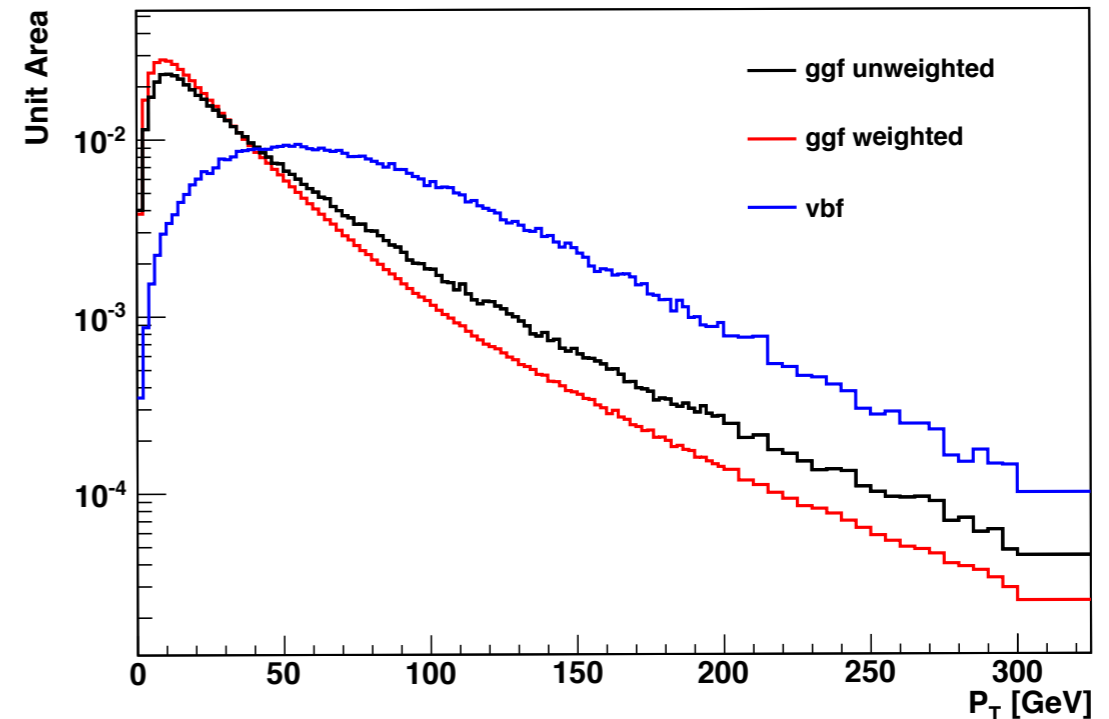
- In  $\gamma\gamma$  the background shape is assumed to be exponential, cuts in  $p_{Tt}$  have effects on  $\gamma\gamma$  background that induce distortion on the  $m_{\gamma\gamma}$  spectrum;
- to increase analysis sensitivity, the analysis is divided into 2 bins ( $p_{Tt} < 40$  GeV and  $p_{Tt} > 40$  GeV)
- the  $\gamma\gamma$  background populates mainly the low  $p_{Tt}$  category, analysis sensitivity improves of about 5%, 10%.
- uncertainties on Higgs  $p_T$  affect the migration between the high and low  $p_{Tt}$  categories, inducing an 8% uncertainty evaluated through scale (renormalisation, factorisation and resummation) and pdf variation.

# Reweighting to HqT2.0

125 GeV Higgs MC



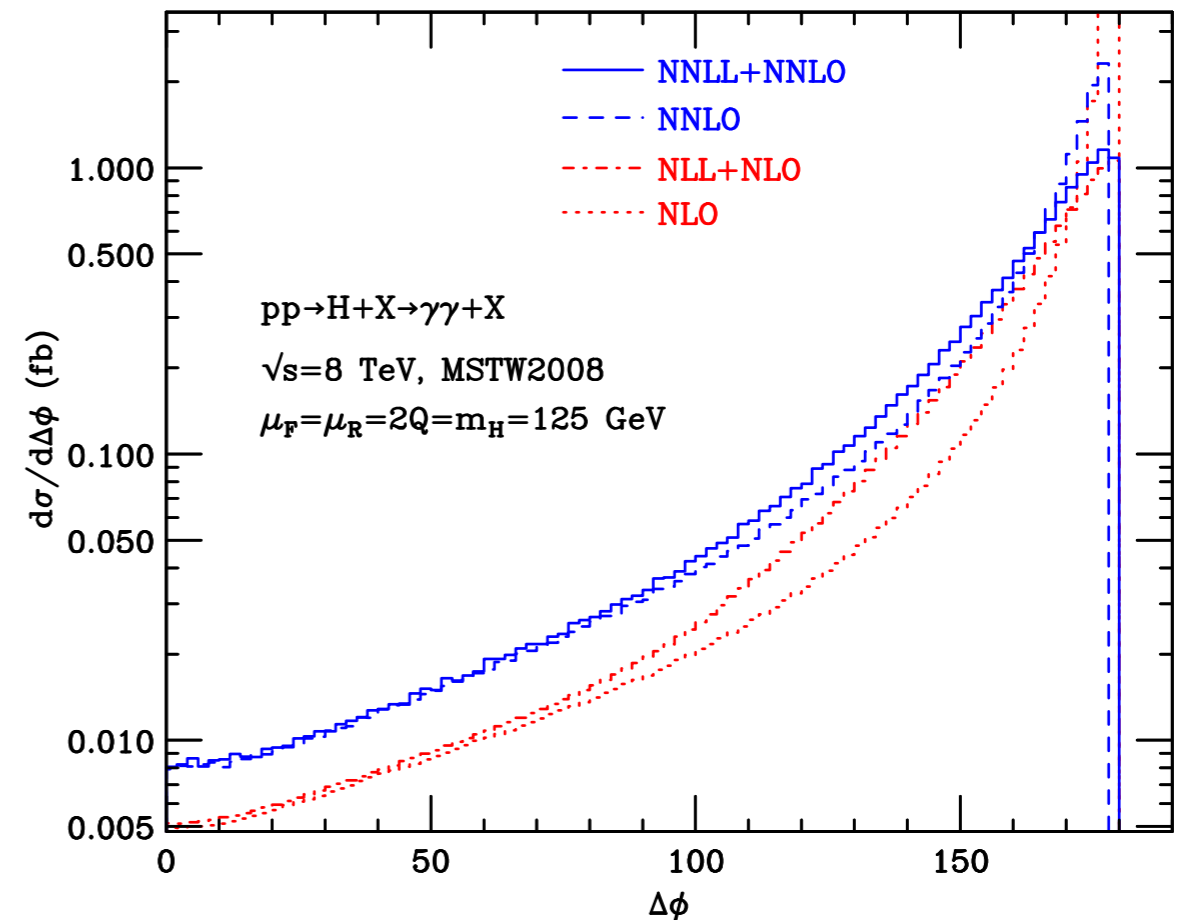
125 GeV Higgs MC



HqT2.0 allows the variation of the renormalisation, factorisation and resummation scale and pdf variation, uncertainties evaluated by reweighting Powheg Higgs  $p_T$  to different HqT2.0 and computing  $p_T > 40$  GeV acceptance systematics;

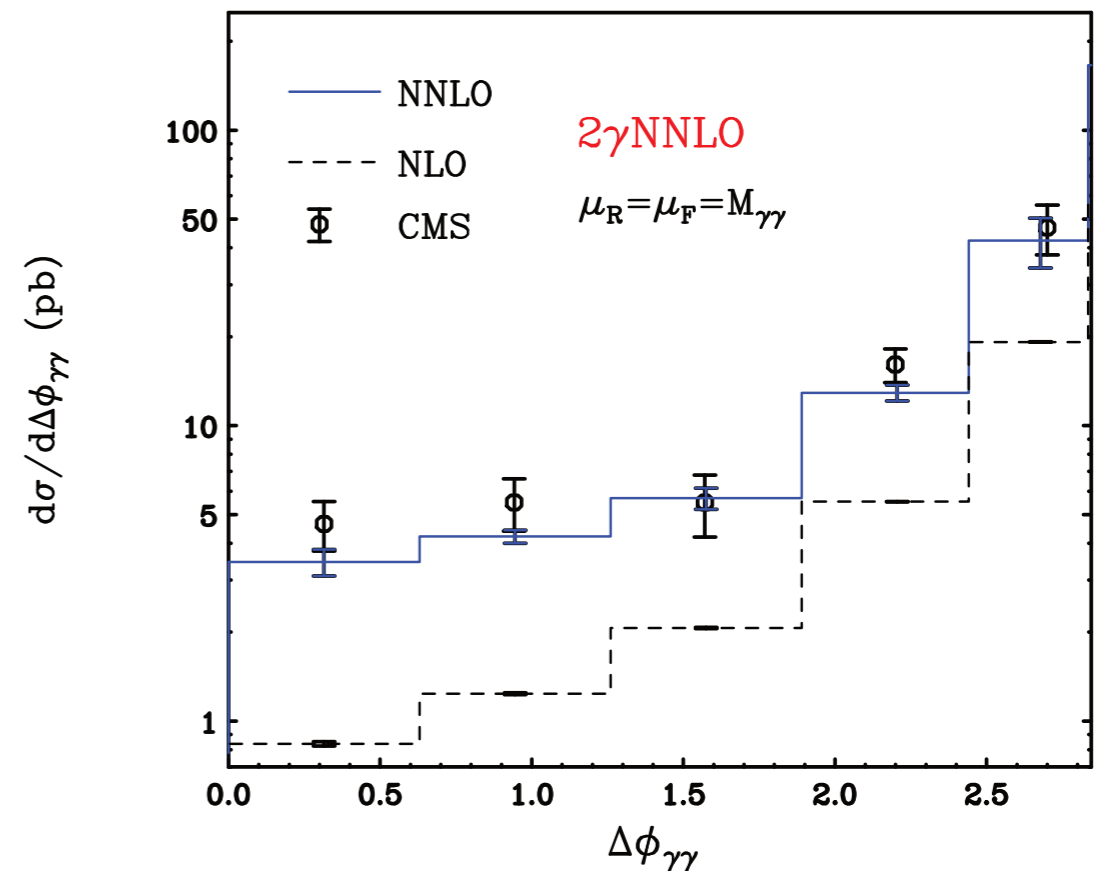
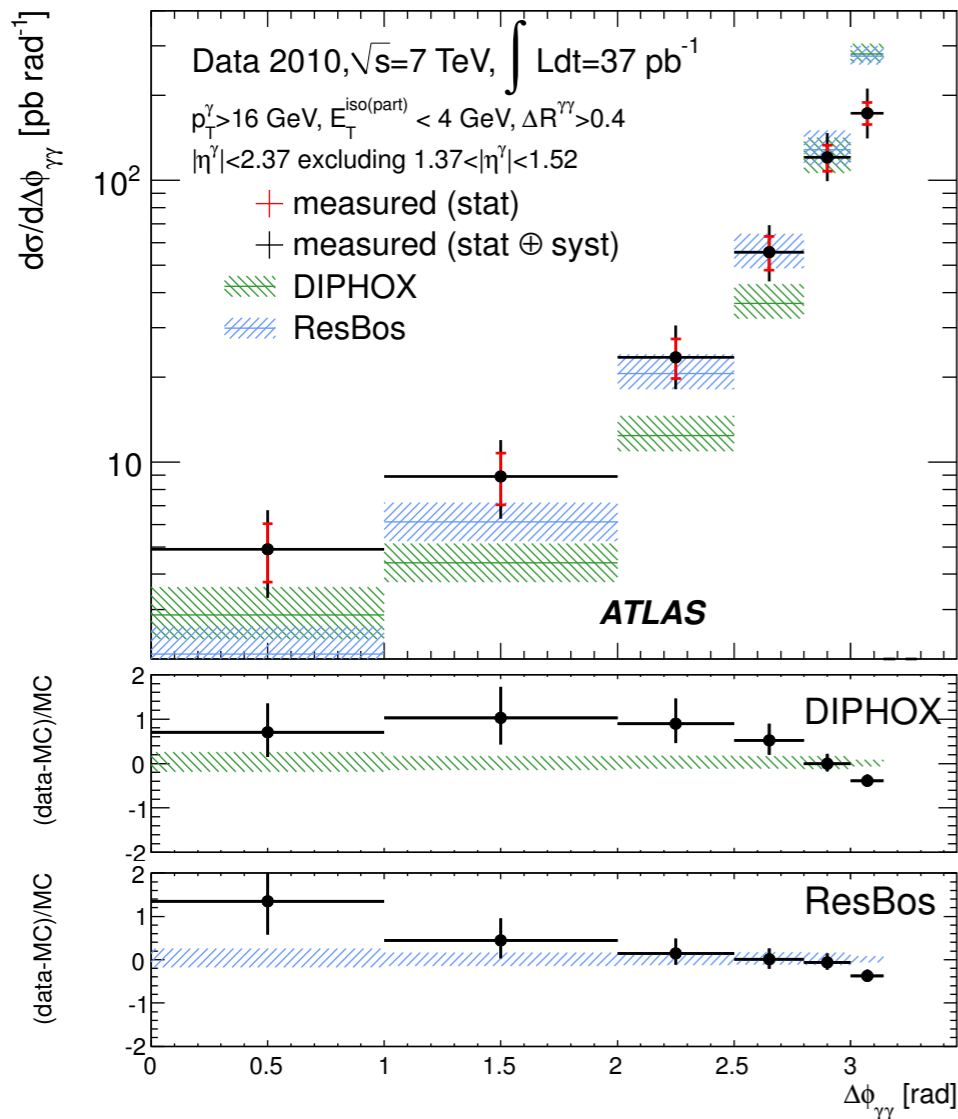
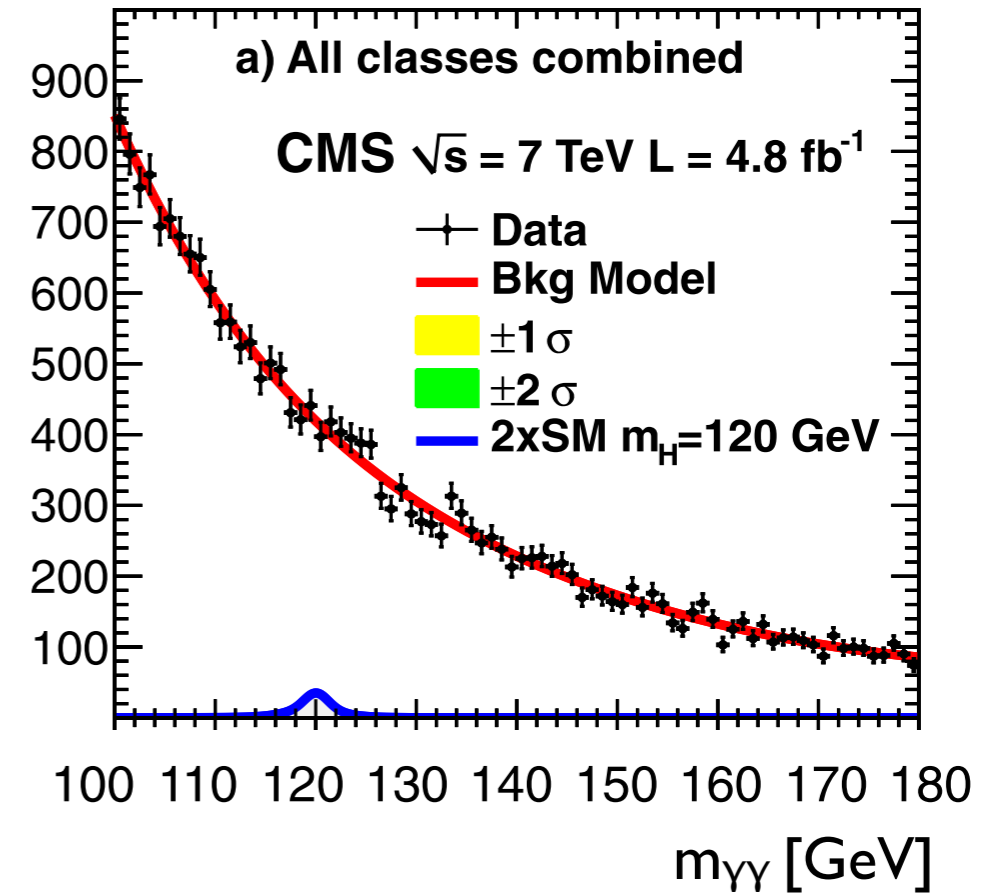
new tool recently available that computes all QCD inclusive observables @NNLO+NNLL (HRES)  
D. de Florian, G. Ferrera, M. Grazzini, D. Tommasini

We can think to normalise the signal yield in  $p_T$  categories preserving NNLO+NNLL accuracy.

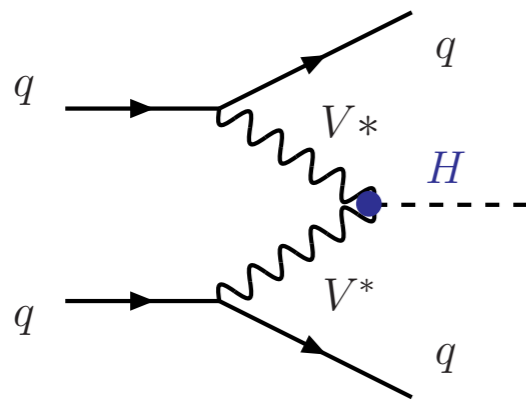


# Background description and spurious signal

- Both ATLAS and CMS use the full spectrum to parametrize the background;
- CMS uses a 5<sup>th</sup> degree polynomial to describe the background and shows that the bias is 5 times smaller than the statistical uncertainties of the fit and is ignored.
- ATLAS uses an exponential function and use RESBOS (NLO +NNLL) and DIPHOX. The bias is introduced as spurious signal in the fitting procedure allowing to reduce signal sensitivity for each probed mass point.



# The VBF selection and jet bin uncertainties



● A different way to exploit VBF topology is to select explicitly the jet topology of VBF events:

● 2 forward jets, with a large rapidity gap ( $\Delta\eta_{jj} \gg 0$ ) (3-3.2 is a typical cut)

● large invariant mass of the jet pair ( $m_{jj} > 400-500 \text{ GeV}$ )

● Jet cuts typically induce larger uncertainties due to the jet energy scale and extra energy in the jet cone introduced by the Underlying Event, anyway the S/B ratio is enhanced a lot by the VBF selection ( $\sim 0.1$  in standard analysis, 1 in VBF topology) with a significant reduction of the number of expected signal events going from  $\sim 50$  to  $\sim 2$ ).

Overall 10% extra sensitivity is gained in the VBF category.

● The VBF process is 0<sup>th</sup> power in  $\alpha_s$ , inducing small scale uncertainty ( $\sim 0.5\%$ ), PDF uncertainty are the dominant uncertainties on the total cross section ( $\sim 3\%$ )

In the VBF selection region we still have a sizable contamination from the ggF process: for  $m_H = 120 \text{ GeV}$  CMS expect 2.01 events from VBF and 0.76 from ggF, the error on the ggF contribution in 2 jet bin dominates the total error on the VBF selected events

# Jet bin uncertainties in the ggF production

The ggF production cross section has PDF uncertainties of  $\sim 8\%$ , scale uncertainties  $\sim 10\%$  (even if it is at NNLO+NNLL).

In several analyses, (in particular  $WW \rightarrow l\nu l\nu$ , CMS  $\gamma\gamma$ ) we divide the dataset in jet bins, this is needed to keep in different bins regions with different S/B ratio and signal yield. (maximise sensitivity against top contamination in  $WW$ , exploiting the VBF topology in CMS  $\gamma\gamma$ )

Jet binning introduces uncertainty due to the introduction of a further scale ( $p_T^{\text{cut}}$ ) in the problem.

Any observable can be expanded as a function of  $\alpha_s$ .

$f(\alpha_s) \sim a_0 + a_1\alpha_s + a_2\alpha_s^2 + \dots$       $\alpha_s$  is computed at a given scale  $\mu_{\text{ren}} \sim m_H, m_H/2 \dots$   
 if summed up to all order  $\mu_{\text{ren}}$  dependence cancels out.  
 residual dependence is taken as uncertainty.

What happens when we apply a  $p_T^{\text{cut}}$  on the jets

$$\sigma_0 = \sigma_{\text{total}} - \sigma_{\geq 1} = \sigma_B [1 - \alpha_s(L^2 + L)]$$

$$\sigma_{\text{total}} \simeq \sigma_B [1 + \alpha_s + \alpha_s^2 + \mathcal{O}(\alpha_s^3)] .$$

$$\sigma_{\geq 1}(p^{\text{cut}}) \simeq \sigma_B [\alpha_s(L^2 + L + 1) + \alpha_s^2(L^4 + L^3 + L^2 + L + 1) + \mathcal{O}(\alpha_s^3 L^6)]$$

$$L = \ln(p^{\text{cut}}/Q)$$

for particular  $p_T^{\text{cut}}$  values  $L^2+L \sim 0$   
 the cross section dependence from  $\mu_{\text{ren}}$  vanishes.

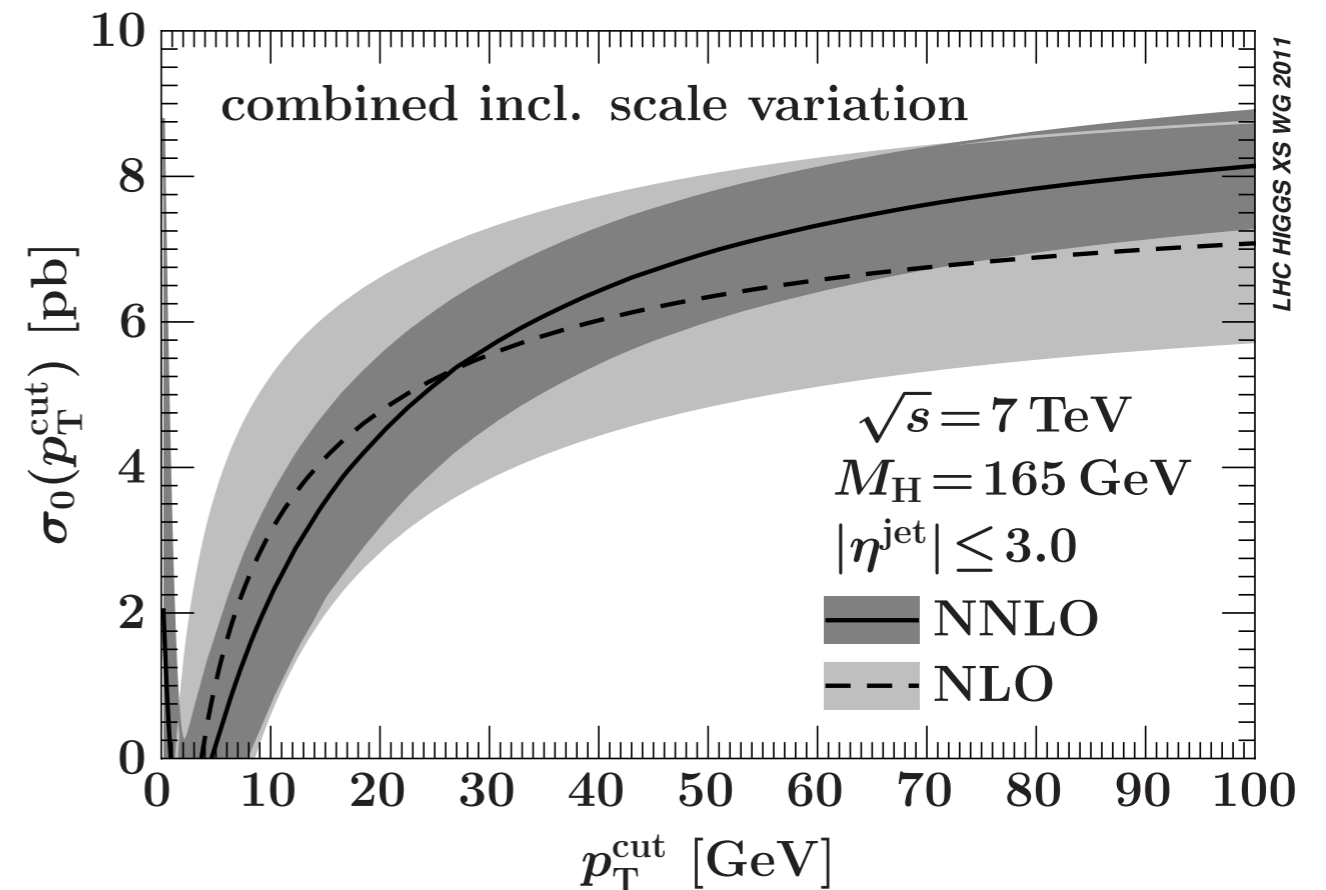
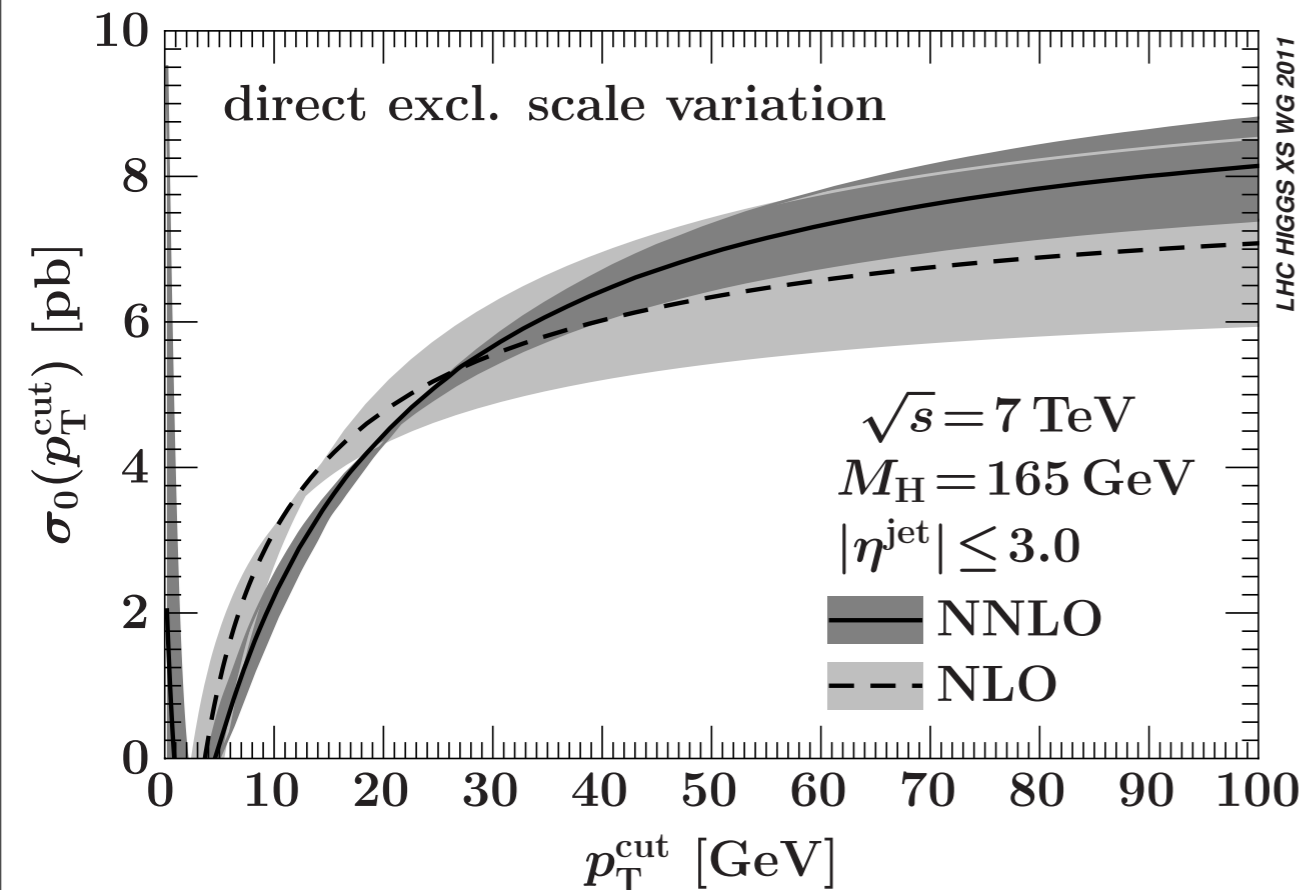
Scale variation is not anymore a reasonable estimate of higher order corrections effects.



# Stewart, Tackmann prescription (arXiv:1107.2117)

$$\sigma_0 = \sigma_{\text{total}} - \sigma_{\geq 1}$$

Evaluate the error on each contribution as independent, and propagate it to the exclusive binning. The uncertainty obtained covers also the Parton Shower uncertainty (that is included in the higher order terms).



The uncertainty are evaluated using HNNLO (S. Catani, M. Grazzini), that is full calculation at  $\mathcal{O}(\alpha_s^4)$   
 The uncertainty is around 20% in the 0 jet bin, increasing with the Higgs mass due to the higher contribution from the 1 jet inclusive.

The 1 jet exclusive is affected by large error (70%) on the 2 jet inclusive:

$$\sigma_1 = \sigma_{\geq 1} - \sigma_{\geq 2} \quad \sigma_{\geq 2} \text{ at } \alpha_s^4 \text{ is just the tree level (LO) contribution.}$$

There exist an  $\alpha_s^5$  calculation for the 2 jet bin included in MCFM (J. Campbell, K. Ellis, C. Williams) it is not used in  $\sigma_1$  otherwise we break the  $\alpha_s$  expansion ( $\alpha_s^5$  terms in  $\sigma_{\geq 1}$  are unknown).



# Cross check by G.P. Salam et al.

- Different schemes for the jet veto at fixed order in  $\alpha_s$  have been compared;
- The three schemes differ for NNNLO terms (therefore difference among the schemes take into account higher order terms not covered by the scale variation)

scheme a

$$f_0^{(a)}(p_T^{\text{cut}}) \equiv \frac{\sigma_0^{(0)}(p_T^{\text{cut}}) + \sigma_0^{(1)}(p_T^{\text{cut}}) + \sigma_0^{(2)}(p_T^{\text{cut}})}{\sigma^{(0)} + \sigma^{(1)} + \sigma^{(2)}}.$$

$\sigma_0^{(i)}$  is evaluated at  $\alpha_s^i$

scheme b

$$f_0^{(b)}(p_T^{\text{cut}}) = 1 - \frac{\sigma_{1\text{-jet}}^{\text{NLO}}(p_T^{\text{cut}})}{\sigma^{(0)} + \sigma^{(1)}}.$$

inclusive

evaluate numerator and denominator at the same numbers of loops

scheme c

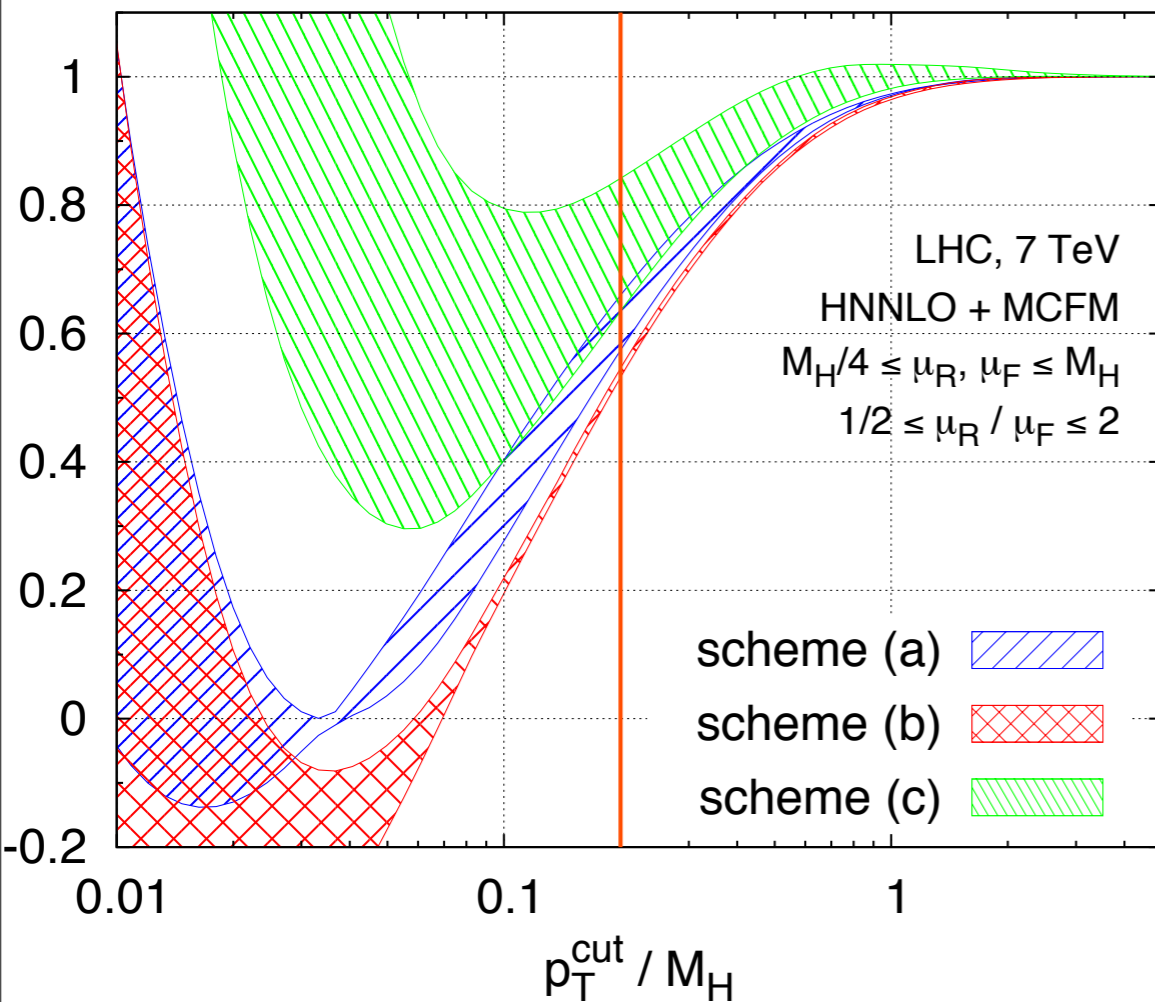
$$f_0^{(c)}(p_T^{\text{cut}}) = 1 - \frac{\sigma_{1\text{-jet}}^{\text{NLO}}(p_T^{\text{cut}})}{\sigma^{(0)}} + \frac{\sigma^{(1)}}{(\sigma^{(0)})^2} \sigma_{1\text{-jet}}^{\text{LO}}(p_T^{\text{cut}}).$$

fixed order  $\alpha_s^2$

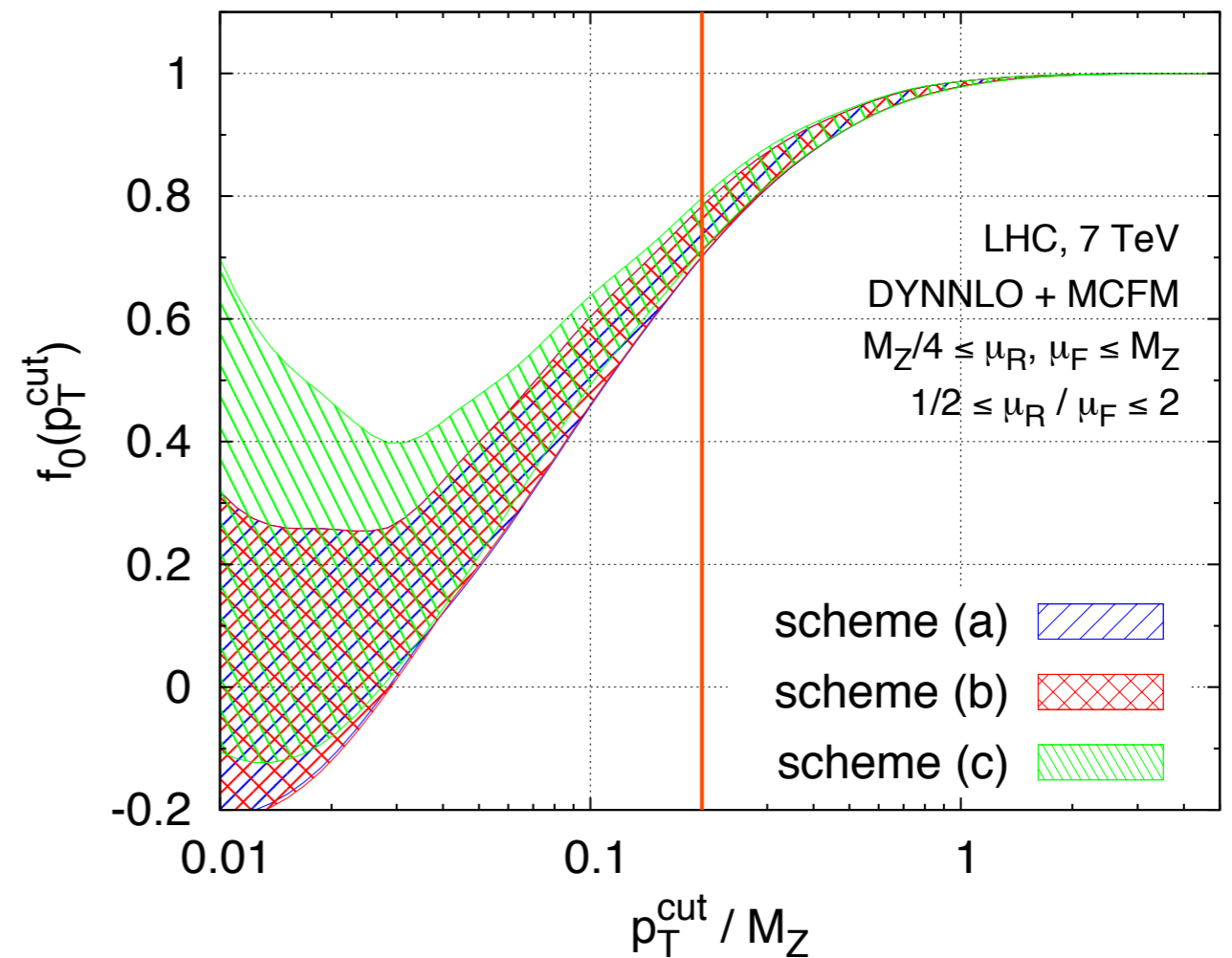
# Cross check by G.P. Salam et al.

- The spread among the schemes is larger than the scale uncertainty (S.T. procedure gives more realistic values for higher order contributions)
- In DY process, there is quite good agreement among the schemes (better convergence of the perturbative expansion)

## Higgs

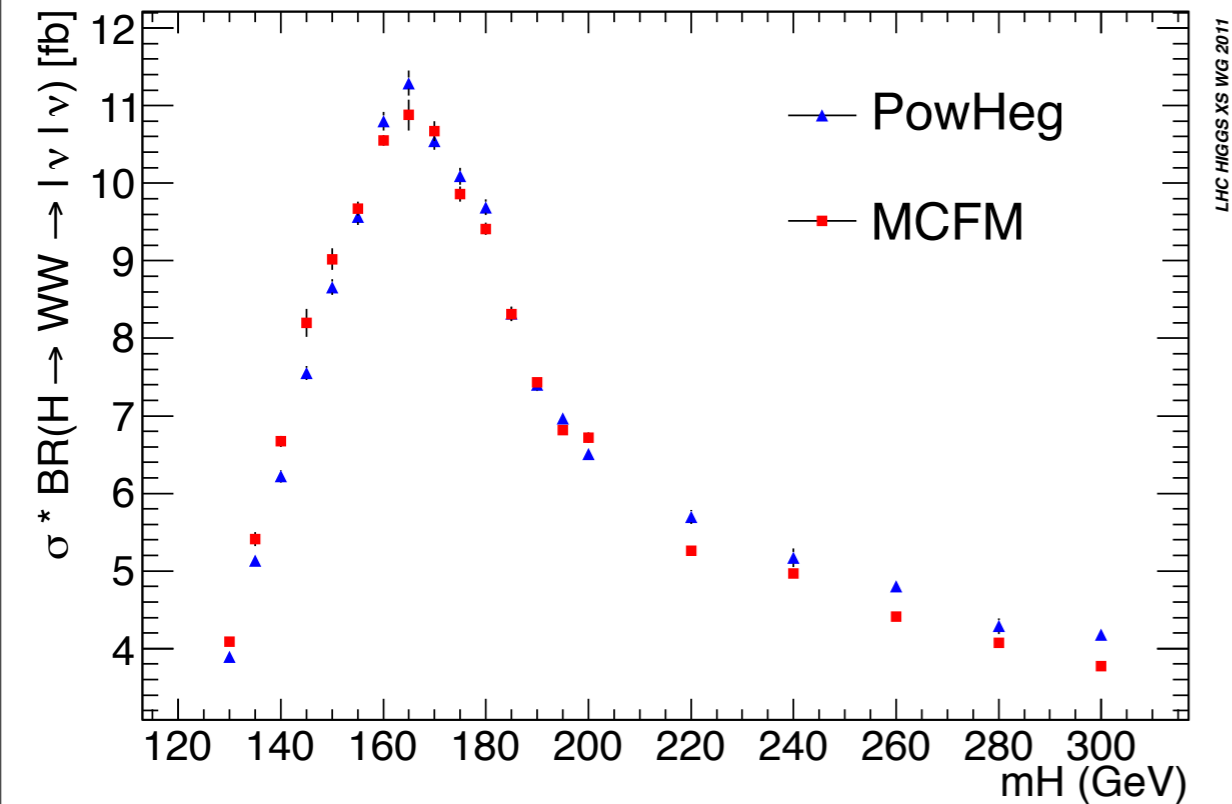


## Z



# MCFM-Powheg+Pythia comparison.

Scale uncertainty obtained by varying  $\mu_R, \mu_F$  by a factor 2 around  $m_H$ .



$M_H$ [GeV]	MCFM [fb]	POWHEG [fb]	Ratio: POWHEG/MCFM
130	$4.09 \pm 0.05$	$3.89 \pm 0.05$	$0.95 \pm 0.02$
135	$5.41 \pm 0.09$	$5.13 \pm 0.06$	$0.95 \pm 0.02$
140	$6.67 \pm 0.07$	$6.22 \pm 0.08$	$0.93 \pm 0.01$
145	$8.20 \pm 0.18$	$7.55 \pm 0.09$	$0.92 \pm 0.02$
150	$9.02 \pm 0.14$	$8.66 \pm 0.10$	$0.96 \pm 0.02$
155	$9.67 \pm 0.09$	$9.57 \pm 0.11$	$0.99 \pm 0.01$
160	$10.55 \pm 0.07$	$10.80 \pm 0.12$	$1.02 \pm 0.01$
165	$10.88 \pm 0.20$	$11.29 \pm 0.16$	$1.04 \pm 0.02$
170	$10.67 \pm 0.13$	$10.54 \pm 0.11$	$0.99 \pm 0.02$
175	$9.86 \pm 0.10$	$10.09 \pm 0.11$	$1.02 \pm 0.01$
180	$9.41 \pm 0.08$	$9.69 \pm 0.10$	$1.03 \pm 0.01$
185	$8.31 \pm 0.09$	$8.32 \pm 0.09$	$1.00 \pm 0.01$
190	$7.43 \pm 0.05$	$7.40 \pm 0.08$	$1.00 \pm 0.01$
195	$6.82 \pm 0.06$	$6.97 \pm 0.07$	$1.02 \pm 0.01$
200	$6.72 \pm 0.07$	$6.51 \pm 0.07$	$0.97 \pm 0.01$
220	$5.26 \pm 0.05$	$5.70 \pm 0.09$	$1.08 \pm 0.02$
240	$4.97 \pm 0.04$	$5.17 \pm 0.12$	$1.04 \pm 0.02$
260	$4.41 \pm 0.02$	$4.80 \pm 0.07$	$1.09 \pm 0.01$
280	$4.07 \pm 0.04$	$4.29 \pm 0.10$	$1.05 \pm 0.02$
300	$3.77 \pm 0.02$	$4.18 \pm 0.06$	$1.11 \pm 0.02$

$M_H$ [GeV]	scale uncertainties
130	23%
160	24%
220	20%

2 jet bin scale uncertainties below 25%

The difference with the Powheg prediction, even if compared after UE, hadronisation and parton shower, is smaller than the scale uncertainty itself.

Taking CMS numbers:

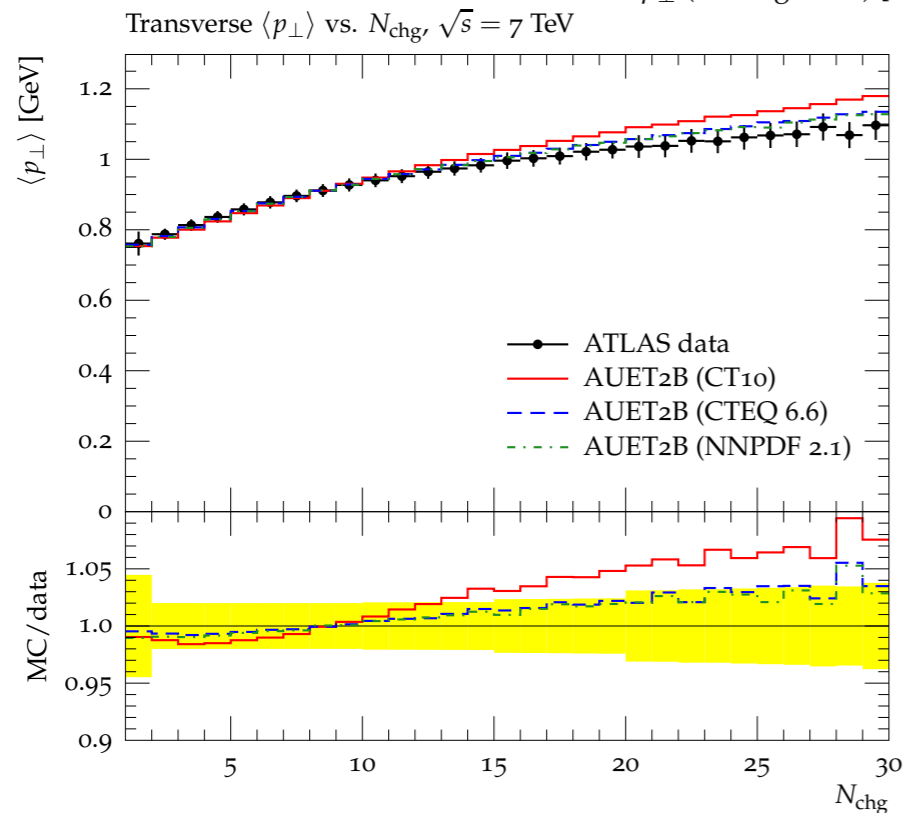
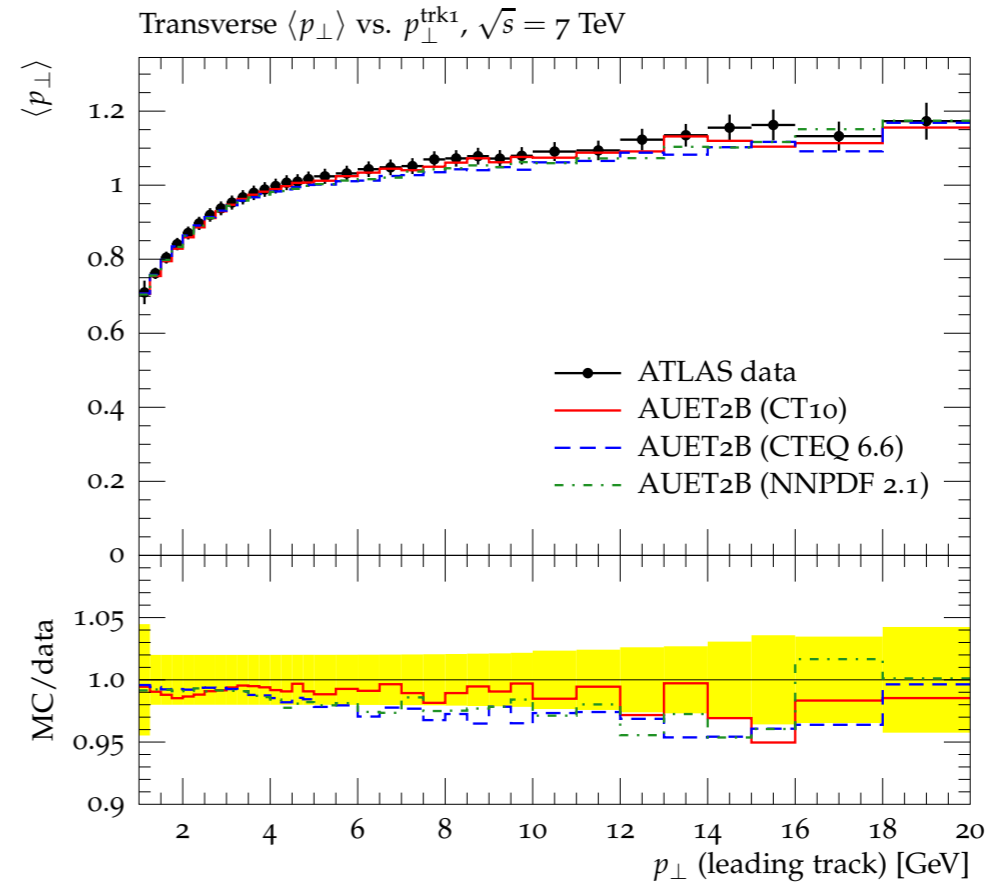
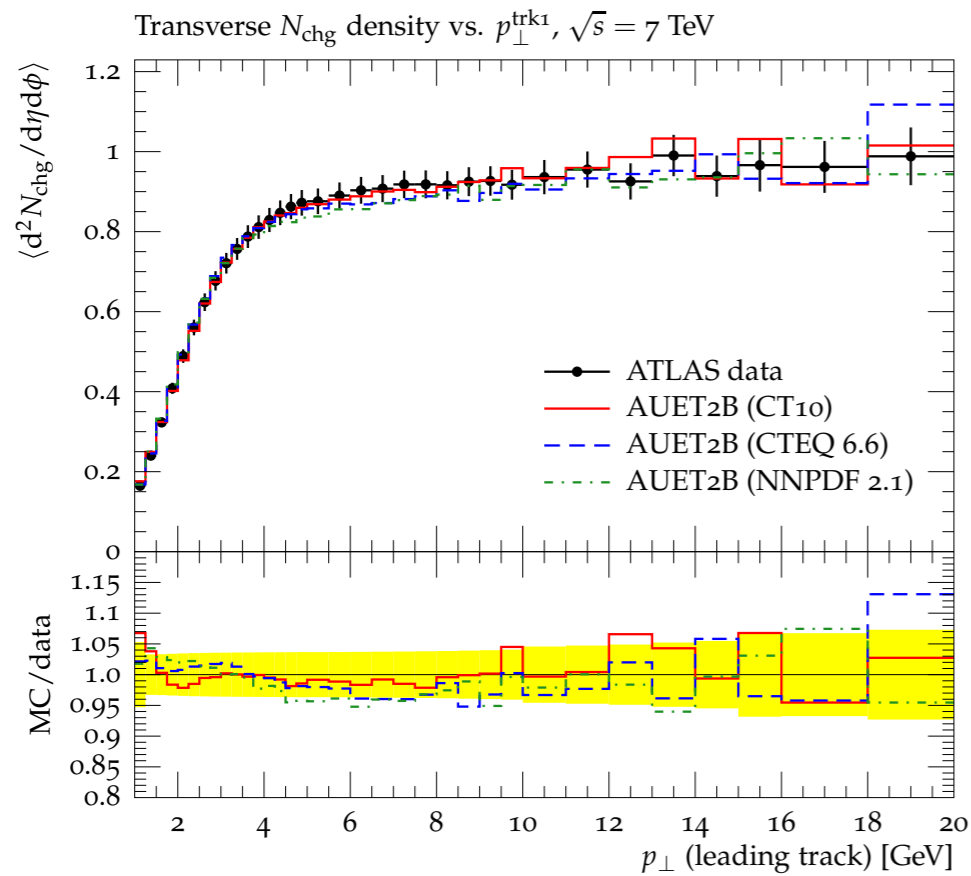
2.1 events from VBF have a theoretical error of about 0.1 events, while the 0.76 events from ggF have an error of 0.2 still dominating the signal uncertainty.

CMS quotes a much larger error 70% from UE in ggF. It is not clear (to me) why it should affect only ggF.

Several tuning have been compared (dt6, p0, propt0 and proq20, z2 (reference) tune), see: [Physics Letters B 710 \(2012\) 403–425](#) for definition.

# UE tuning in ATLAS (Pythia6)

Tuning is performed by looking at UE sensitive observables (track multiplicity, track  $p_T$  spectrum) Pythia6



Param. name	Function	Sampling range
PARP(77)	High- $p_{\perp}$ suppression of colour reconnection	0.0 – 1.0
PARP(78)	Strength of colour reconnection	0.0 – 1.0
PARP(82)	MPI $p_{\perp}$ cutoff at $\sqrt{s} = 1800$ GeV	1.5 – 2.5
PARP(84)	Rel. radius of core proton matter distribution	0.0 – 1.0
PARP(90)	MPI cutoff energy evolution exponent	0.15 – 0.25

PDF	PARP(77)	PARP(78)	PARP(82)	PARP(84)	PARP(90)
CTEQ 6.6	0.505	0.385	1.87	0.561	0.189
CT10	0.125	0.309	1.89	0.415	0.182
NNPDF 2.1 NLO	0.498	0.354	1.86	0.588	0.177

Table 3: Tuned MPI parameters for the AUET2B PYTHIA6 tunings to NLO PDFs.

# UE tuning in ATLAS (Pythia6)

Tuning is performed by looking at UE sensitive observables (track multiplicity, track  $p_T$  spectrum) Pythia6

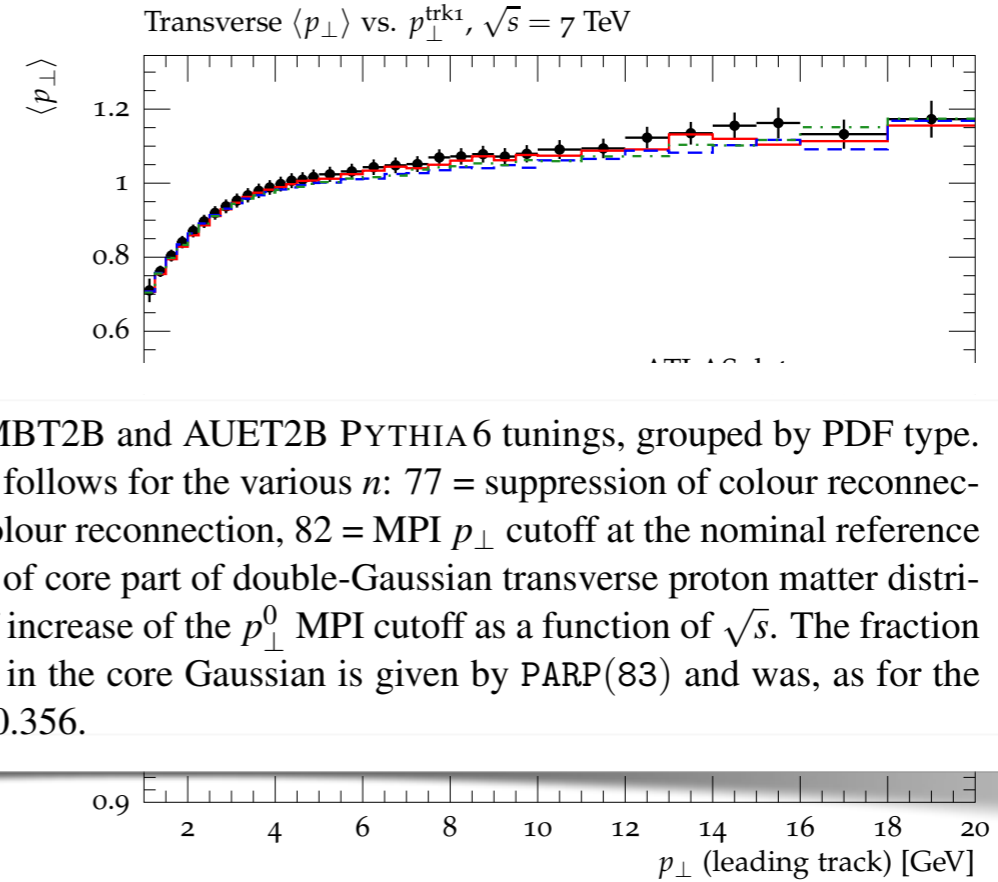
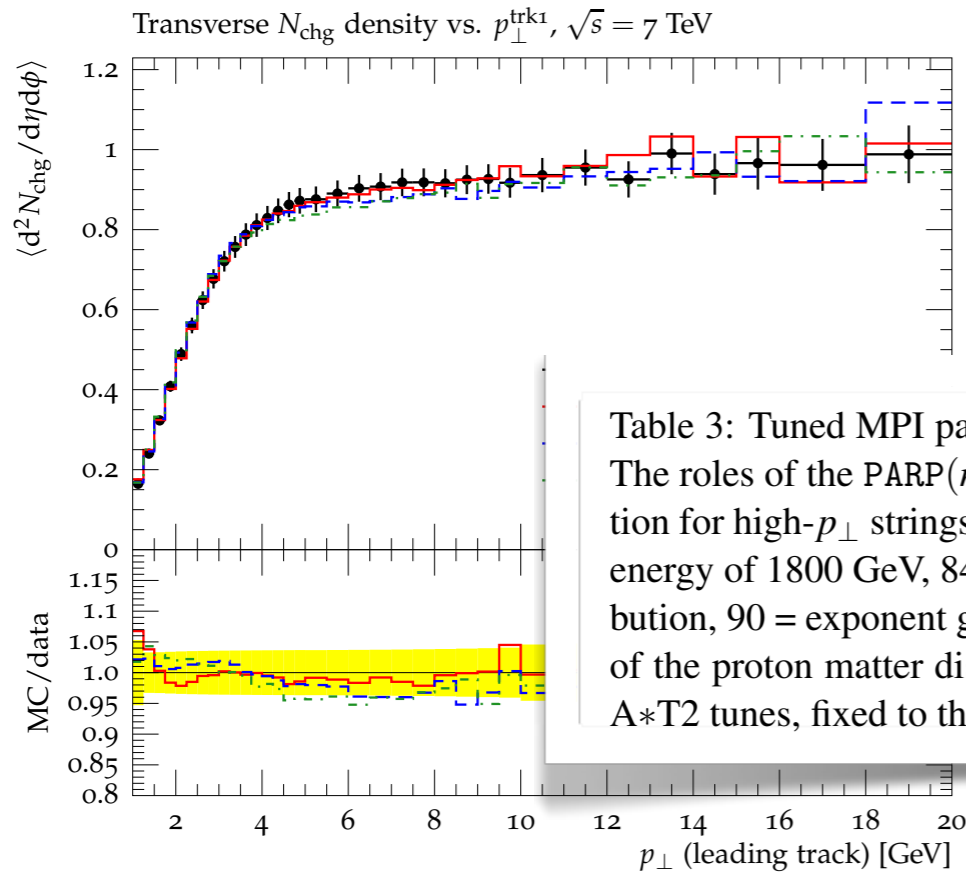
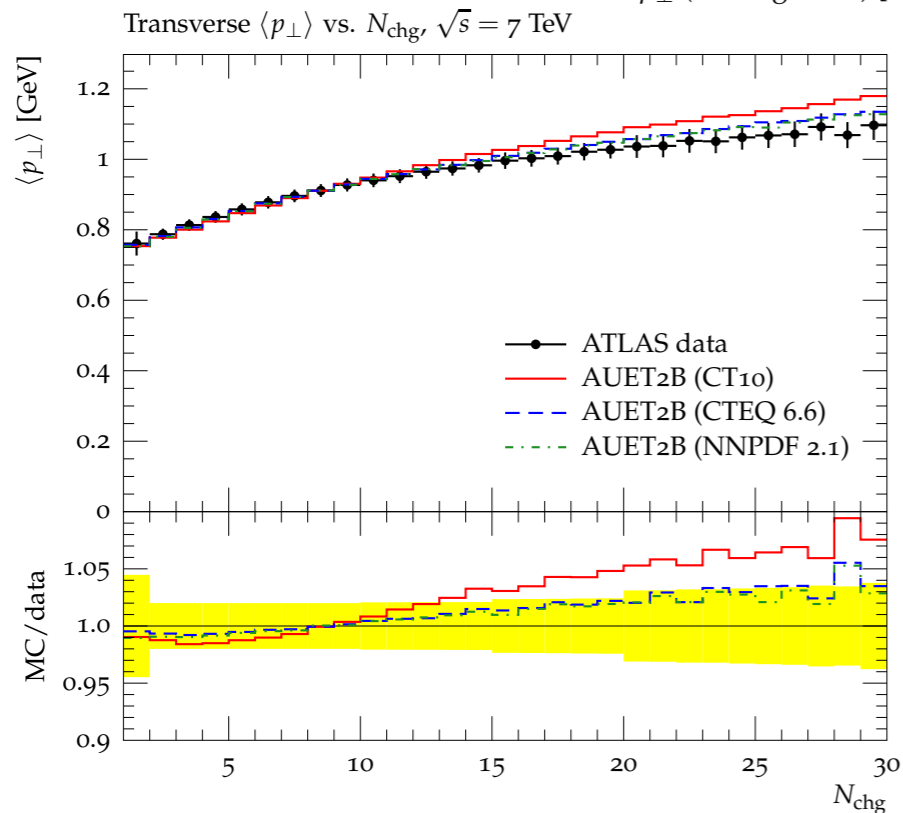


Table 3: Tuned MPI parameters for the AMBT2B and AUET2B PYTHIA6 tunings, grouped by PDF type. The roles of the PARP( $n$ ) parameters are as follows for the various  $n$ : 77 = suppression of colour reconnection for high- $p_{\perp}$  strings, 78 = strength of colour reconnection, 82 = MPI  $p_{\perp}$  cutoff at the nominal reference energy of 1800 GeV, 84 = fractional radius of core part of double-Gaussian transverse proton matter distribution, 90 = exponent governing the rate of increase of the  $p_{\perp}^0$  MPI cutoff as a function of  $\sqrt{s}$ . The fraction of the proton matter distribution contained in the core Gaussian is given by PARP(83) and was, as for the A\*T2 tunes, fixed to the AMBT1 value of 0.356.



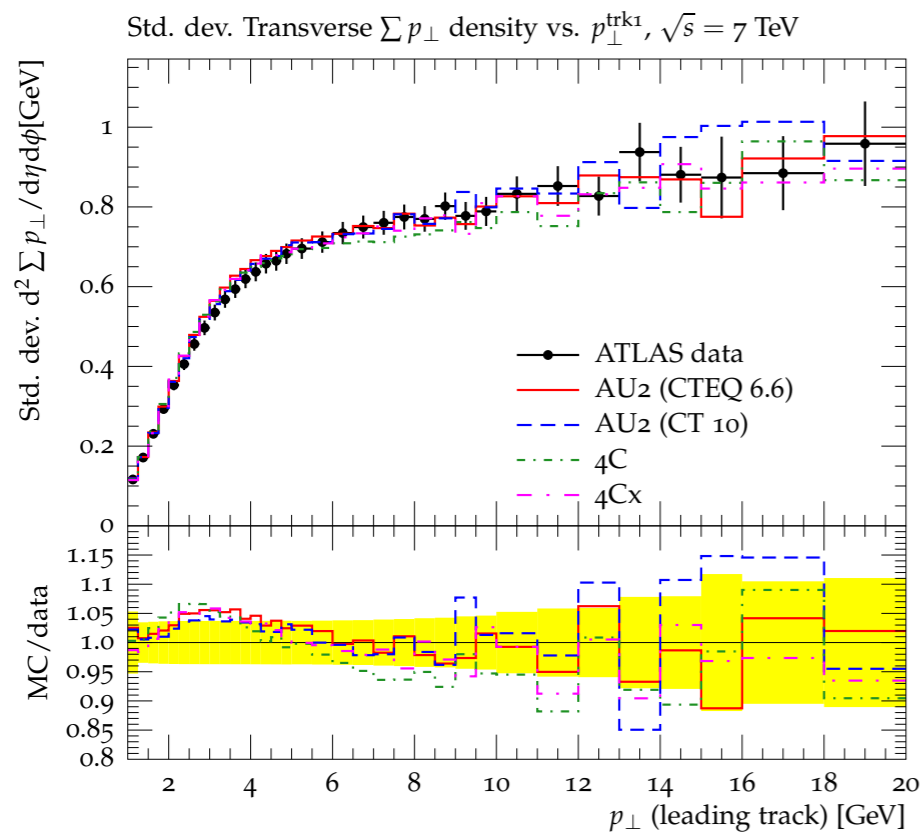
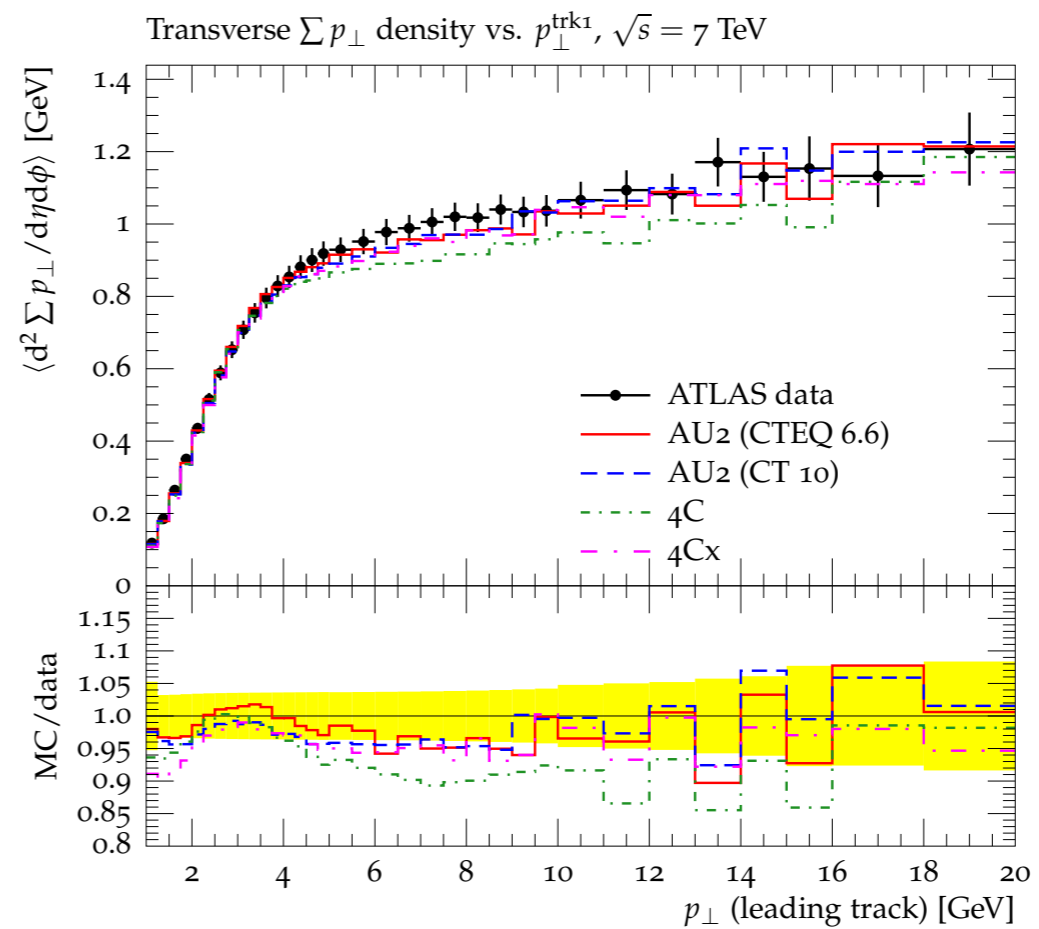
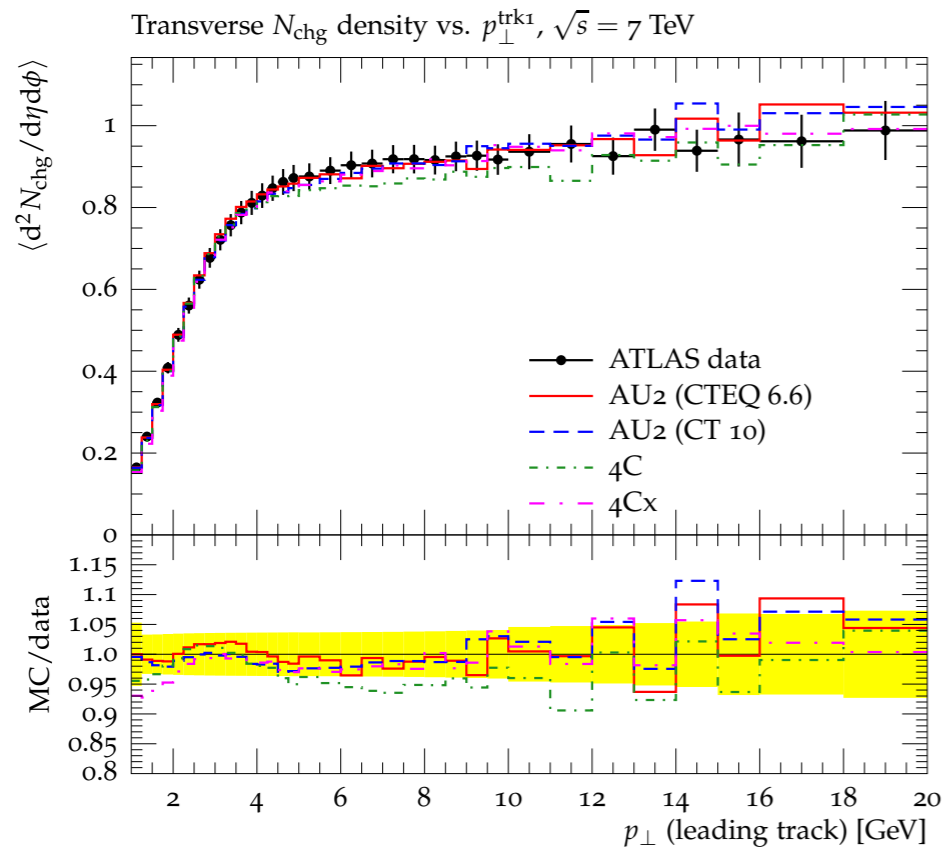
Param. name	Function	Sampling range
PARP(77)	High- $p_{\perp}$ suppression of colour reconnection	0.0 – 1.0
PARP(78)	Strength of colour reconnection	0.0 – 1.0
PARP(82)	MPI $p_{\perp}$ cutoff at $\sqrt{s} = 1800$ GeV	1.5 – 2.5
PARP(84)	Rel. radius of core proton matter distribution	0.0 – 1.0
PARP(90)	MPI cutoff energy evolution exponent	0.15 – 0.25

PDF	PARP(77)	PARP(78)	PARP(82)	PARP(84)	PARP(90)
CTEQ 6.6	0.505	0.385	1.87	0.561	0.189
CT10	0.125	0.309	1.89	0.415	0.182
NNPDF 2.1 NLO	0.498	0.354	1.86	0.588	0.177

Table 3: Tuned MPI parameters for the AUET2B PYTHIA6 tunings to NLO PDFs.

# UE tuning in ATLAS (Pythia8)

Tuning is performed by looking at UE sensitive observables (track multiplicity, track  $p_T$  spectrum)



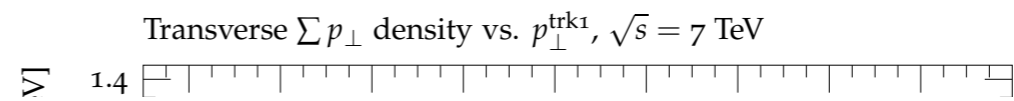
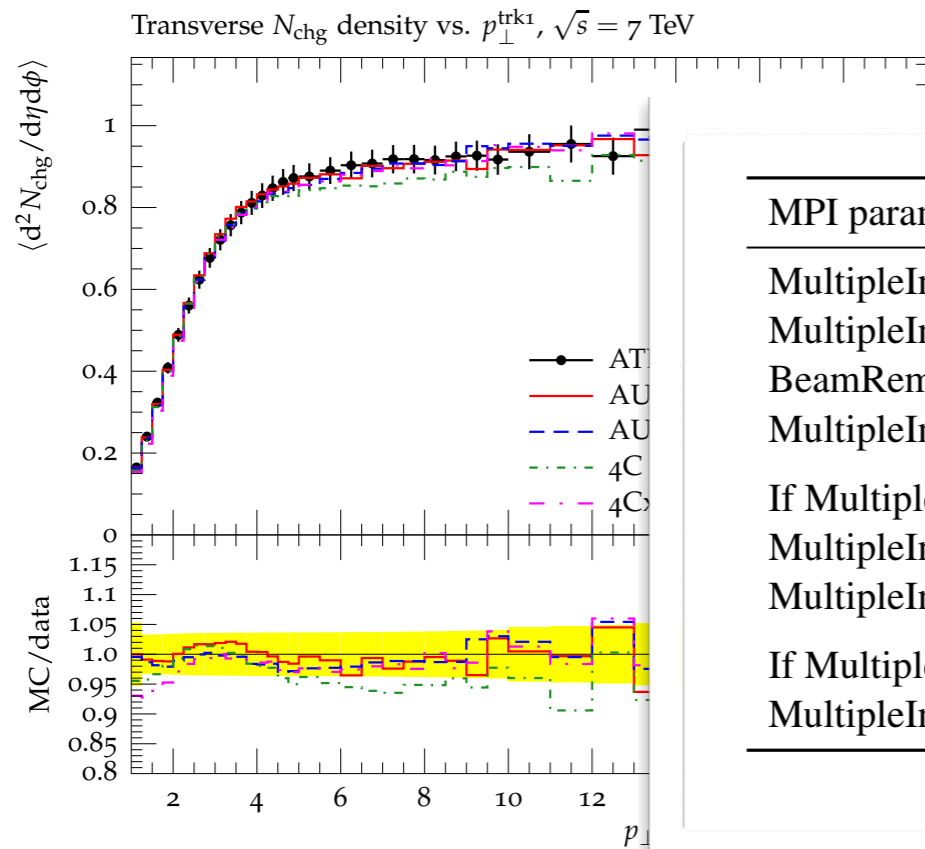
PDF	pT0Ref	ecomPow	a1	reconnectRange
CTEQ 6L1	2.18	0.22	0.06	1.55
MSTW2008 LO	1.90	0.30	0.03	2.28
CTEQ 6.6	1.73	0.16	0.03	5.12
CT10	1.70	0.16	0.10	4.67
MRST2007 LO*	2.39	0.24	0.01	1.76
MRST2007 LO**	2.57	0.23	0.01	1.47

Table 4: Tuned MPI parameters for the A2/AU2 Pythia 8 tunings.



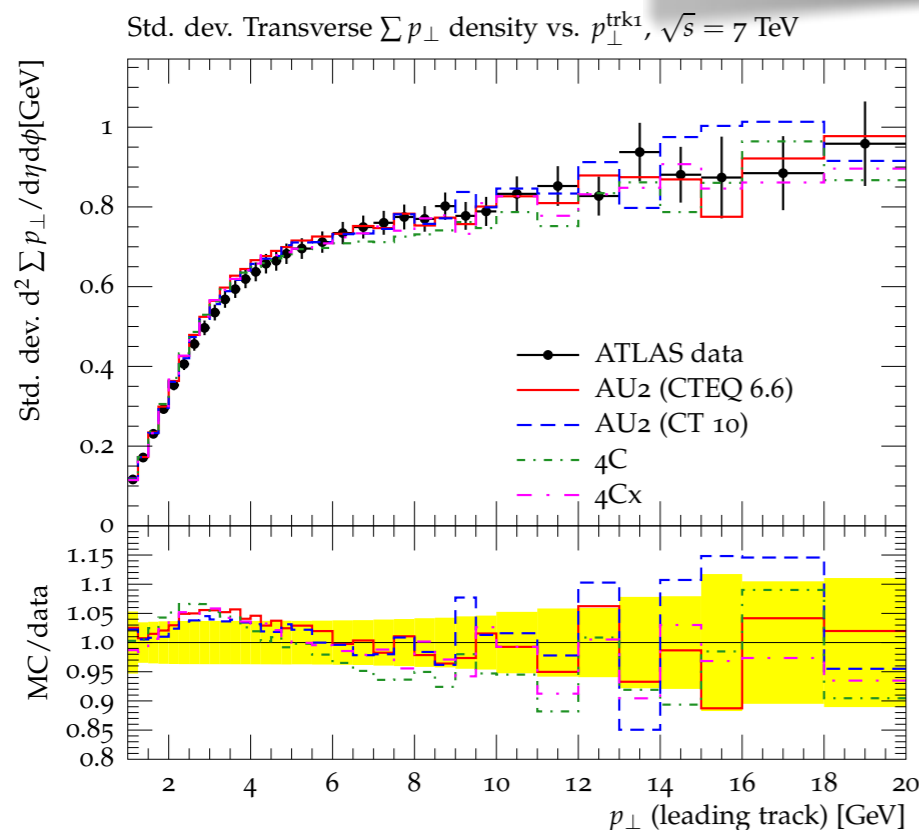
# UE tuning in ATLAS (Pythia8)

Tuning is performed by looking at UE sensitive observables (track multiplicity, track  $p_T$  spectrum)



MPI parameter	Equivalent PYTHIA 6 parameter	Tune 4C value
MultipleInteractions:pT0Ref	PARP(82)	2.085
MultipleInteractions:ecmPow	PARP(90)	0.19
BeamRemnants:reconnectRange	PARP(77), PARP(78)	1.5
MultipleInteractions:bProfile	MSTP(82)	3
If MultipleInteractions:bProfile = 2 (double-Gaussian matter dbn.)		
MultipleInteractions:coreFraction	PARP(83)	–
MultipleInteractions:coreRadius	PARP(84)	–
If MultipleInteractions:bProfile = 3 (exp/Gaussian overlap dbn.)		
MultipleInteractions:expPow	PARP(83)	2.0

Table 7: Pythia 8 MPI parameters

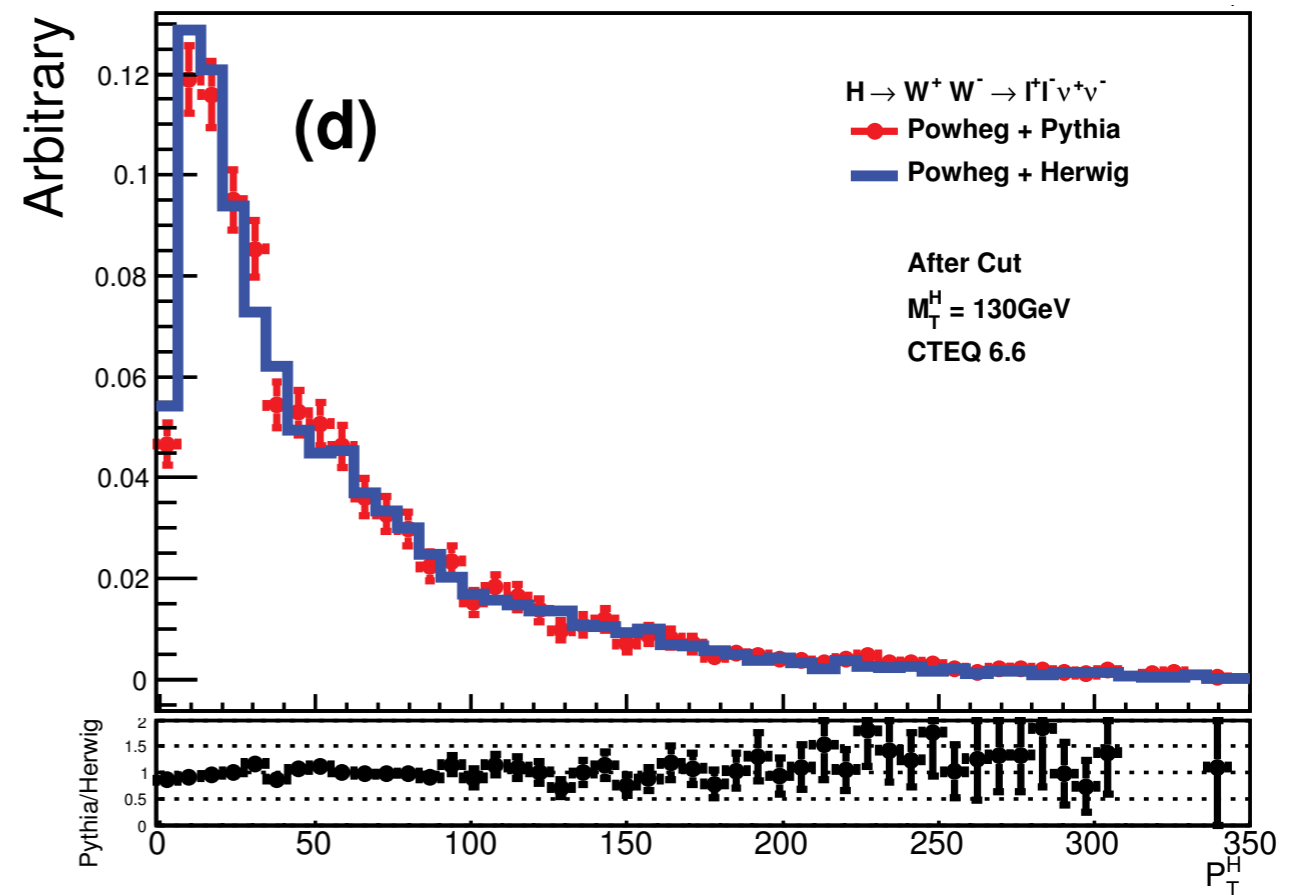
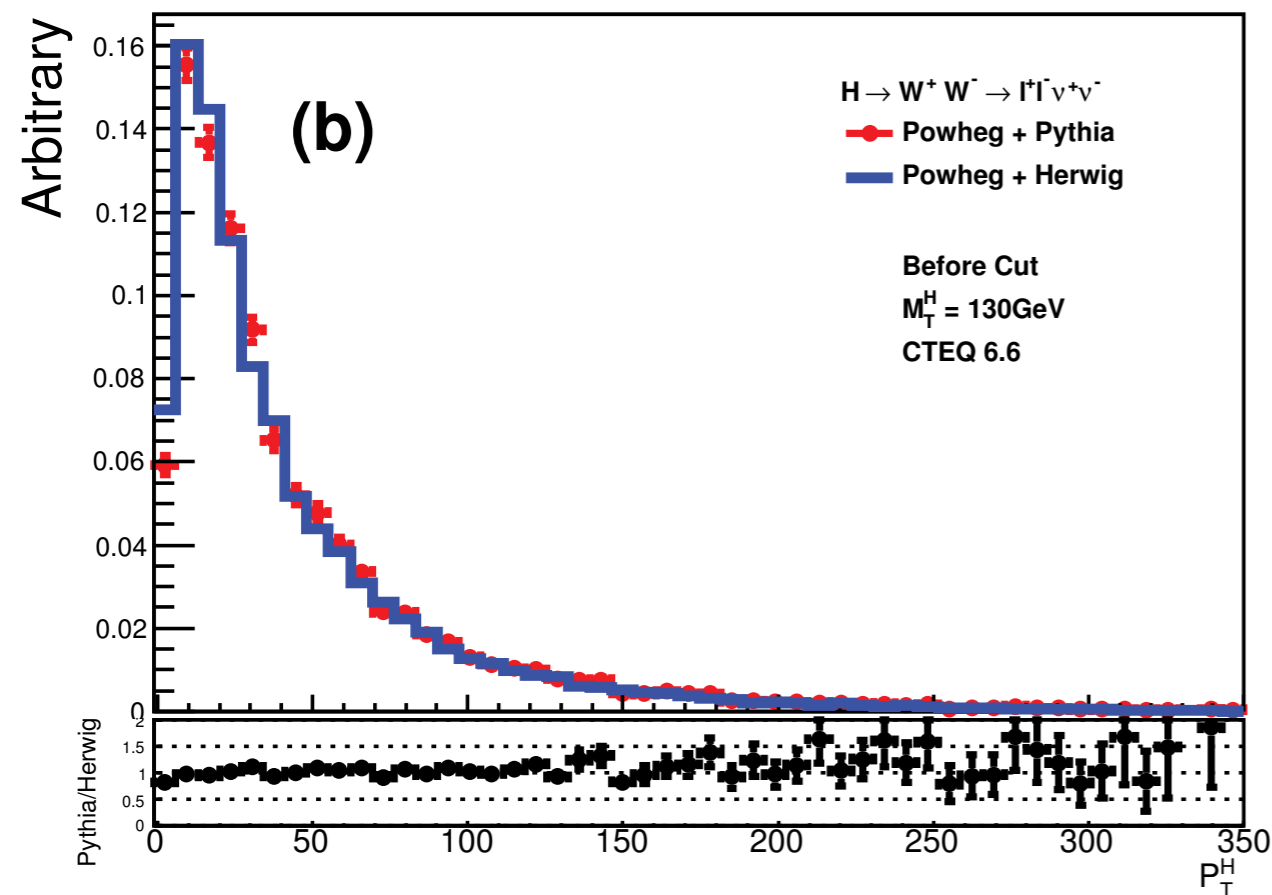


PDF	pT0Ref	ecomPow	a1	reconnectRange
CTEQ 6L1	2.18	0.22	0.06	1.55
MSTW2008 LO	1.90	0.30	0.03	2.28
CTEQ 6.6	1.73	0.16	0.03	5.12
CT10	1.70	0.16	0.10	4.67
MRST2007 LO*	2.39	0.24	0.01	1.76
MRST2007 LO**	2.57	0.23	0.01	1.47

Table 4: Tuned MPI parameters for the A2/AU2 Pythia 8 tunings.

# Parton shower effects.

- Parton shower is the best we can do to have a detailed description of what happens in the detector. Herwig and Pythia are slightly different
  - Herwig order the showers to small angles, so that late in the shower we have more collinear particles than at the beginning.
- Pythia is instead virtuality ordered (highest  $Q^2$  branches first), effect on Higgs observables has been studied switching off UE to decouple the UE modelling issue.
- study performed with and without cuts typical of  $H \rightarrow WW \rightarrow l\nu l\nu$  analysis



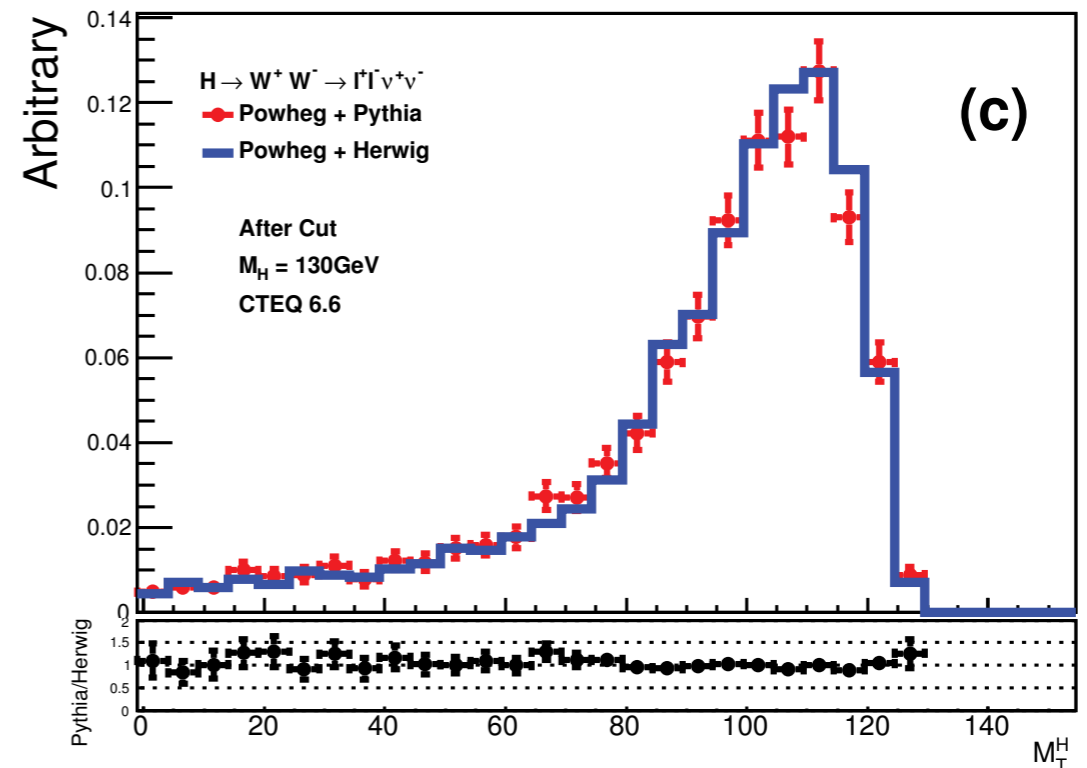
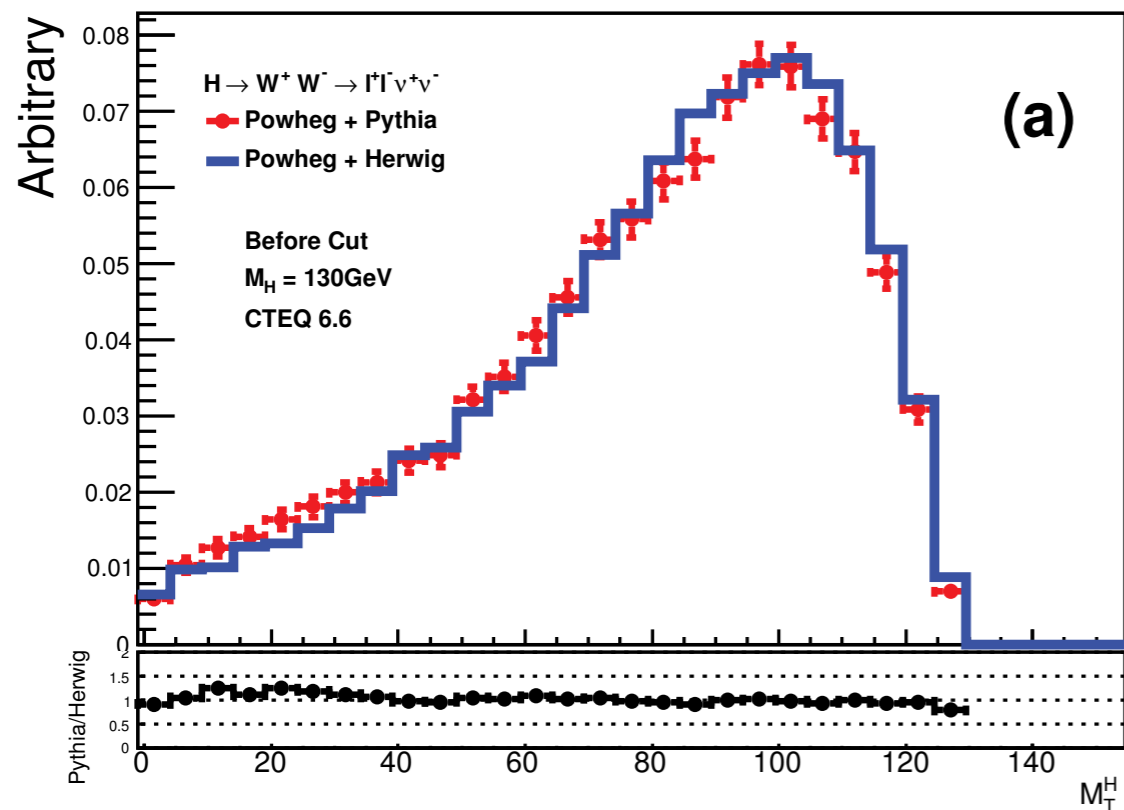
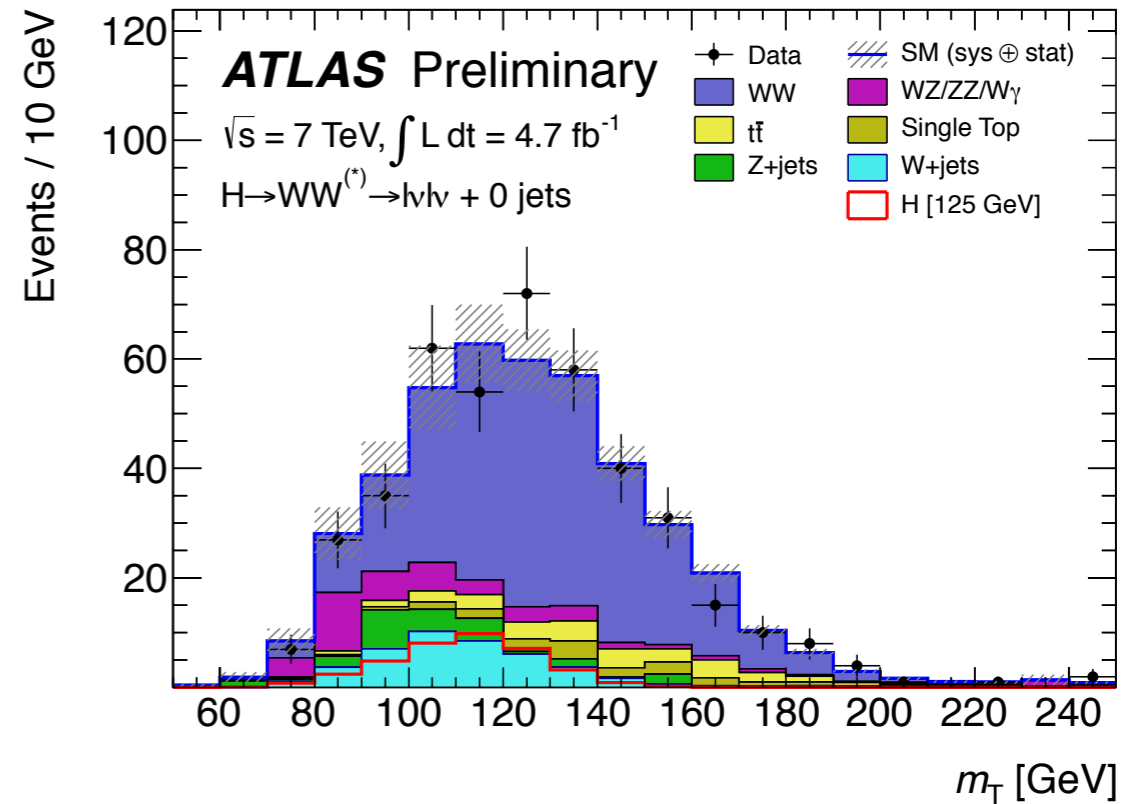


# Effect on the $m_T$ distribution

$$m_T = \sqrt{(E_T^{\ell\ell} + E_T^{\text{miss}})^2 - (\mathbf{p}_T^{\ell\ell} + \mathbf{p}_T^{\text{miss}})^2}$$

$m_T$  is the Higgs mass if all leptons are in the transverse plane.

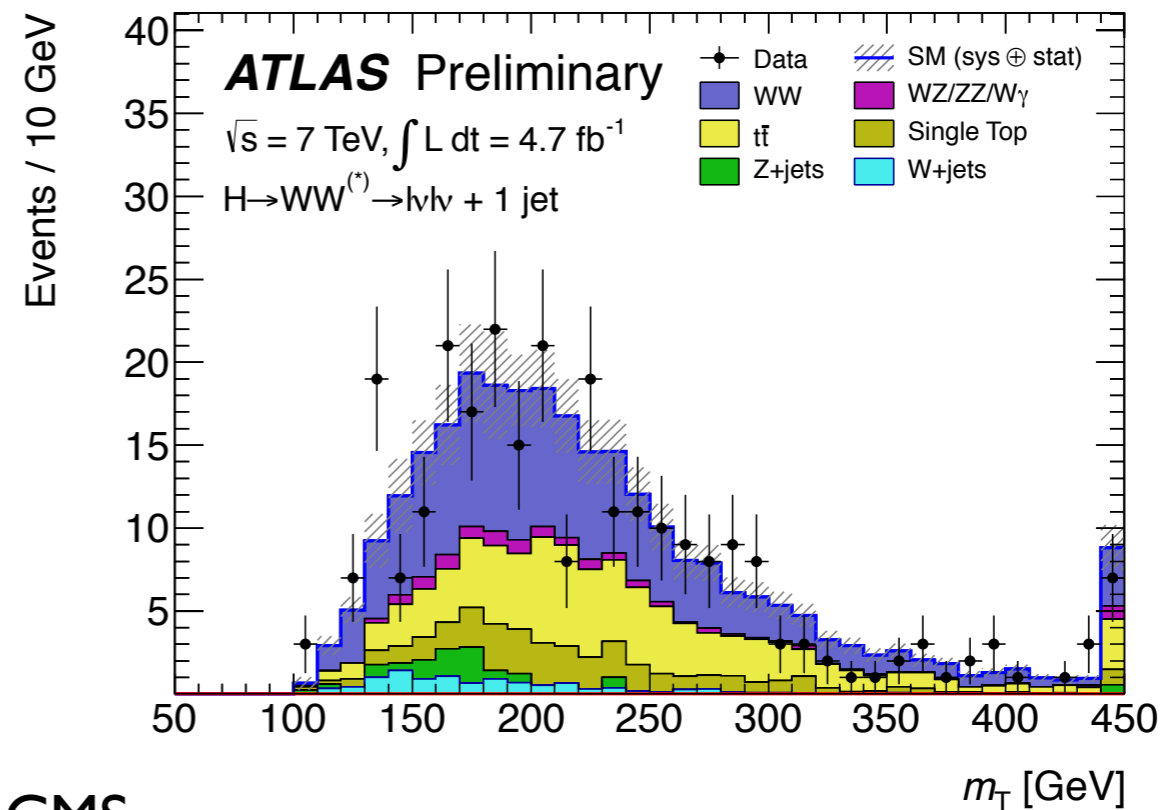
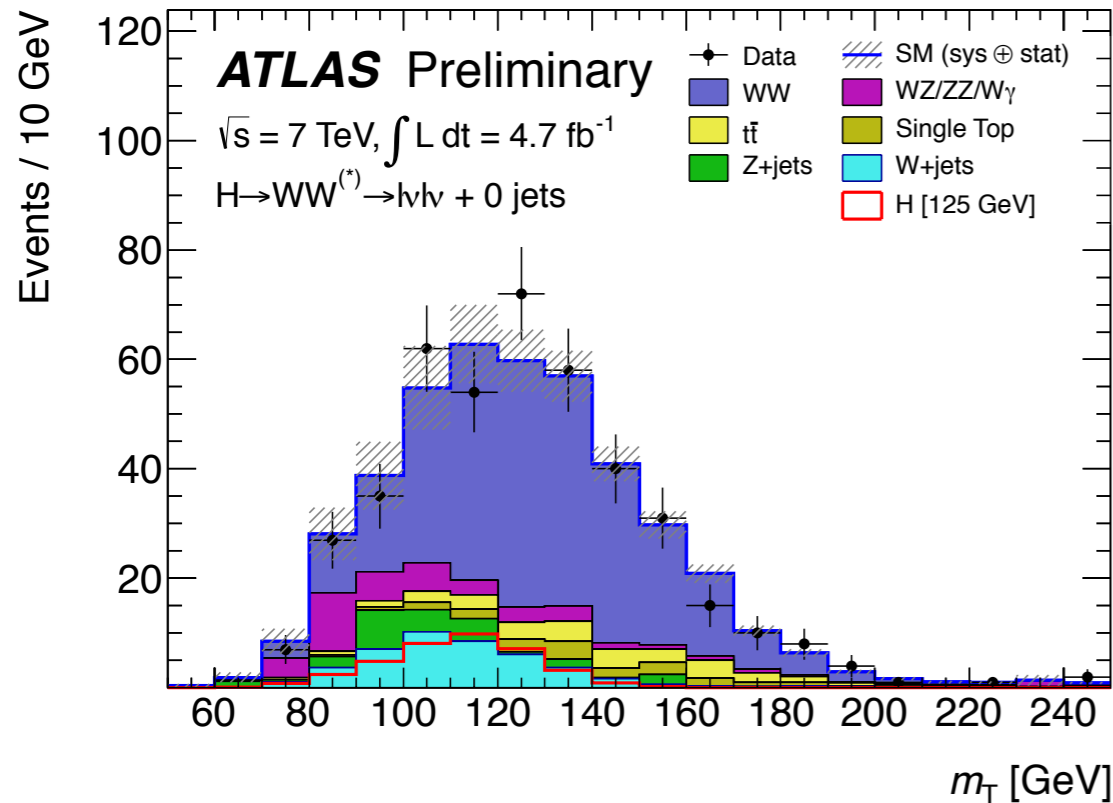
$$E_T^{\ell\ell} = \sqrt{(\mathbf{p}_T^{\ell\ell})^2 + m_{\ell\ell}^2}, |\mathbf{p}_T^{\text{miss}}| = E_T^{\text{miss}} \text{ and } \mathbf{p}_T^{\ell\ell}$$



# The $H \rightarrow WW \rightarrow l\nu l\nu$ channel.

- It is the most sensitive channel in the region  $122 < m_H < 200$  GeV
- Excludes alone the region  $130 < m_H < 260$  GeV (ATLAS)  $129 < m_H < 270$  GeV (CMS)
- It is affected by several backgrounds:

In the high mass region, is dominated by the  $pp \rightarrow WW \rightarrow l\nu l\nu$ , in the low mass region many other background source become important:



Main backgrounds

ATLAS

CMS

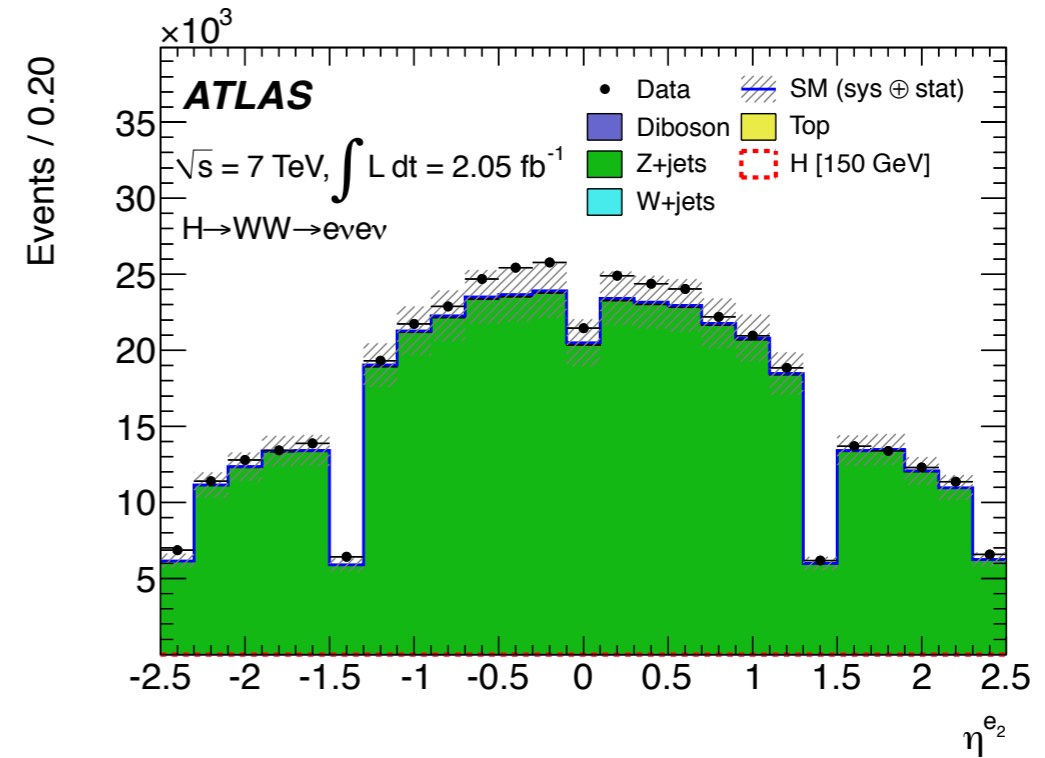
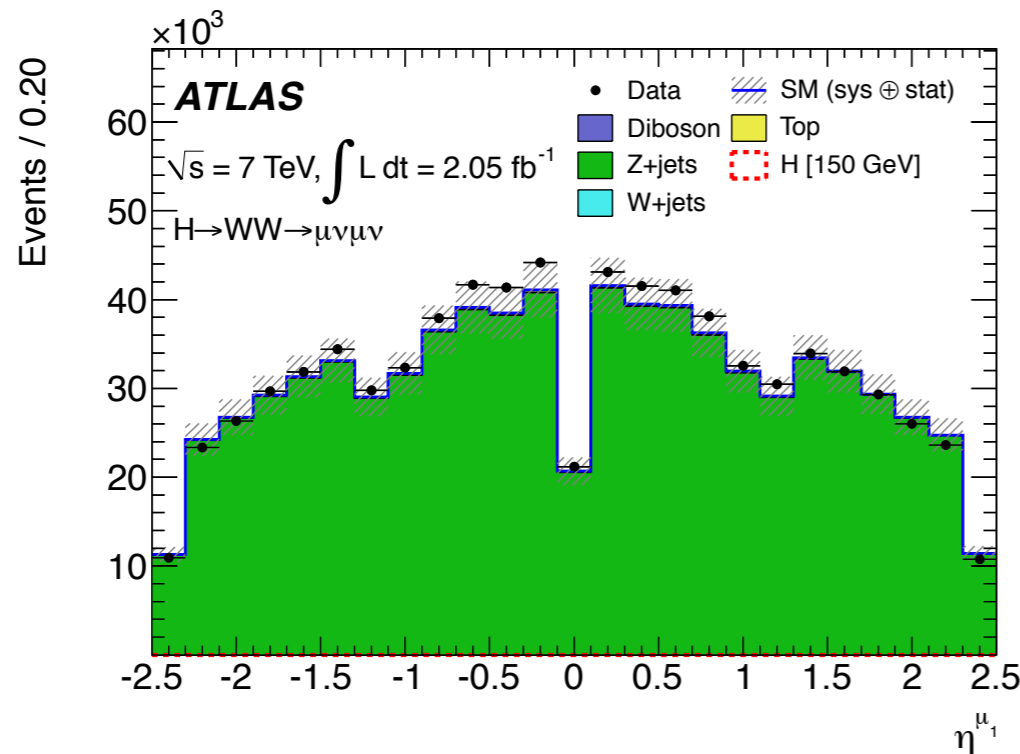
- WW
- top
- single top
- Z/ $\gamma^*$
- W $\gamma$
- W $\gamma^*$

- MC@NLO+Herwig (NLO)
- MC@NLO+Herwig (NLO)
- AcerMC (LO)
- ALPGEN+HERWIG (MULTILEG)
- ALPGEN+HERWIG (MULTILEG)
- MADGRAPH+Pythia (LO)

- MADGRAPH+Pythia (LO)
- Powheg+Pythia (NLO)
- Powheg(Wt)(NLO), Pythia(all others)(LO)
- Powheg+Pythia(NLO)
- Pythia (LO)
- MADGRAPH+Pythia (LO)

# DY simulation.

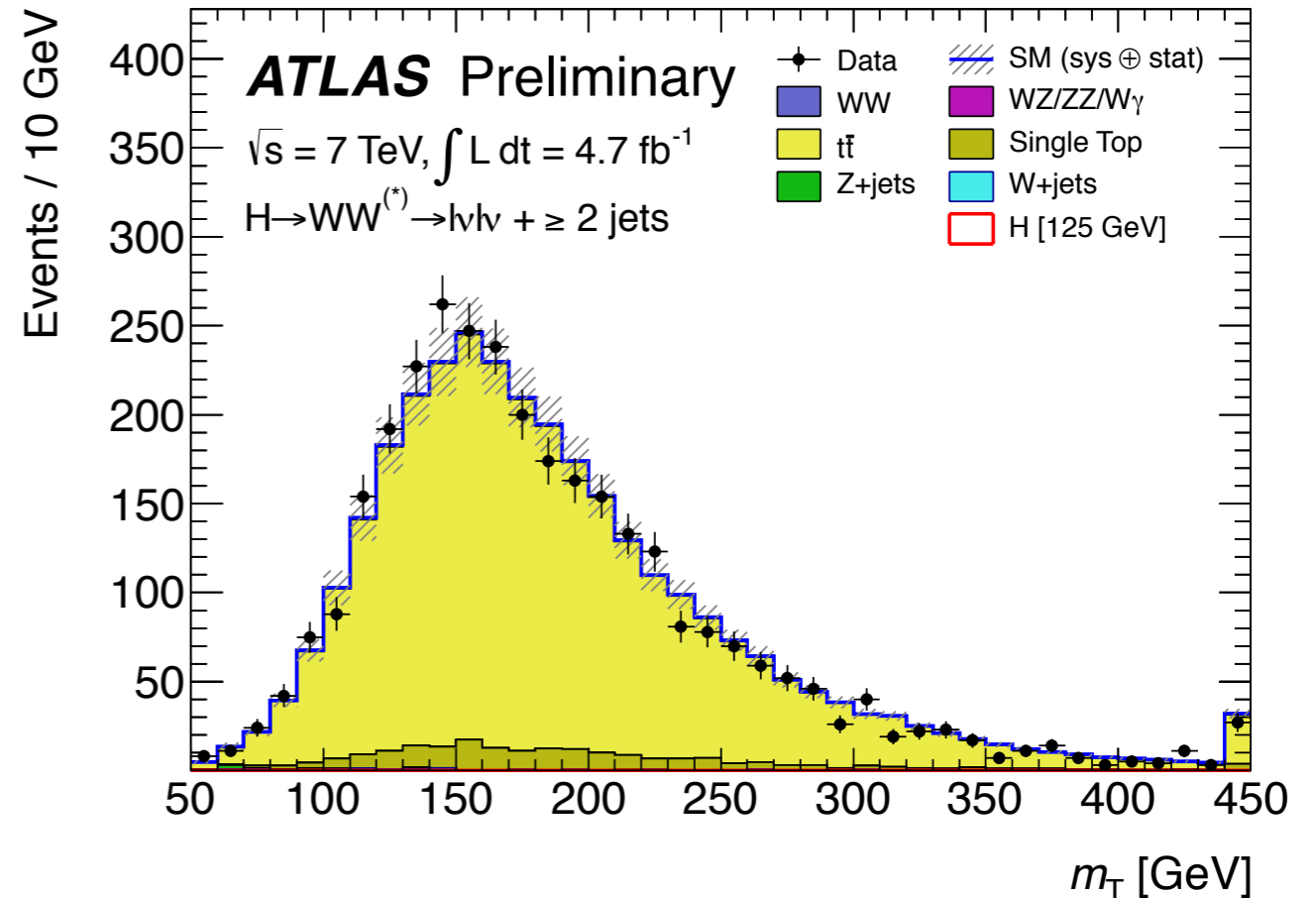
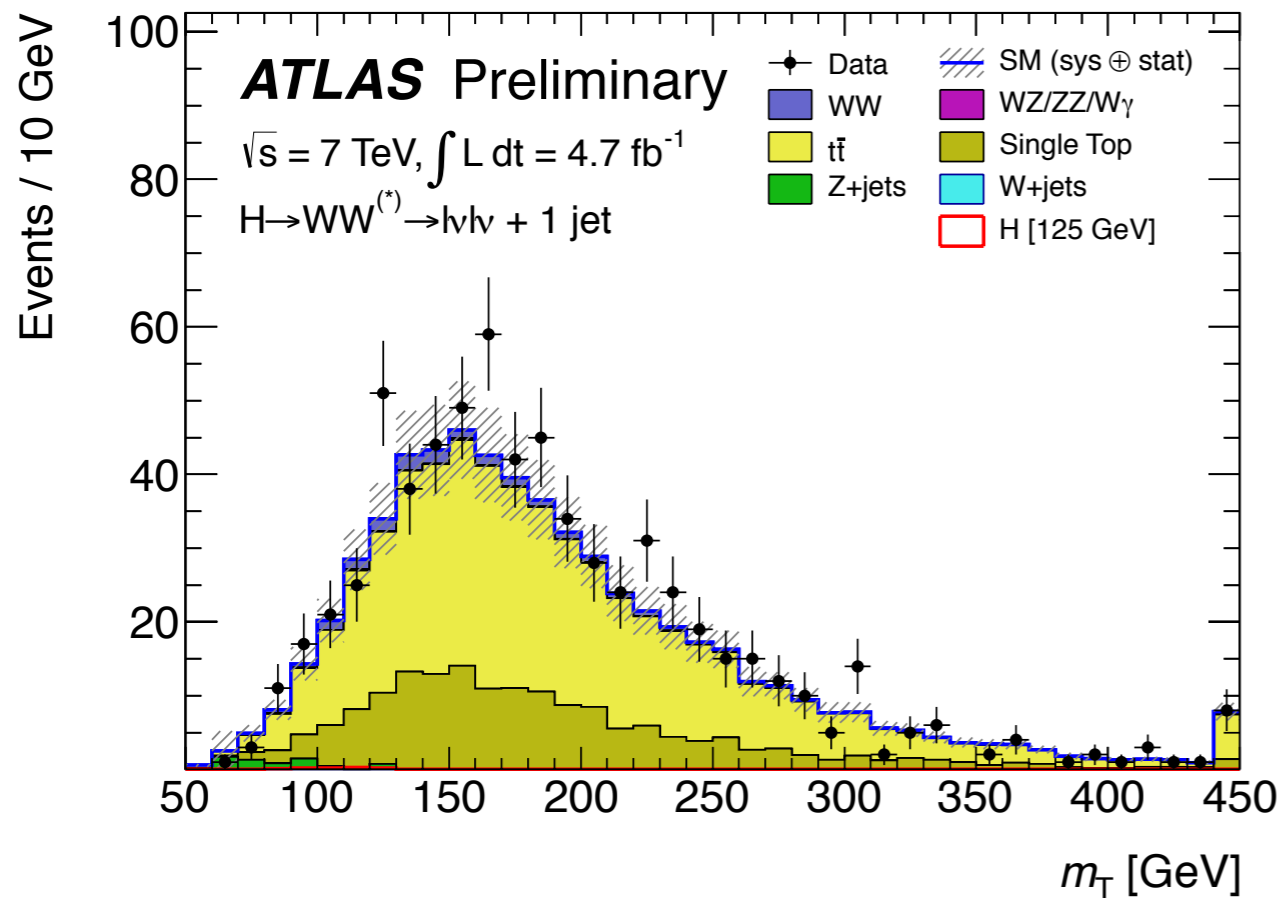
- Pythia is not able to describe correctly the jet distributions (pseudorapidity of the jets, jet multiplicity, jet  $p_T$  distribution)
- ALPGEN+Herwig with CTEQ6L1 pdf's doesn't describe correctly the  $\eta$  distribution of the leptons



- Using pdf reweighting to MRST LO\* give much better agreement on the pseudorapidity distributions (unfortunately I cannot show them because we don't have an approved plot...., sorry for that!!)
- Jet multiplicity and pseudorapidity distributions are preserved after PDF reweighting.

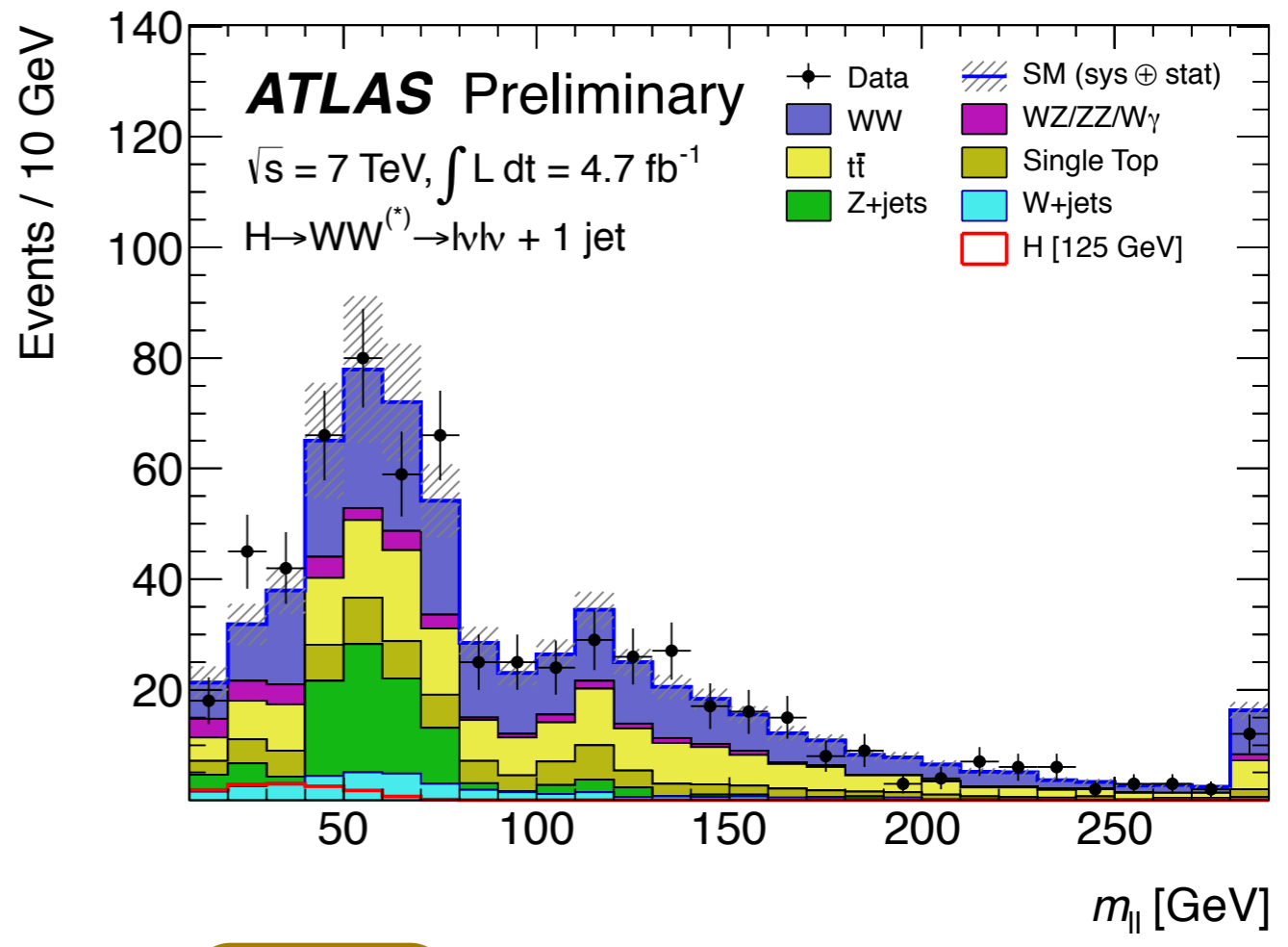
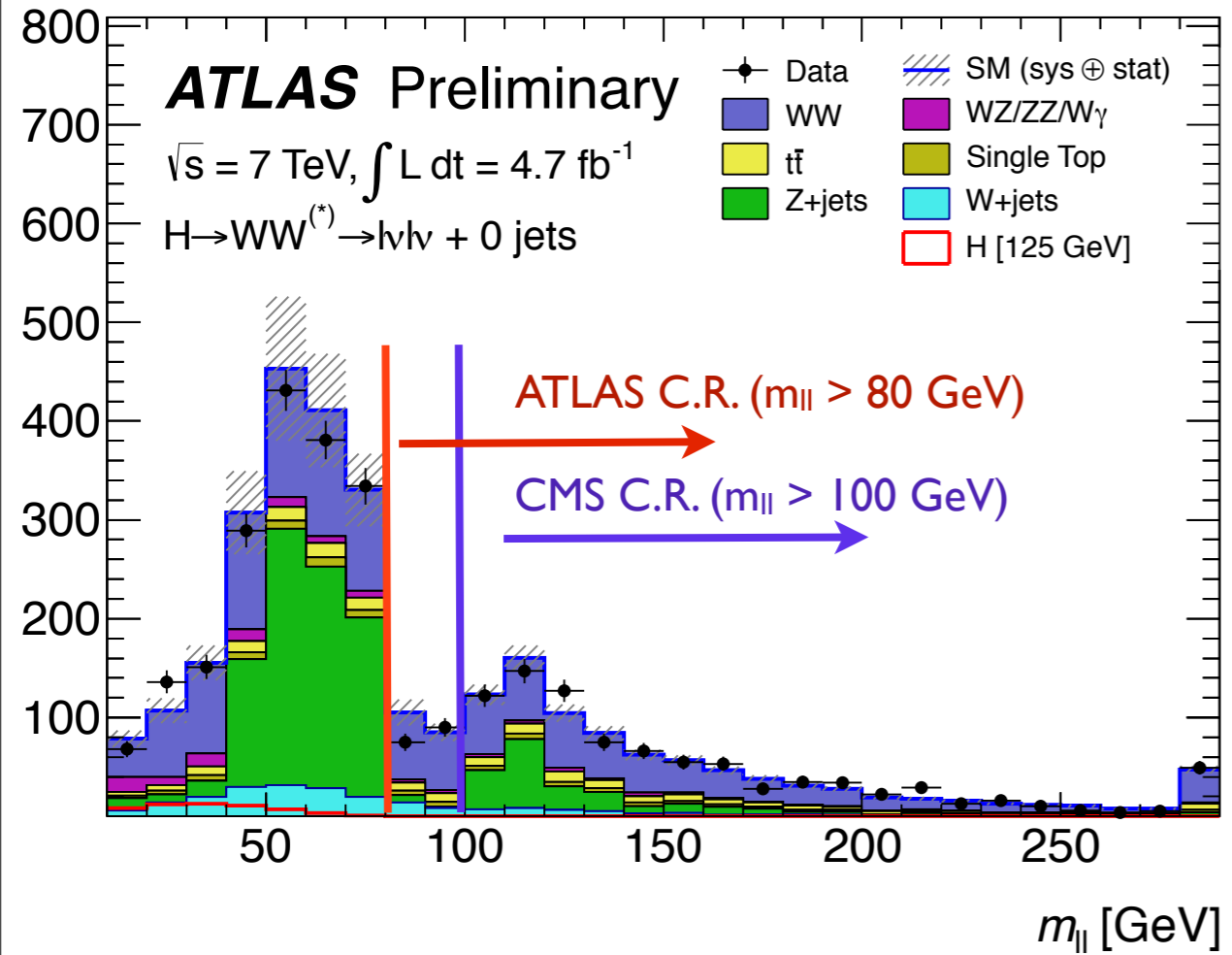
# Top description.

MC@NLO performs quite well in the description of the top. There are some normalisation problem (probably due to the Herwig old decay table affecting b-tagging and anti-b-tagging efficiencies), but the kinematic variables looks in good agreement after a total normalisation correction ( $\sim 10\%$ ,  $20\%$ ).



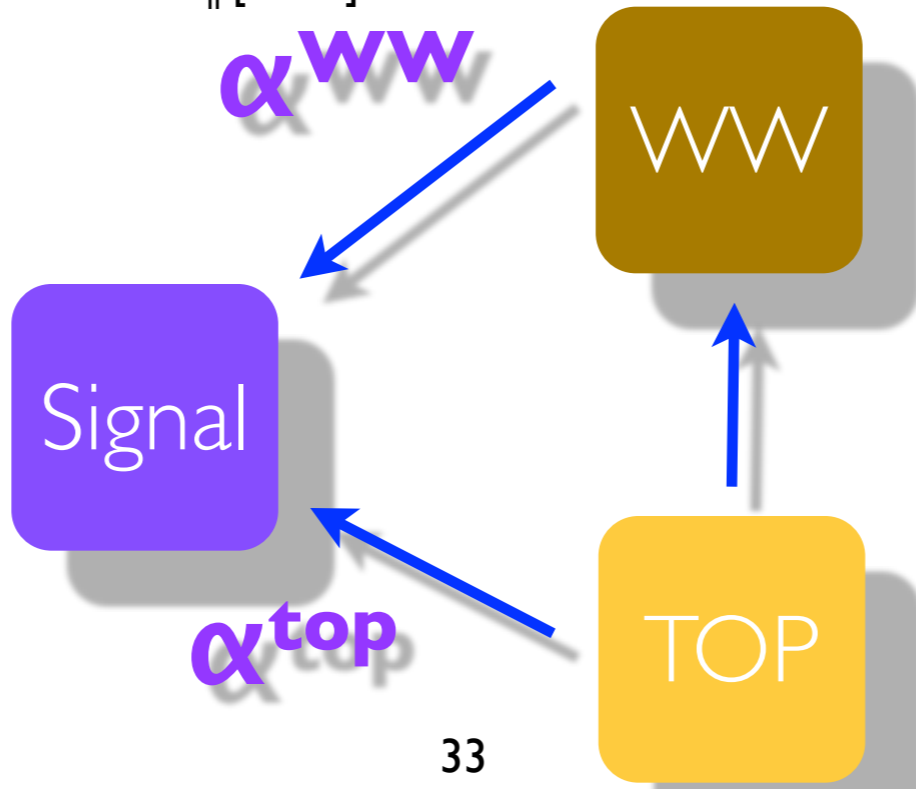
some discrepancy is instead observed in the  $m_{jj}$  distribution (actually corrected by normalising the top in a b-tag control region after the  $m_{jj}$  cut).

# WW background



In 0j only  $\alpha^{WW}$  is used, while in 1jet we need to subtract top contamination from WW C.R.

This recipe is applied for  $m_H < 200 \text{ GeV}$



$\beta$  no theor error, largely dominated by JES and b-tag efficiency

# Uncertainties on the extrapolation parameters

In order to minimise theoretical bias in the background normalisation, WW in 0j and 1j bin and top background in the 1 jet bin are normalised in the control regions.

The background yield in the signal region is determined according to the formula:

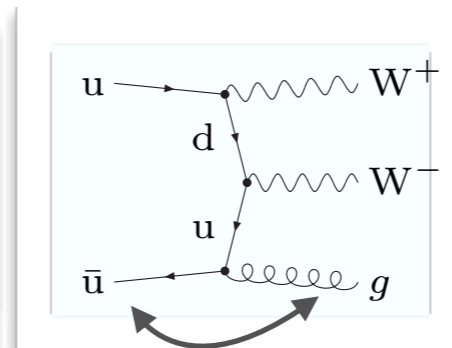
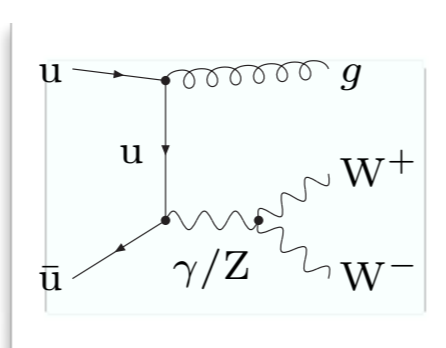
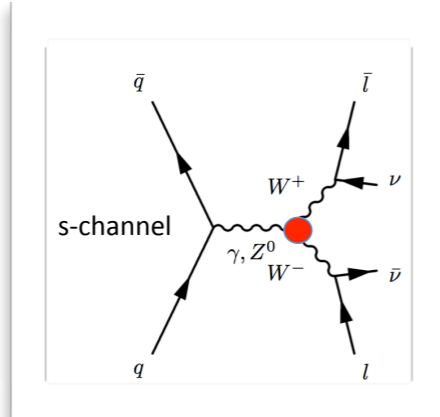
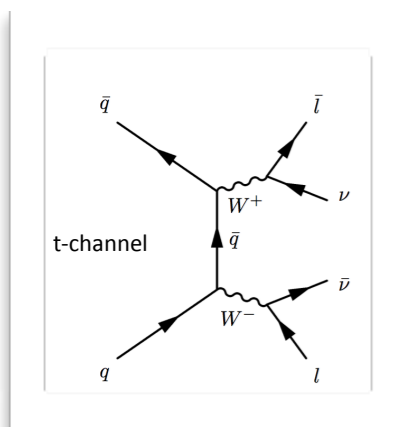
$$N_{0j}^{WW} = \alpha_{0j}^{WW} N_{0jC.R.}^{WW}$$

$$N_{1j}^{WW} = \alpha_{1j}^{WW} N_{1jC.R.}^{WW}$$

Theoretical uncertainties on  $\alpha^{WW}$  and central values are evaluated through scale variation and pdf using MC@NLO. MC@NLO include both qq/qg initiated process, taking into account spin correlation and off-shell W's.

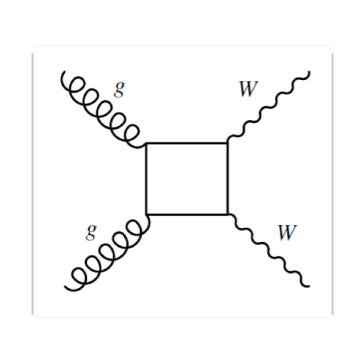
LO

NLO



qg/qq

NNLO



gg not present in MC@NLO because it is an  $\alpha_s^2$  process. Due to high gluon luminosity sensible contribution, central WW cross section corrected with gg2WW. Scale and pdf uncertainty due to gg2WW neglected (gg2WW contribution to  $\alpha$  is  $< 3\%$ , scale uncertainties dominates (30%) giving an error  $< 1\%$ )

# WW background for $H \rightarrow WW$ : uncertainties on $\alpha$ parameters.

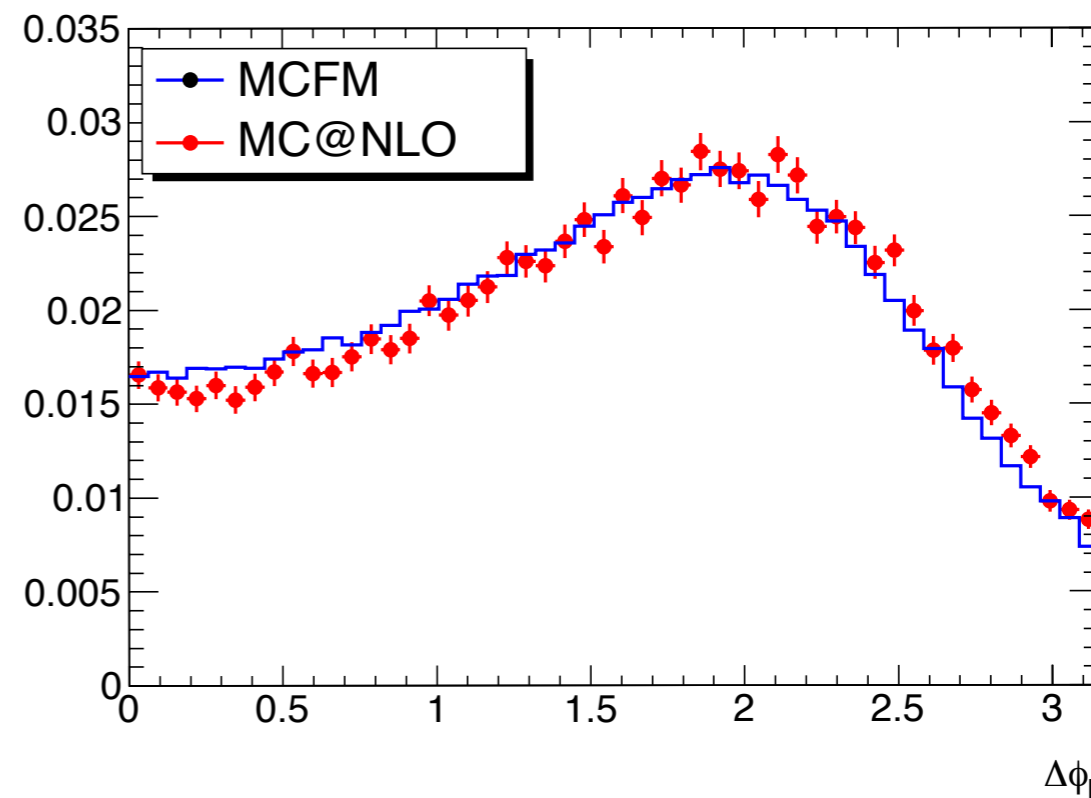
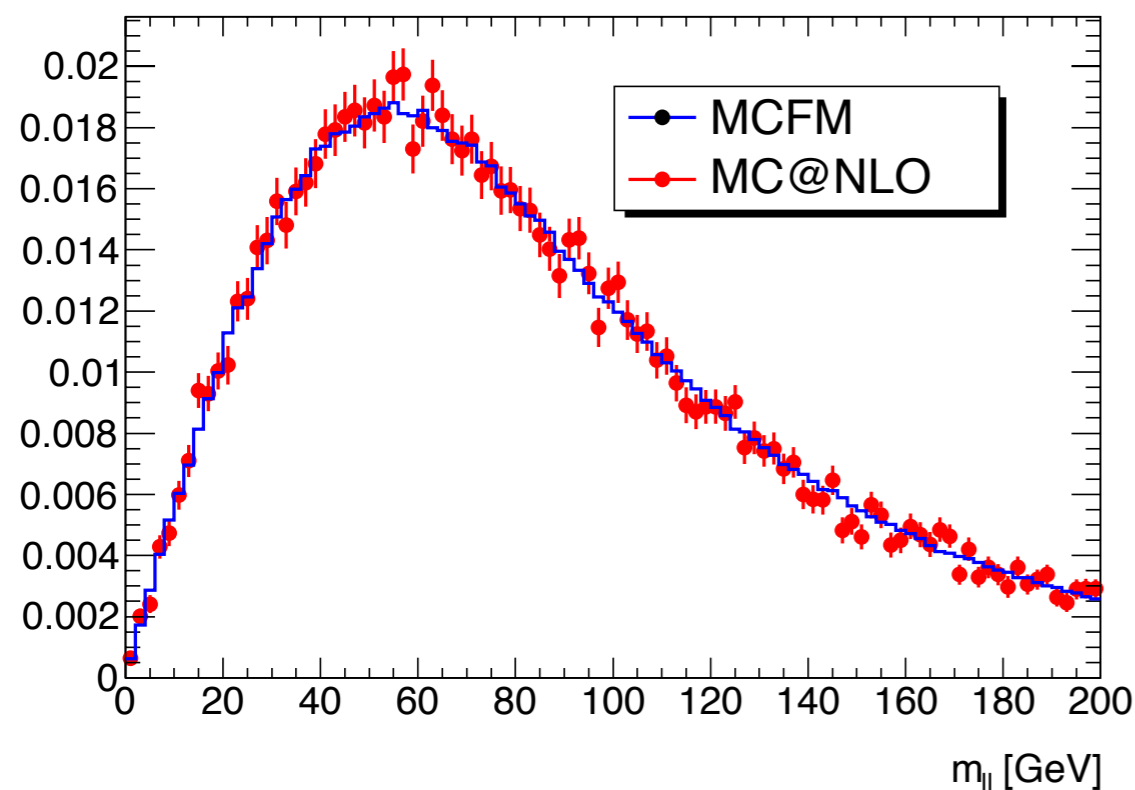
The scale variation is obtained using the prescription:  $1/2 \leq \xi_f/\xi_r \leq 2$      $1/2 \leq \xi_f \leq 2$

$$\mu_r = \xi_r \mu_0 \quad \mu_f = \xi_f \mu_0 \quad \text{with } 1/2 \leq \xi_r \leq 2 \quad \mu_0 = \frac{\sqrt{p_{T1}^2 + M_{W1}^2} + \sqrt{p_{T2}^2 + M_{W2}^2}}{2}$$

	scale	pdf CTEQ 6.6 error set	pdf central (CTEQ6.6, MSTW2008, NNPDF2.1)	Modelisation
$\alpha_{WW}^{0j}$	2.5%	2.6%	2.7 %	3.5%
$\alpha_{WW}^{1j}$	4%	2.5%	1.4 %	3.5 %
correlation	1			

**Table 26:** Scale and pdf uncertainties on WW extrapolation parameters  $\alpha$  in the ATLAS analysis.

Modelisation from MC@NLO-MCFM comparison without jet counting (full inclusive in number of jets).



$$\frac{\alpha(MC@NLO)}{\alpha(MCFM)} = 0.980 \pm 0.015$$

Takes into account contribution of single resonant diagrams and exact spin correlation for off-shell W's.



# WW background estimation at high mass (1/2).

For high  $m_H$  ( $> 200$  GeV) the signal  $m_{ll}$  distribution moves in the WW C.R., it is not possible to define a signal free control region.

Both ATLAS and CMS move to fully MC predicted event rate in jet bins at high  $m_H$ , ATLAS (MC@NLO), CMS (MADGRAPH)

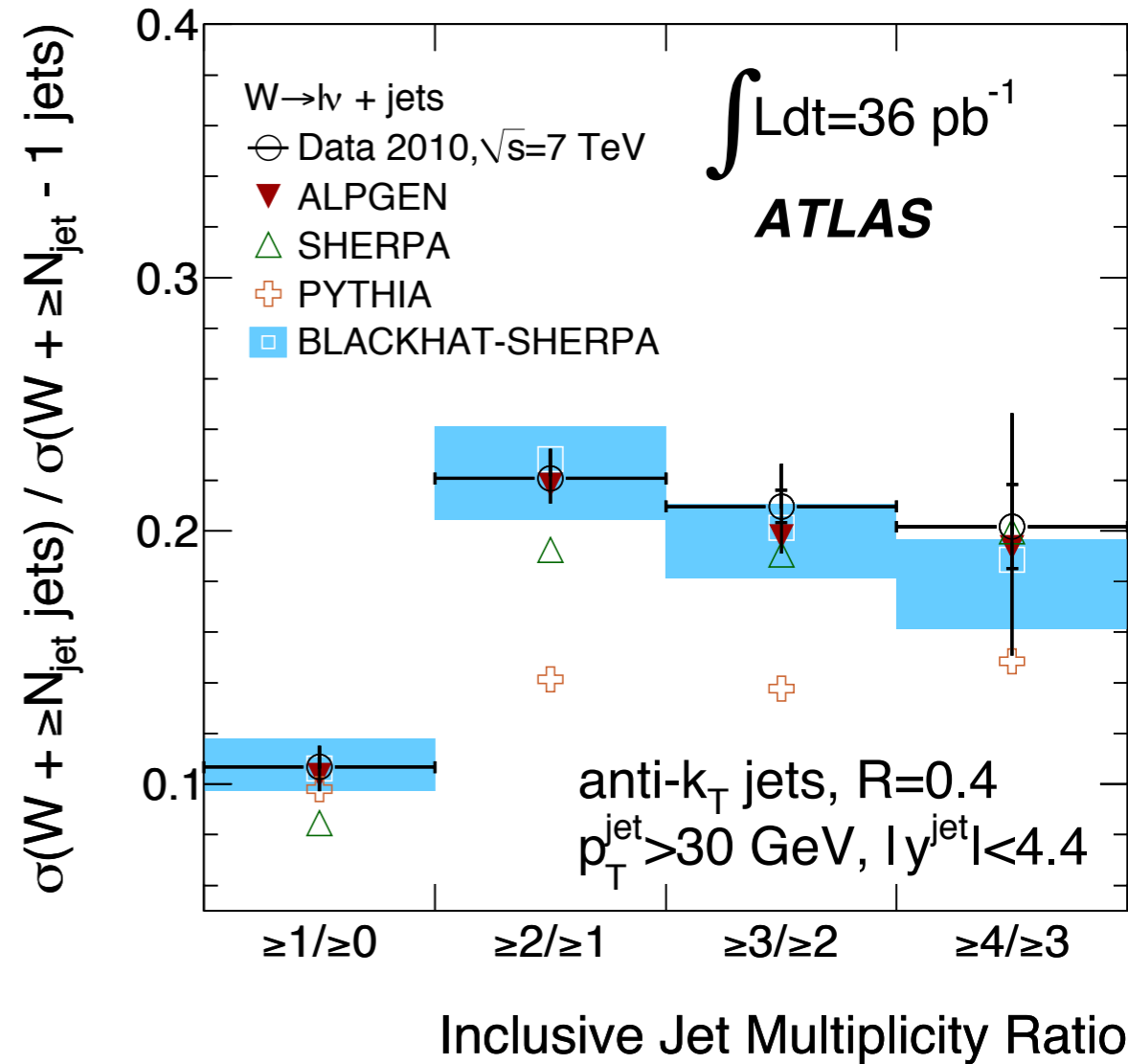
Scale uncertainties from MC@NLO are not enough (the 2 jet channel is produced only through parton shower in MC@NLO), ATLAS needs to compare with better calculations:ALPGEN, MADGRAPH.

The ratio  $\sigma_{\geq N+1}/\sigma_{\geq N}$  is usually well reproduced by ALPGEN

Add as systematic error discrepancies in  $\sigma_{\geq 2}/\sigma_{\geq 1}$  between ALPGEN and MC@NLO

ALPGEN includes VBF  $qq \rightarrow WW \rightarrow H \rightarrow WW$  with  $m_H = 120$  GeV, anyway both W's are on shell therefore the contribution from the Higgs is negligible (t-channel contribution also negligible).

	ALPGEN	MC@NLO
$\sigma_{>=1}/\sigma_{>=0}$	0,353	0,299
$\sigma_{>=2}/\sigma_{>=1}$	0,360	0,256
$\sigma_{>=3}/\sigma_{>=2}$	0,1124	0,06



fractional uncertainties (%).

	Scale	Model.	Total
$\sigma_{>=0}$	3,00	0,00	3,00
$\sigma_{>=1}$	6,0	0,00	6,00
$\sigma_{>=2}$	9,00	40,73	42,00
$\sigma_{>=3}$	10,0	98,28	99,00



# WW background estimation at high mass (2/2).

$$f_0 = \frac{\sigma_{\geq 0} - \sigma_{\geq 1}}{\sigma_{\geq 0}}$$

$$f_1 = \frac{\sigma_{\geq 1} - \sigma_{\geq 2}}{\sigma_{\geq 1}}$$

$$f_2 = \frac{\sigma_{\geq 2}}{\sigma_{\geq 1}}$$

scale uncertainties on exclusive jet fractions

	$f_0$	$f_1$	$f_2$
value	0.70	0.22	0.08
error (%)	3%	18%	38%

Inclusive 2 jets induce a large uncertainty in the 1 jet bin but not in the 0 jet bin.

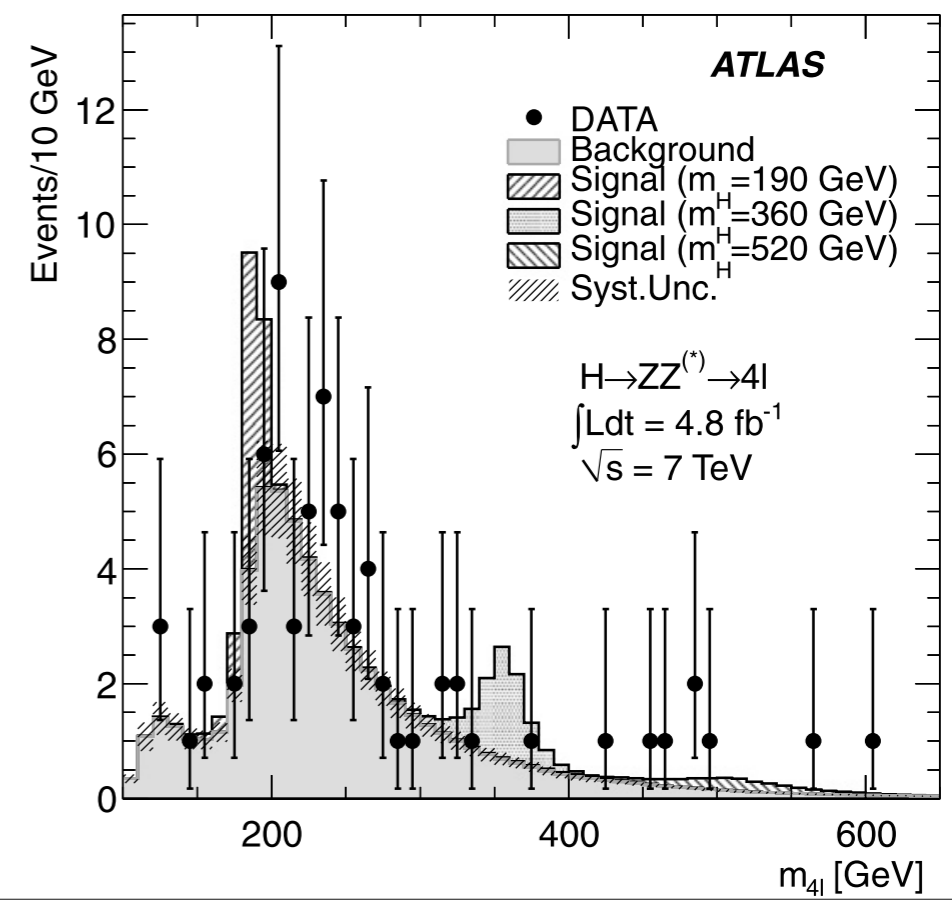
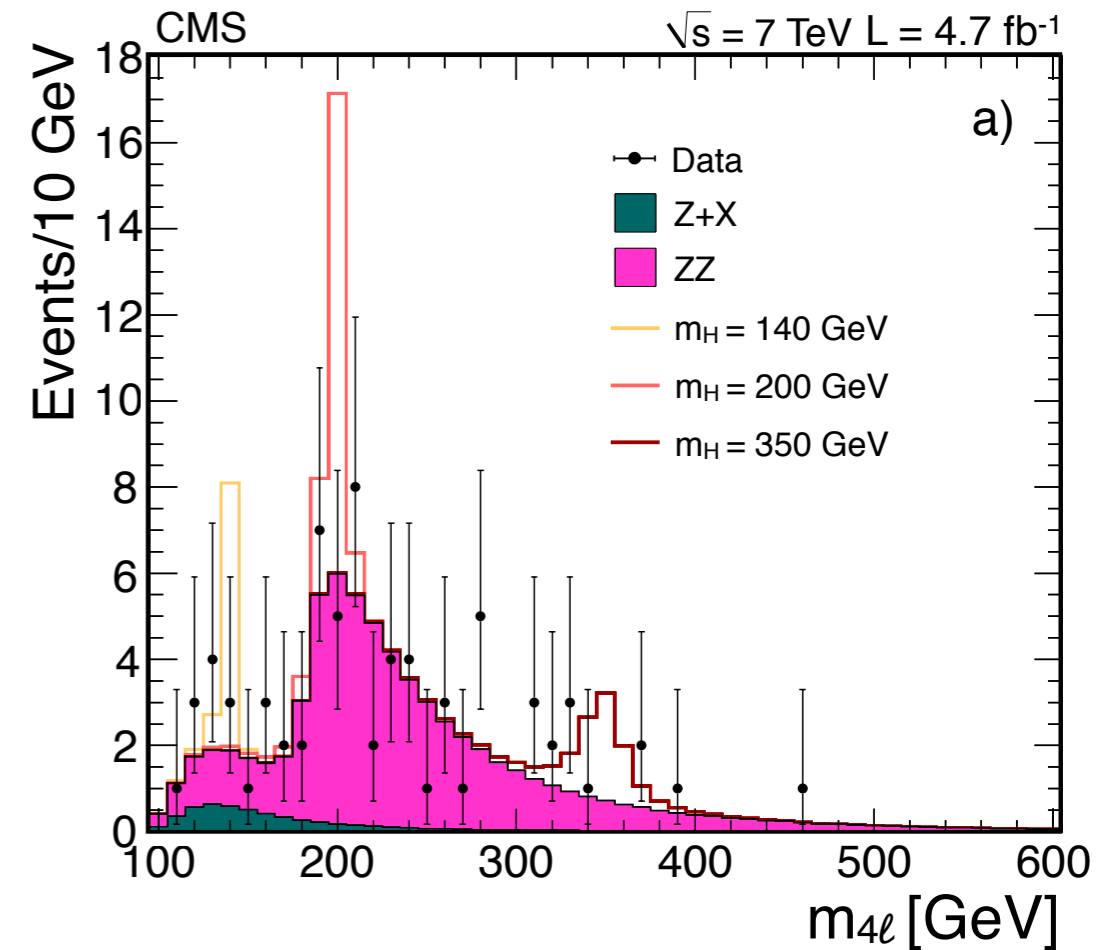
$$N_0 = f_0 A_0 \sigma L \quad N_1 = f_1 A_1 \sigma L$$

Acceptance is defined as all the other analysis cuts except the jet binning.

		scale error	%	pdfs
		<b>0j</b>		$f_0 A_0$
mH (GeV)	<b>110 - 200</b>		4,00	2%
	<b>200 - 300</b>		5,00	
		<b>1j</b>	5,00	
mH (GeV)	<b>110 - 200</b>		3,4	$f_1 A_1$
	<b>200 - 300</b>		3,00	2%

$$H \rightarrow ZZ^* \rightarrow 4l$$

- Search in the 4l final state  $\mu^+\mu^-\mu^+\mu^-$ ,  $e^+e^-e^+e^-$ ,  $e^+e^-\mu^+\mu^-$ ;
- Require one Z on shell: ATLAS 15 GeV around the Z mass, CMS 50-120 GeV window;
- The other lepton combination is requested in 12 GeV  $< m_Z < 120$  GeV in the CMS case, and an  $m_{4l}$  dependent cut in the ATLAS case going from 15 GeV to 60 GeV for  $m_{4l}$  from 120 to 200 GeV;
- signal simulated in both ATLAS and CMS with Powheg NLO MC.
- In the 4mu, 4e case Powheg misses the interference between same flavour same charge leptons configurations, correction performed at cross section level using Prophecy4f MC generator (A. Denner, S. Dittmaier, A. Muck)



# Background simulation

## ATLAS

## CMS

Z+light jets

ALPGEN+HERWIG

MADGRAPH

Z+bbar, ccbar

ALPGEN+HERWIG

MADGRAPH

ttbar

MC@NLO+HERWIG

Powheg

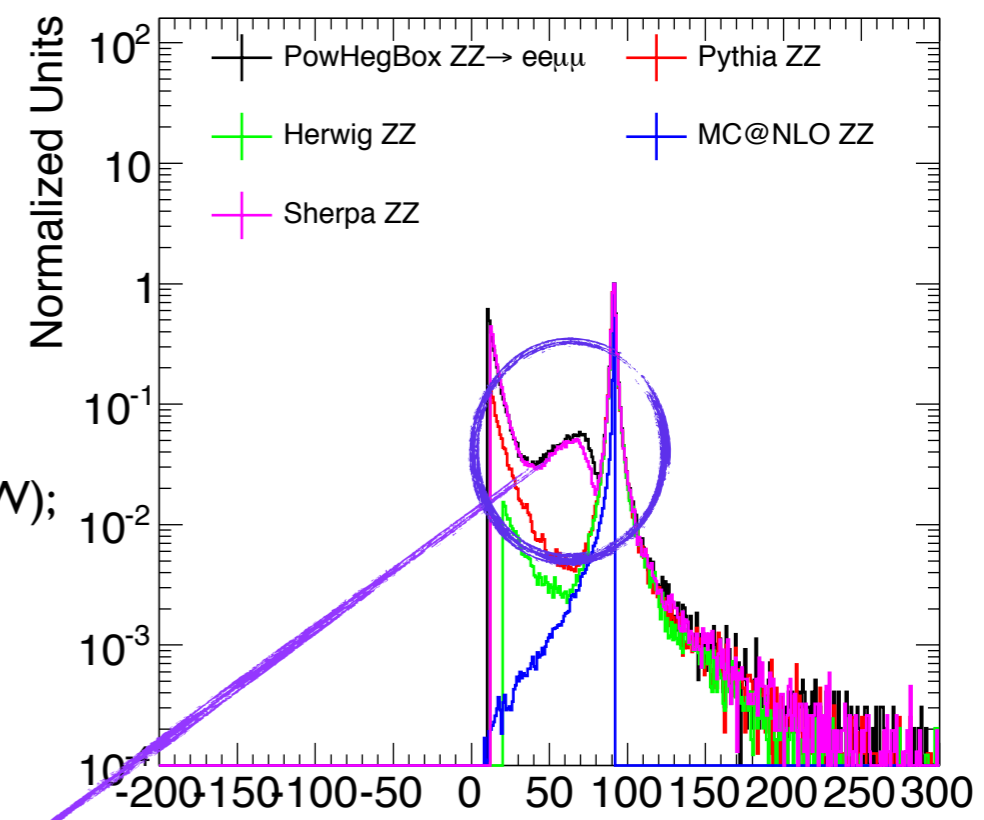
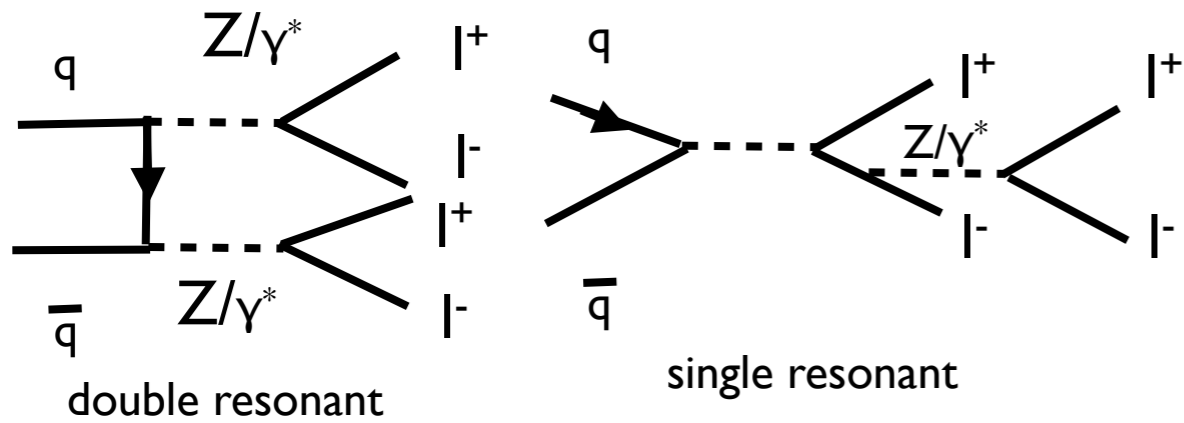
$pp \rightarrow ZZ \rightarrow 4l$

Pythia

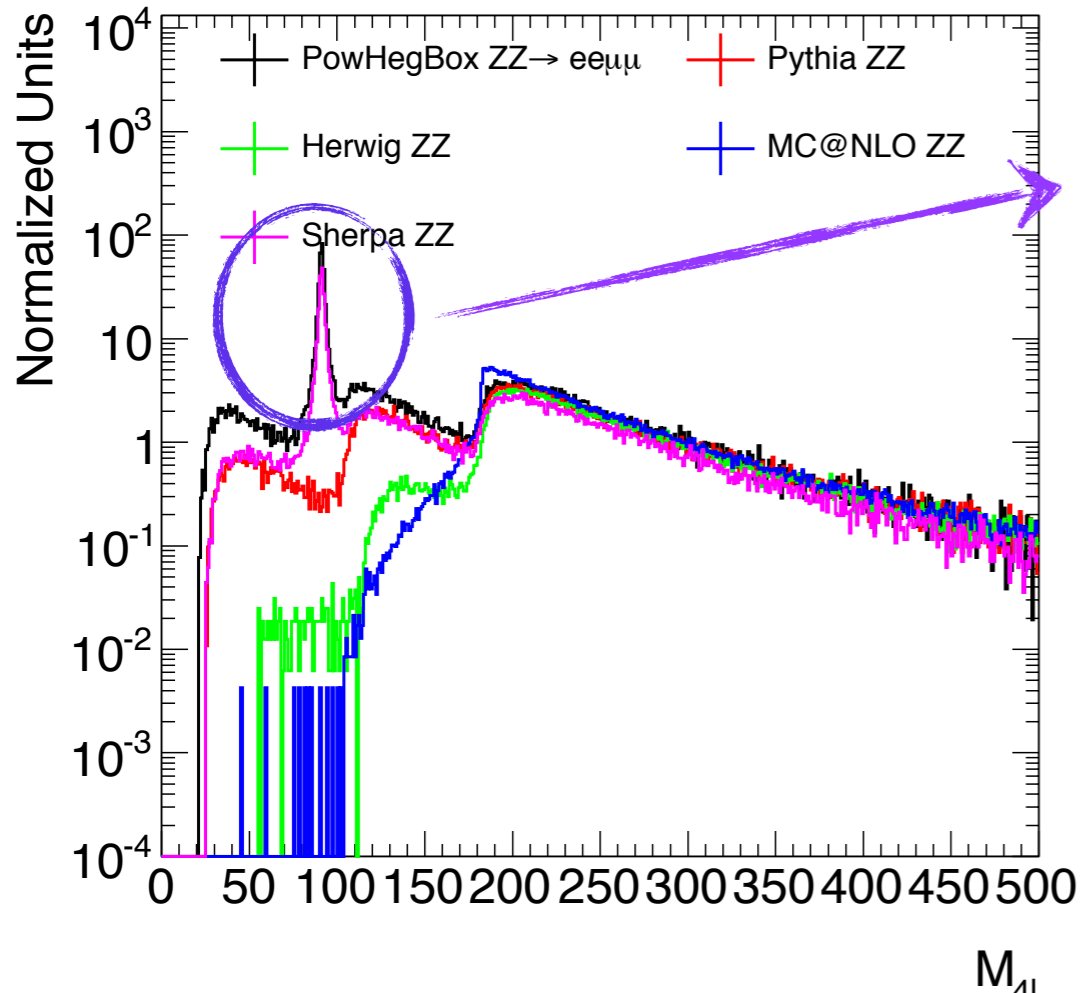
Powheg

- The background is largely dominated by  $pp \rightarrow ZZ \rightarrow 4l$ , in the low mass region  $m_{4l} < 180$  GeV  
Some contribution from reducible background appears
- Z+jets with jet mis-id as electrons, Z+bbar with muons from B decay passing isolation cuts.
- Reducible background is evaluated with data driven techniques (reverting isolation and identification criteria starting from MC normalisation in control region).
- ZZ background is taken from MC.

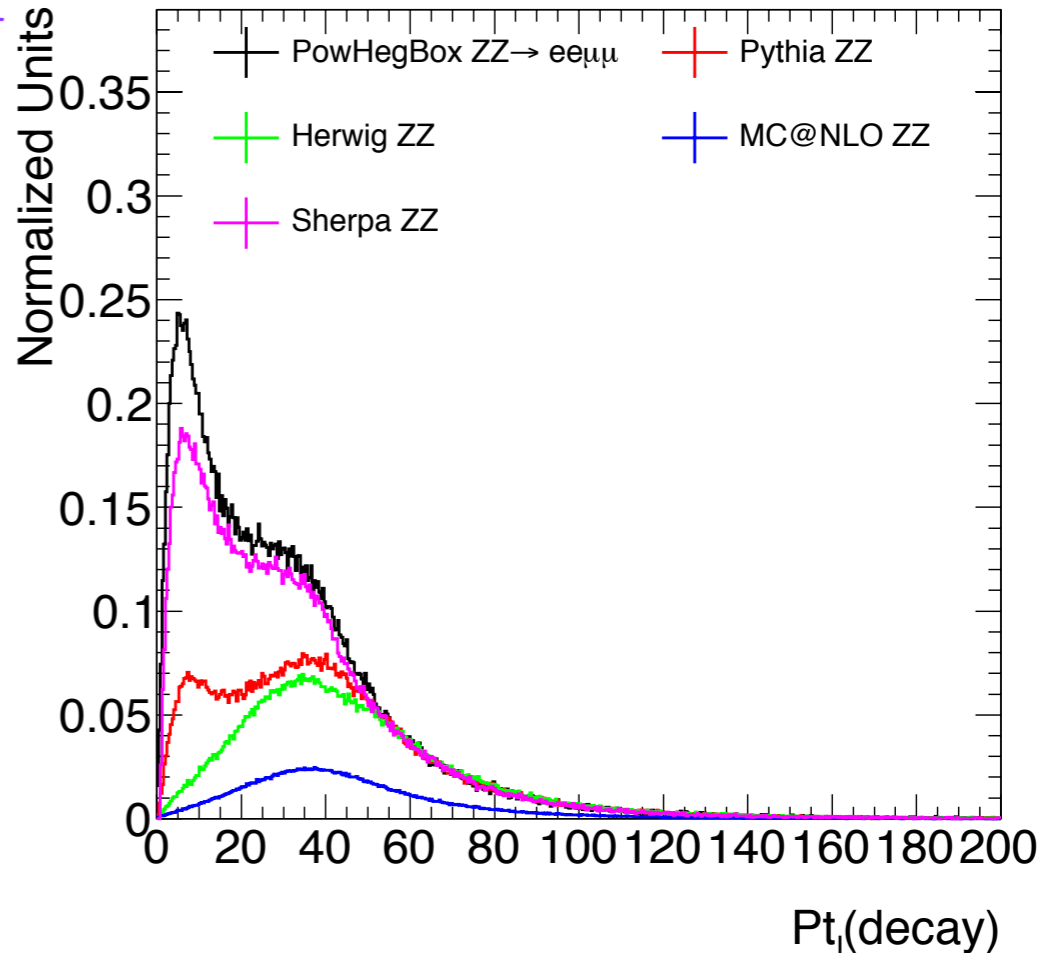
# The $pp \rightarrow ZZ \rightarrow 4l$ background



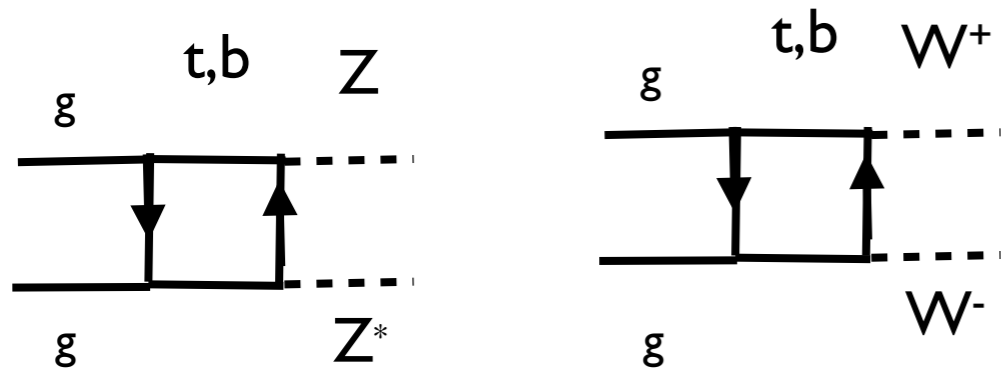
- MC@NLO just considers the Z process (on shell and parametrised with a BW);
- Pythia doesn't include single resonant contribution;
- Both of them are included in MCFM (parton level MC);
- ATLAS reweights Pythia  $M_{4l}$  distribution to MCFM
- CMS uses Powheg that includes all contributions.
- Differential uncertainties are computed by CMS (using std. ren, fact scale variation)



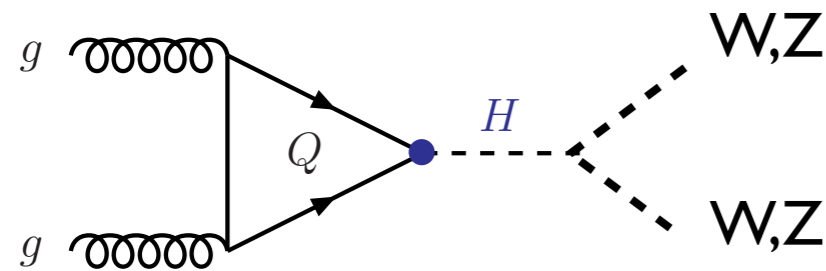
Single resonant contribution



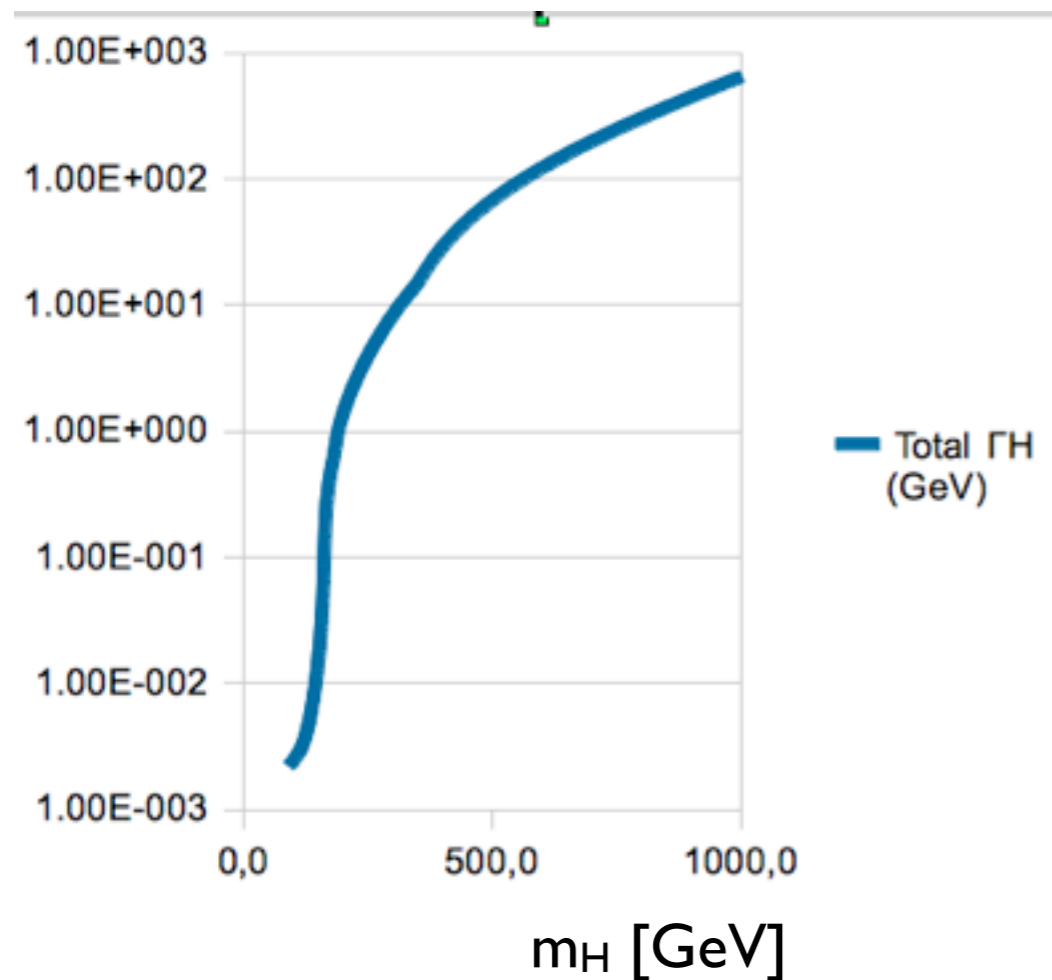
# The $gg \rightarrow ZZ, WW$ background



At order  $\alpha_s^2$ , is not included in MC@NLO  $pp \rightarrow WW$  because NLO in  $qq \rightarrow W^+W^-$  is  $O(\alpha_s)$ . Its contribution is anyway enhanced by the  $gg$  luminosity. Inclusively in  $WW$  is  $\sim 5\%$  of the  $WW$  rate. It is increased up to a factor 2 by the signal selection cuts.



Interference effects can be important for large values of  $m_H$ . The Higgs becomes broader at larger  $m_H$  values.



For  $m_H > 300$  GeV the Higgs, due to the broad structure, can largely interfere with the background.

The effect has been evaluated at LO in MCFM.

A conservative uncertainty on this effect has been roughly estimated and is of the order  $150\% \times M_H^3$  (TeV)

It gives an effect of 4% at 300 GeV, 30% at 600 GeV, 75% at 800 GeV.

Work is on going to implement the interference and the proper Higgs line shape in aMC@NLO.

# Heavy Higgs line shape

For very high mass the Higgs becomes more and more close to a broad hadronic resonance and shows all typical features of states like  $\sigma$ ,  $f_0$ ,  $a_0$

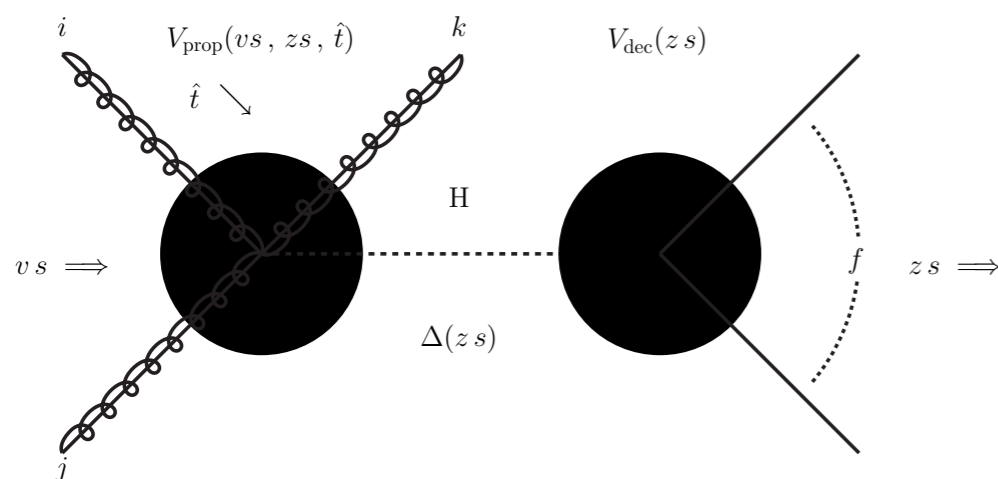
- 1) Strong deviation from BW behaviour;
- 2) Opening threshold effects in the width;
- 3) width dependent from the mass of the final state;
- 4) interference with continuum background;

You can substitute the  $\pi^+\pi^-$  with  $W^+W^-$  and  $ZZ$

MC@NLO implements an Higgs line shape that is a BW with  $\Gamma = f(m_H)$

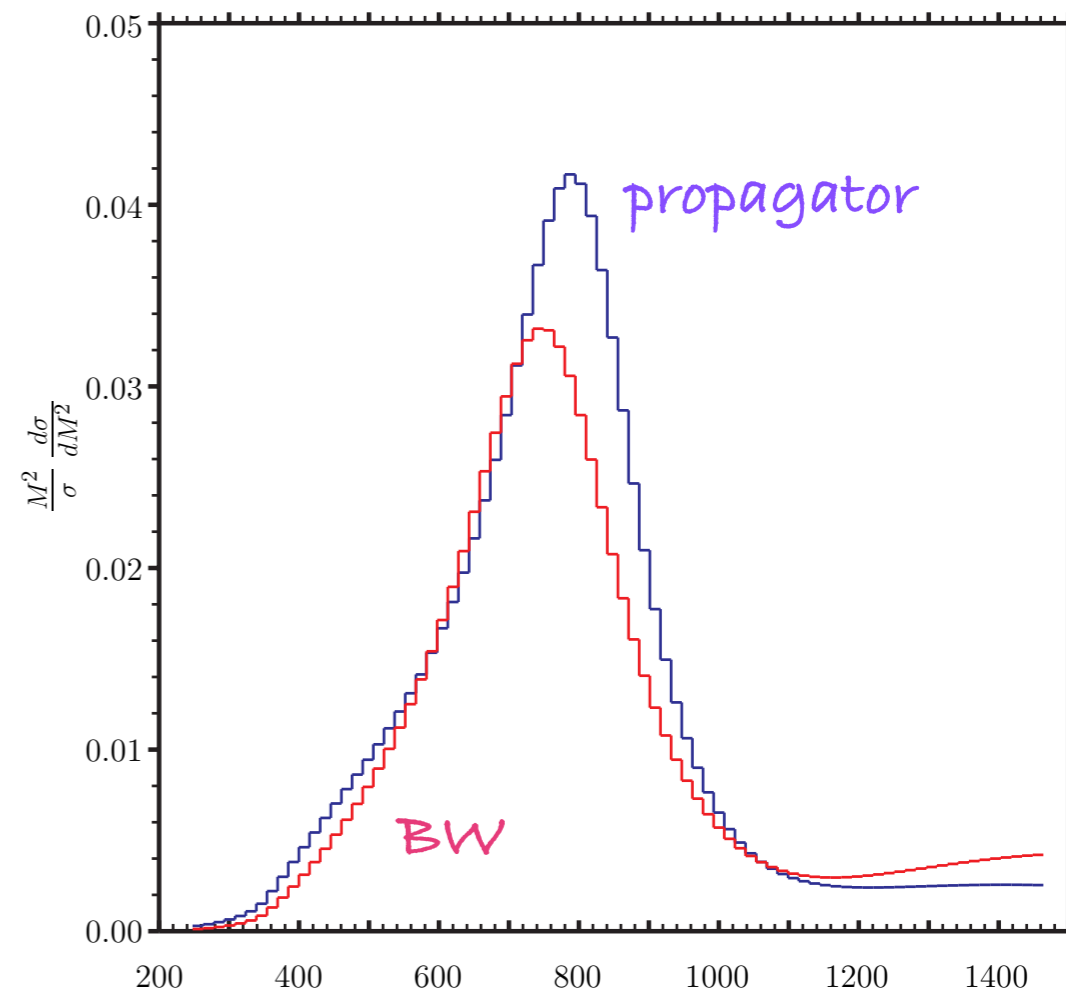
Powheg implements  $\Gamma = f(s)$   $s = m^2$  of the decayed system ( $\rho$  like parametrisation)

More complete calculation (will be implemented in Powheg and aMC@NLO) use the complex pole scheme: the line shape is given by unitarity conditions and the full QFT scattering amplitude (Flatte' for  $f_0$ )



$$\Rightarrow \sigma_{ij \rightarrow H+k}(v_s, \hat{t}, z_s) \frac{v z s^2}{|z s - s_H|^2} \frac{\Gamma_{H \rightarrow f}(z s)}{(z s)^{1/2}} + \text{NR}$$

$$= \sigma_{ij \rightarrow H+k}(v_s, \hat{t}, s_H) \frac{v s |s_H|^{1/2}}{|z s - s_H|^2} \Gamma_{H \rightarrow f}(s_H) + \text{NR}'$$



# Interference effect at work?

Actually G. Passarino doesn't agree with this interpretation.

LO implementation of interference effect in MCFM shows that at least the interference is not fully described.

Seymour scheme:  
emulates the S-B  
interference effects

Zero width approximation (ZWA):

$$\frac{1}{\Delta(Q, m_H)} \rightarrow \frac{\pi}{m_H \Gamma_H(m_H)} \delta(Q^2 - m_H^2)$$

Naive Breit-Wigner (BW):

$$\frac{1}{\Delta(Q, m_H)} = \frac{1}{(Q^2 - m_H^2)^2 + m_H^2 \Gamma_H^2(m_H)}$$

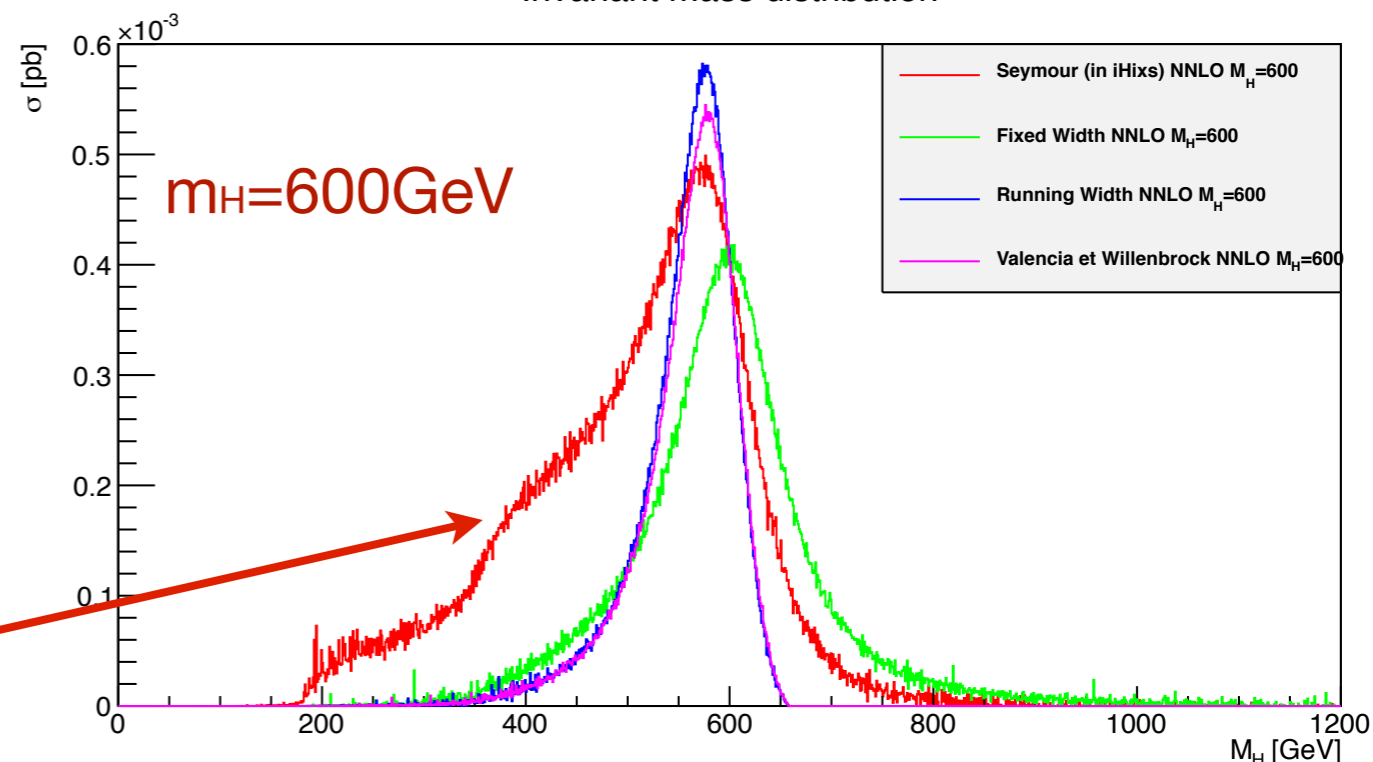
Breit-Wigner with running width:

$$\frac{1}{\Delta(Q, m_H)} = \frac{1}{(Q^2 - m_H^2)^2 + Q^2 \Gamma_H^2(Q)}$$

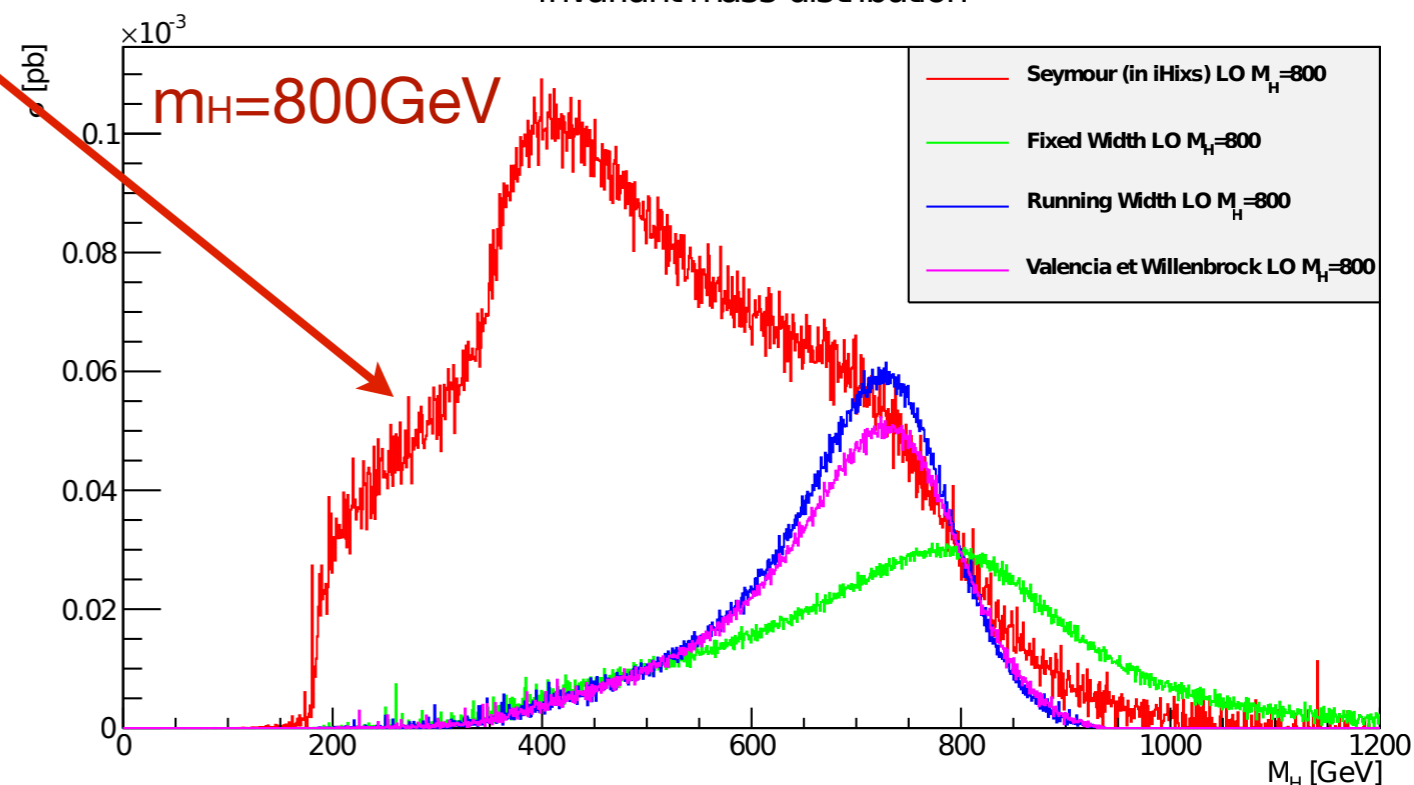
Seymour scheme [21]

$$\frac{1}{\Delta(Q, m_H)} = \frac{m_H^4 / Q^4}{(Q^2 - m_H^2)^2 + \Gamma_H^2(m_H^2) \frac{Q^4}{m_H^2}}$$

Invariant mass distribution



Invariant mass distribution





# Conclusions

All of this we need to do these plots:

